STUDIES OF FLUID DISTRIBUTION WITH MAGNETIC FIELDS AND ANALYSIS OF ULTRA COMPACT OBJECTS WITH CENTRIFUGAL FORCE REVERSAL

THESIS

SUBMITTED TO THE
UNIVERSITY OF RAJASTHAN
FOR THE DEGREE OF

DOCTOR OF PHILOSOPHY

(FACULTY OF SCIENCE)

CO-SUPERVISOR :
PROF A.R. PRASANNA
PHYSICAL RESEARCH LABORATORY
NAVRANGPURA
AHMEDABAD-380 009

SUPERVISOR :
PROF. G.N. PUROHIT
DEPARTMENT OF MATHEMATICS
UNIVERSITY OF RAJASTHAN
JAIPUR-302 004

BY
ANSHU GUPTA

MARCH 1997

CERTIFICATE

This is to certify that **Ms. Anshu Gupta** has written the thesis on the topic entitled **'Studies of fluid distribution with magnetic fields and analysis of ultra compact objects with Centrifugal Force Reversal'** under our joint supervision. As far as, we know her work is original and it has not been done earlier anywhere else. She has worked for more than 100 days each year either in Jaipur or at Ahmedabad.

Prof. A. R. Prasanna
Co-Supervisor
Theory Division,
Physical Research Laboratory,
Ahmedabad.

Prof. G. N . Purohit
Supervisor
Head, Deptt. of Mathematics,
University of Rajasthan,
Jaipur.

dedicated to...
who add meaning
to my existence.

ACKNOWLEDGEMENTS

First and foremost, I would like to express my thanks and profound gratitude to my thesis supervisors Prof. G. N. Purohit and Prof. A. R. Prasanna for providing me with the necessary guidance and direction.

I am particularly grateful to Prof. Prasanna for his kind understanding and never ending patience during the course of this work. I have been benefited extensively from his deep knowledge and understanding of General relativity and Astrophysics. Without his discerning, yet discreet guidance this work would have never been completed.

My special thanks are due to Dr. Sai Iyer and Dr. S. Mohanty for their sustained interest in my work and for their useful comments that have helped in adding to the clarity of ideas presented here. It has been a pleasure to know and to work with them.

It is a pleasure to explicitly acknowledge the kind help extended to me by Sai whenever I approached him regarding any problems either in Physics or in Computations.

Thanks are due to Dr. Sitaram for his useful suggestions. I am thankful to Prof. Das and other academic faculty of theory group for their encouragement and help.

It is a pleasure to thank Dr. Dhurandhar, Dr. Kembhavi, Dr. Bala Iyer and Dr. Sathayaprakash for giving me a broader perspective of the ongoing research in the field of relativistic astrophysics.

Discussions with Amruta, Hiranmaya and Pradip have been very useful. I wish to record my thanks to them.

My sincere thanks to Dr. D. S. Chauhan and the office staff at Department of Mathematics, University of Rajasthan, Jaipur for their help regarding the registration formalities.

I also wish to thank all the PRL staff; at theory floor, in particular Mr. Viswanathan and at Library, Computer Center and other supporting facilities for their kind co-operation.

I am extremely grateful to Kunu for not only going through the whole manuscript meticulously more than once but also to provide me with moral support and ever-ready help.

My heart-felt thanks are due to Aparna, Kamath, Sandeep and Watson for their timely help.

Poulose has always been a very helpful and supportive friend, batch-mate and office-mate. I wish to thank him for all those exciting discussions and arguments we had shared.

Special thanks are due to my batch-mates, all other RS's and PDF's at PRL and at various research institutes for their nice and enjoyable company.

I gratefully acknowledge the selfless help and kind support of my friends here and elsewhere. The memories of cheerful moments shared with them will always be a treasure to cherish.

Nobody can ever acknowledge the contributions of parents and family members enough, hence I will not attempt to do that.

Publications/ Pre-prints

- Centrifugal force and ellipticity behaviour of a slowly rotating ultra compact object,

  Anshu Gupta, Sai Iyer and A. R. Prasanna

  Class. and Quant. Grav. 1996 **13** pp. 2675.

- Structure of External Electromagnetic Field around a Slowly Rotating Compact Object and Charged Particle Trajectories Therein,

  A. R. Prasanna and **Anshu Gupta** 1997

  to appear in *Il Nuovo Cimento B.*

- Behaviour of the centrifugal force and of ellipticity for a slowly rotating fluid configuration with different equations of state

  Anshu Gupta, Sai Iyer and A. R. Prasanna

  (Communicated to Class. and Quant. Grav.).

- Effects of rotation and equations of state on the structure of the electromagnetic field inside a slowly rotating body,

  Anshu Gupta and A. R. Prasanna

  in preperation.

- Čerenkov radiation by charged particles in an external gravitational field and detection of cosmic strings,

  Anshu Gupta, Subhendra Mohanty and Manoj K. Samal

  (PRL Preprint No. PRL-TH-95/12, astro-ph/9509022, In communication Phys. Rev. D (Rapid Communications)).

Preface

The main aim of the thesis is to understand the role of general relativity, particularly of the significant characteristics like inertial frame dragging and centrifugal force reversal in the context of ultra compact fluid distributions and their magneto-spheres. With the discovery of quasars, pulsars and x-ray binaries in the sixties and seventies, it was realized that gravity needs to be discussed in the framework of general relativity for describing high energy astrophysical phenomena. Apart from the dynamics of these systems, general relativistic effects become more important in the understanding of equilibrium configurations and their stability.

Pulsars are modeled after rotating magnetized neutron stars. Even though much effort that had gone into the study of the structure and dynamics of electromagnetic fields in the above context, it is not sufficient for a full understanding. Most of the studies have restricted themselves either to the Newtonian formalism or have at best considered the static spacetime metric (Schwarzschild geometry), which represents a non-rotating body, thus missing the information which can be obtained by considering metric which includes rotational effects. Due to the non-linearity of Einstein's field equations, it is difficult to get exact analytical solutions in general. Whereas it is well known that black-hole physics has to be discussed using the Kerr-geometry, for rotating compact objects like neutron stars, one needs to look for appropriate solutions describing the interior as well as the exterior. One of the ways is to solve

Einstein's field equations numerically, and the other method is to get analytical solutions with some approximations. Hartle, in 1967, developed a formalism to calculate the equilibrium configuration of slowly rotating relativistic bodies treating the rotation upto second order in angular velocity. In that formalism, rotation was considered as the perturbation on a non-rotating body. Later, it was extended by Hartle & Thorne (1968) for considering equilibrium models with different equations of state. The advantage of this formalism compared to the numerical method which demands a lot of computational power, is that despite approximations it can be used for discussions on pulsars as the observed angular velocity of various pulsars is within the range where slow rotation approximation is valid. In other words, if the angular velocity is less than the Keplerian angular velocity then the Hartle-Thorne procedure can be used.

The composition and distribution of matter in neutron stars are not yet understood clearly. Several equations of state are considered as representative models for the neutron star's matter distribution and their interaction. Considering a few of these realistic equations of state and using the Hartle-Thorne formalism, we have attempted to study the consequent effects of rotation and matter distribution on the structure of electro-magnetic fields, centrifugal force, motion of particles and related phenomena, some of which arise only due to relativistic effects and have no analogies in Newtonian physics.

We have found that rotation does have an important bearing upon the magnetic field

topology as well as on the behaviour of ellipticity of the fluid distribution. The trajectories of charged particles in a dipole magnetic field and quadrupole electric field superposed on the external spacetime of a very slowly rotating mass (represented by a first order correction to the Schwarzschild geometry) show distinction of the orbits for co- and contra-rotating particles as compared to the particle orbits around a non-rotating body. Further, we found that for very stiff equations of state there is substantial increment ($\approx 25\%$) in the field strength near the center of the body due to rotation. Ellipticity and centrifugal force of a slowly rotating contracting system show extrema as a result of relativistic effects. Whereas the centrifugal force shows maxima for both homogeneous and inhomogeneous distributions, the ellipticity shows a negative behaviour in the case of inhomogeneous distributions indicating that the system gets prolate and not oblate.

Contents

Chapter 1

Introduction

The importance of the studies of compact objects endowed with magnetic field and rotation was realized after the discovery of pulsars by Hewish and his group (Hewish et al. 1968), when Gold (1968) suggested that the observed pulsars could be rotating neutron stars with surface magnetic field of around 10^{12} G. The idea for the existence of neutron star was proposed by Baade & Zwicky (1934), indicating these objects to be highly dense, small in size and very strongly bounded gravitationally. They also suggested the formation of such objects in supernova explosions, when the core of the star collapses under its own weight till the neutron degeneracy pressure can overcome gravity thus leading to an equilibrium compact object. Oppenheimer & Volkoff (1939) did the first calculation for these stable equilibrium objects assuming the matter composition to be an ideal gas of free neutrons at very high density. Though in the next 25-30 years very few studies were devoted in this direction with Harrison et al. (1958), Cameron (1959) discussing the equations of state of such objects while Hoyle et al. (1964) suggested that the neutron star produced in supernova explosion to be a rapidly rotating object, (see Tsuruta & Cameron 1966 also) possessing strong magnetic fields (Woltzer 1964). The discoveries of x-ray sources by Giacconi et al. (1962) and quasars by Sandage (1961) and Schmidt (1963), generated lot of interest in the studies of compact objects like neutron stars and black holes. But the confirmation of the existence of such objects was only accepted with the observation of pulsars which possibly are rotating neutron stars. As the gravitational potential of these compact objects can be very large $M/R \approx 0.4 - 0.5$, it has been suggested time and again that one needs to bring in the framework of general relativity for describing the gravitational field of these compact objects. Despite the amount of work gone into the studies of equilibrium structure, composition and emission mechanism of these objects which we will be briefly discussing in the following sections of this chapter, there still exist a number of unresolved problems.

In this thesis we have basically studied the role of general relativity, particularly of the significant characteristics like inertial frame dragging and centrifugal force reversal in the context of ultra compact fluid distributions and their magnetospheres. In other words we have attempted to study the consequent effects of rotation and matter distribution on the structure of electromagnetic fields, centrifugal force, motion of particle and related phenomena, some of which arise only due to relativistic effects and have no analogies in the framework of Newtonian physics.

We present in this chapter a brief outline of the discussion of electromagnetic fields on curved spacetime, inertial forces in general relativity and of slowly rotating fluid configurations in the framework of general relativity, which indeed forms the basis of the studies made and presented in the following chapters.

1.1 Electromagnetic fields and compact objects

Almost all the celestial bodies possess magnetic fields and electric fields within and around them. Puzzles regarding the origin, evolution and their effects on the dynamical and physical processes are not yet resolved. Various theories exist connecting their generation and evolution with thermal instabilities, heating mechanisms etc. A review by Doglinov (1988) discusses it in detail for various celestial bodies. Further, in the case of massive compact objects like pulsars and quasars, the interactions between electromagnetic field and strong gravitational field also become very important. Besides, the motivation to understand the dynamics of these objects, the studies of electromagnetic interactions with strong gravitational field is a subject of theoretical interest in its own right.

According to Einstein's mass-energy relationship, $E = mc^2$, any form of energy is [illegible] to mass, thus having an associated gravitational field with it. In general relativity gravitational field is manifested in the form of curvature of spacetime. Hence, in the presence of an electromagnetic field around a massive body, the geometry of spacetime is not only affected by matter distribution but also due to electromagnetic fields. Similarly, electromagnetic fields also get influenced by the massive body. This interaction between the fields is studied by solving the Einstein's field equations alongwith the Maxwell's equations in curved spacetime. Solution of these coupled set of the Einstein - Maxwell equation should in principle give the metric potential g_{ij} of the background geometry of spacetime and the vector potential A_i electromagnetic field.

In general, analytical solutions to the Einstein-Maxwell equations are not always possible. Instead it is rather simpler to get solutions if the Einstein field equations are decoupled from the Maxwell equations, which means that curvature of spacetime is assumed to be affected only by the distribution of matter. This could be so, if the energy due to electromagnetic field is very small as compared to the gravitational potential energy. In most of the astrophysical situations, one can work with this assumption since, for magnetic field as high as 10^{12} G, the corresponding energy is $\approx 10^{24}$ ergs which is very small as compared to the gravitational potential energy $\approx 10^{40}$ ergs due to $1 M_{\odot}$ object.

With such basic assumption, Cohen & Wald (1971) and Hanni & Ruffini (1973) calculated the quasi-static electric field of a point charge in a static background both inside and outside the radius at which the source was located. Whereas, Ginzburg & Ozernoi (1965) obtained the solution with a dipole magnetic field, multipole moments of quasi-static magnetic field outside the spherically symmetric static body were derived by Anderson & Cohen (1970). All these solutions were asymptotically flat. Further, Petterson (1974) also obtained the multipole expansion of the magnetic field by solving the Maxwell's equations in curved spacetime which he used to derive the magnetic field inside and outside a quasi-static current loop around a Schwarzschild black hole.

Cohen et al. (1974), Chitre & Vishveshwara (1975) and Petterson (1974, 1975) discussed the solution of electromagnetic field in the Kerr geometry which basically represents the rotating black hole and has very important relevance in the studies of quasar emission mechanism of quasars. Studies of electromagnetic field due to a stationary charge in the source free region (Cohen et al. 1974) and due to an uncharged current loop in the equatorial plane (Chitre & Vishveshwara 1975) were extended by Petterson (1975). He first obtained the stationary axisymmetric electromagnetic fields around a rotating black hole using NP formalism (Newman & Penrose 1962) as described by Teukolsky (1973) and calculated the field of a loop in the equatorial plane which has both current and a net charge. Further, he used it for obtaining the minimum energy configuration of a black hole surrounded by a current loop. Once the black hole reaches that state, no charge accretion will occur.

Though these studies laid the basic foundation for the studies of electromagnetic interaction in static and stationary spacetime geometries and are also useful in the studies of black hole physics, they do not contribute substantially to the analysis of pulsar emission mechanism. The reason for this is, the pulsars are rotating objects and there does not exist any exact solution which describes the geometry of spacetime around a rotating object. Though Kerr metric is an exact solution for a rotating system, it is only valid for a rotating black hole. Black hole represents that state of a body when the whole dynamics cease, thus the solution representing that stage is not applicable to study the stellar structures like neutron stars and pulsars.

Just before the discovery of pulsars, Pacini (1967) proposed a magnetic dipole model in which the rotational energy of neutron star was converted into the electromagnetic radiation and in that field the particle motion was discussed. Later Ostriker & Gunn (1969), Goldreich & Julian (1969) and Ruderman & Sutherland (1975), gave some models for the pulsar emission mechanism and the formation of magnetosphere but they did not consider any relativistic effects in their studies. In the last decade, effects of spacetime curvature are included in the studies of pulsar beam width (Kapoor & Datta 1985; Kapoor 1991), effect of light bending in x-ray pulsars and x-ray bursts (Meszaros & Riffert 1987, 1988; Riffert & Meszaros 1988), pair production attenuation of gamma rays (Riffert et al. 1989; Meszaros et al. 1989) and gamma ray emission from radio pulsars (Gontheir & Harding 1994), but all these studies considered only the dipole magnetic field in the static background. Recently, Sengupta (1995) has discussed the effects of induced quadruple electric field due to a rotating dipole magnetic field. However, in his studies though the rotation was considered, the dragging of inertial frame which is one of the important general relativistic effects arising due to the rotation of the source, was neglected.

Since particle motion in any of the fields reflects the structure of that field, it is useful to study the particle trajectories in the given field. There have been a large number of studies of charged particle trajectories in electromagnetic fields on curved spacetime (Prasanna & Varma 1977; Prasanna & Vishveshwara 1978; Chakraborty & Prasanna 1982; Stuchlik 1983; Balek et al. 1989) using Schwarzschild, Kerr, Ernst etc. as the background geometries. Prasanna (1980) provides an excellent review on this topic of charged particle motion in electromagnetic fields on curved spacetime. Further, Stuchlik (1983) discussed the particle trajectories considering the non-zero cosmological constant. In the Kerr-de Sitter spacetime mainly latitudinal motion is studied whereas properties of purely radial trajectories are studied in Schwarzschild-de Sitter background, besides analyzing the existence and stability of circular orbits. Circular orbits of ultra-relativistic particles with high specific charge are discussed by Balek et al. (1989). More recently, Prasanna & Sengupta (1994), have discussed the particle motion on Schwarzschild background in the presence of a toroidal magnetic field. As our interest in the present study is to look at the effects of inertial frame dragging on the magnetosphere of a compact object, we first consider the solution of Maxwell's equations in the exterior spacetime of a slowly rotating massive object represented by linearized Kerr geometry and then study the charged particle trajectories in that field. It is found that the trapped bound orbits exist both for co- and contra-rotating particles for various combination of the physical parameters.

1.2 Inertial forces in general theory of relativity

For the understanding of an equilibrium configuration and its stability, the role of forces acting on the system is very important. In Newtonian formalism a spherically symmetric fluid distribution attains equilibrium when the gravitational force balances the pressure gradient force (Chandrasekhar 1967),

$$\frac{dp}{dr} = -\frac{GM(r)}{r^2}\rho \tag{1.1}$$

(p is the total pressure, $M(r)$ is the mass enclosed in the shell of radius r and ρ is the density) and a test particle orbiting around a central object remains in a circular orbit when the centrifugal force generated due to its rotation cancels the effect of the gravitational force. In case of general theory of relativity, description of the particle motion and the equilibrium configuration are in the language of curvature of spacetime, which is basically represented in terms of metric component g_{ij} and its derivatives. Particle trajectories are nothing but the geodesic equations given as

$$\frac{d^2x^i}{ds^2} + \Gamma^i_{jk}u^j u^k = 0 \tag{1.2}$$

in that curved spacetime, which expresses the total acceleration in terms of connection coefficients (Γ^i_{jk}) but separate terms do not represent the forces analogous to their Newtonian counterparts. The familiarity of Newtonian approach to understand the dynamics of a system in terms of the forces acting on the system is often simpler and helps to get a clearer picture of the physical process in comparison to the geometrical quantities of general relativity. Abramowicz et al. (1988) (hereafter ACL) have shown that it is possible to introduce the concept of inertial forces within the realm of general theory of relativity. They showed that in a conformally projected 3-space of the 4-dimensional spacetime, the total force can be split in such a way that different terms correspond to centrifugal, gravitational and Coriolis force like in Newtonian mechanics. This specific frame is called optical reference geometry (ORG) as it was found that null-lines of 4-spacetime are geodesics in such a projected 3-space.

Since then many of the dynamical studies are being carried out in optical reference geometry which have not only shown many new or counterintuitive features (Abramowicz & Prasanna 1990 (hereafter AP) ; Prasanna & Chakrabarti 1990; Chakrabarti & Prasanna 1990; Iyer & Prasanna 1993) but have also helped to understand the behaviour of certain other processes which were already found in the earlier studies and were not in the agreement with their Newtonian interpretation (Seguin 1975; Anderson & Lemos 1988; Chandrasekhar & Miller 1974; Miller 1977).

One of the surprising features which had been noticed with this approach was the behaviour of centrifugal force. It was found that a test particle orbiting in a circular orbit at $r \leq 3m$ (m is the mass of the body in geometrized units) around a static and spherically symmetric body experiences the centrifugal force acting towards the center [AP], which was a very unexpected result, as in Newtonian physics it is well established that the centrifugal force on a particle always acts radially outward irrespective of its distance from the central body. They also found that as a consequence of reversal in the direction of centrifugal force, 1. the reversal of Rayleigh criterion for local stability with respect to infinitesimal, axially symmetric, quasi-stationary perturbations, and 2. the inward transport of angular momentum by the viscous torque around a black hole, which was found by Anderson & Lemos (1988) could be explained.

Simultaneously, studies by Prasanna & Chakrabarti (1990), Chakrabarti & Prasanna (1990) were devoted for stationary and axisymmetric case by considering Kerr spacetime in optical reference geometry. They found that the centrifugal force and Coriolis force depend upon the angular momentum of the source and the test particle, and the reversal of sign for these forces occur at several locations. These studies were done by considering the Boyer-Lindquist coordinates which has the restriction of the ergosurface being the static limit surface, and hence the behaviour of these forces could be analyzed only beyond the ergosurface and not from the event horizon onwards as in the Schwarzschild case. This was rectified by Iyer & Prasanna (1993), using the locally non-rotating frame (LNRF) (Bardeen et al. 1972), which is one of the most suitable coordinate frames for discussing the dynamics of rotating configurations in general relativity. It was found that, though the centrifugal force reverses its sign twice below $r = 2m$ which is of no consequence to any outside observer, it also reverses the direction once between $2m \leq r \leq 3m$ i.e. between the ergosurface and the surface of the centrifugal force reversal in the case of a non-rotating body. The shift of location is inwards from $r = 3m$, as the angular momentum of the black hole increases from 0 to m. Stuchlik (1990) studied the Schwarzschild-de Sitter spacetime using ORG and discussed about the circular photon orbits, whereas Vokrouhlicky & Karas (1991), Prasanna (1991),Prasanna & Iyer (1991), Aguirregabiria et al. (1995, 1996a, b) discussed charged particle motion in the presence of electric and magnetic fields adopting this approach. Further, Nayak & Vishveshwara (1996 a, b) studied the inertial forces in various other spacetimes like Kerr Newmann, Reissner-Nordstorm and Ernst using the covariant definition of inertial forces and the generalization of optical reference geometry for stationary and axially symmetric spacetime (Abramowicz et al. 1993, 1995). They also discussed about the connection of centrifugal force and gyroscopic precession with the circular photon orbits.

While the above studies were made to see the dynamical behaviour around a rotating and/or charged black hole, Abramowicz & Miller (1990) explained the change in behaviour of ellipticity of a contracting body using optical reference geometry as found by Chandrasekhar & Miller (1974). While studying the structure of a slowly rotating, contracting body with homogeneous matter distribution in general relativistic framework, Chandrasekhar and Miller found that around $R \approx 2.3R_s$ (where $R_s = 2m$ is the Schwarzschild radius) ellipticity attains a peak instead of monotonic increase in contradiction with the Newtonian physics. They speculated this effect to be one of the consequences of dragging of inertial frame arising due to the rotation of the body. Abramowicz and Miller used the Newtonian force balance equation for a slowly rotating spheroid and by substituting the centrifugal force as obtained in [AP] for static spacetime found the maximum of ellipticity . Since they found the peak of ellipticity without even considering the background geometry of a rotating body it was apparent that this behaviour was not due to dragging of inertial frame and could be explained in terms of the modified form of the centrifugal force. A number of groups (de Felice 1991a, b, 1994; Barrabes et al. 1995) attempted to understand these anomalies with different viewpoints, like analyzing the concepts of local and global outward and inward directions. Sonego & Massar (1996) presented an assessment of the split of these inertial forces and showed that the centrifugal force expression can also be derived by separating the variables in the Hamilton-Jacobi and Klein-Gordon equations.

In our studies we have adopted [AP] approach and have studied the ellipticity and the centrifugal force of a contracting system. Abramowicz and Miller had used the metric representing a non-rotating body while discussing a slowly rotating contracting body, thus missing out the corrections due to rotation. We have considered the Hartle-metric (Hartle 1967; Hartle & Thorne 1968), which represents a rotating body and made the studies for homogeneous distribution (chapter 4) as well as for inhomogeneous matter distribution (chapter 5).

1.3 Equilibrium structure of compact objects

As was mentioned in the beginning of this chapter, the necessity of general theory of relativity in astrophysical studies was realized with the discovery of quasars and x-ray sources. One of the initial steps in this direction needed was to obtain the equilibrium structure of these compact objects, in the framework of general relativity. The solution of Einstien's field equations describe the equilibrium structure of a fluid distribution in terms of the geometry of spacetime as expressed by the metric components and its derivatives.

One of the simplest systems to be solved is, spherically symmetric static fluid distribution. Tolman (1939) obtained a number of exact solutions for such distribution which not only included the then existing solutions: Einstien's cosmological solution, Schwarzchild's exterior and interior solution and de-Sitter solution, but had few new solutions which were relevant in the studies of stellar structure. The field equations were written in such a way that it was somewhat easier to obtain the solution by taking an ansatz for one of the metric potential. At the same time Oppenheimer & Volkoff (1939) studied the equilibrium configuration consisting of neutrons, using the equation of state for a cold Fermi gas and compared their results with suitably chosen special cases of analytical solutions obtained by Tolman. This was the beginning of the studies of stellar structure considering the effects of strong gravitational field. In the subsequent period of time, Tsuruta & Cameron (1967), Tooper (1966), Fowler (1964, 1966) also studied the non-rotating stellar structure described by the static and spherical symmetric distribution. An extensive review on the theory of stellar structure for spherical symmetric static body is given by Thorne (1967).

Around the same time, importance of rotation was also noticed in most of the astrophysical objects. Meltzer & Thorne (1966), Wheeler (1966) discussed the role of rotation in the damping of neutron star's oscillations and the possible source of energy in supernova remnant, whereas Fowler (1966) indicated its importance in connection with the existence of supermassive objects. Objects having higher masses than the non-rotating configuration which can be stable against the gravitational collapse, come in the category of supermassive objects. Due to the stability criterion, it was realized that such strongly gravitating bodies could not remain in equilibrium unless there existed a force to counterbalance the gravity. Rotation of supermassive stars was considered as one of the possible mechanism. It was calculated by Fowler that a non-rotating supermassive star was gravitationally unstable if its mass was greater than $10^6 M_\odot$, whereas, including the effects of rotation in the post Newtonian approximation, the upper mass limit was found to be $10^8 M_\odot$. Thus to understand these objects more accurately, it was required to develop the theory of rotating stellar objects.

A non-rotating body is described by spherically symmetric and static configuration, thus all the quantities are only functions of the coordinate r and there are three independent field equations with four unknowns: pressure p, energy density ρ and two metric components, one of which is connected with mass $m(r)$ (Oppenheimer & Volkoff 1939). Considering an equation of state, this set of ordinary differential equations is either solved analytically or numerically. As the rotation is introduced, the spherical symmetry breaks down and the system acquires an axisymmetry and stationary state, and the quantities no more remain θ - independent, hence the field equations become partial differential and non-linear. Getting the exact solution for such equations is very cumbersome and tedious (Butterworth & Ipser 1976) and not always possible too. In that case, there are two ways to study these rotating objects in the framework of general relativity : approximation method and numerical method.

In the later case, the whole set of field equations can be solved numerically, and a number of works in recent years have adopted this approach (Shapiro & Teukolsky 1985; Friedman et al. 1986; Bonazzola et al. 1993; Eriguchi et al. 1994; Cook et al. 1994 and the references therein), but the numerical calculations require enormous amount of computational power. On the other hand there exists an approximation scheme which was formulated by Hartle (1967) and was used to give models for white dwarfs and neutron stars (Hartle & Thorne 1968). Hartle adopted a perturbation technique (Chapter 2 contains the formalism of this method), in which he considered the rotation of the object to be slow such that it could be considered as the perturbation over a non-rotating body. This approximation is valid for values of angular velocity which are below the Keplerian velocity. Despite its limitations for being an approximate solution, it is an appropriate tool to study the neutron star models. A typical neutron star of mass $M \approx 1 M_{\odot}$ and radius $R \approx 10$ km, has the critical angular velocity as $\Omega_{crit.} \approx 1/10km$ in geometrised units equivalent to $\approx 3 \times 10^4$ cycles per second. Whereas, even the millisecond pulsar with the period as small as 0.001 second corresponds to an angular velocity $\approx 10^3$ cycles per second, which is still an order less than the $\Omega_{crit.}$.

Using Hartle method Datta & Ray (1983) and Ray & Datta (1984), obtained the lower limits on the neutron star's mass and moment of inertia and upper limits on the radius for a stable configuration. Further Datta et al. (1992, 1995a, b) studied the effects of rotation on the eigenfrequencies of radial pulsation, on the disk luminosity and stellar angular momentum and in the studies of crustal density profile for the various neutron star models. Chandrasekhar & Miller (1974) and Miller (1977) studied quasi-stationary semi-adiabatic contraction of slowly rotating bodies considering this formalism for homogeneous and inhomogeneous matter distribution respectively. In recent years Weber & Glendenning (1992), have also used this to check several models represented by various equations of state with the data on pulsar periods and found that the minimum periods achieved by pulsars can be easily calculated by this approximation scheme even after putting the stringent limit on the upper value of the angular frequency. Our studies are basically made using Hartle metric, and numerical integration procedure for various parameters.

1.4 Composition of compact objects

To understand the structure of a compact object, the knowledge about its matter distribution is very much essential. One of the simplest but ideal case is when it is an incompressible fluid distribution. In that case density is constant throughout the configuration. It is useful to study such distribution for getting some general understanding about the objects, but to apply it in the real astrophysical situations, studies of more realistic fluid distributions are required. There have been a large number of studies in this regard starting from the pioneering work by Oppenheimer & Volkoff (1939) to the recently discussed equations of state by Glendenning (1985), Wiringa et al. (1988) etc.

A compact object like neutron star is usually divided into, the following four density regions:

- Near the surface of the star the density is upto 10^6 gm cm^{-3} and the matter distribution is like a lattice of bare nuclei immersed in a gas of relativistic and degenerate electron gas. The equation of state which basically relates the pressure with energy density i.e. $p = p(\rho)$, is influenced by temperature and magnetic fields but does not contribute much to the mass and the radius of the star.

- The next region has the density range 10^6 gm cm$^{-3} \leq \rho \leq 4.3 \times 10^{11}$gm cm^{-3}, where the protons inside the nuclei undergo inverse beta-decay: $e^- + p \rightarrow n + \nu$ (e^-, p, n & ν are electron, proton, neutron and neutrino respectively) providing the neutron rich region.

- The third density region begins at about 4.3×10^{11}gm cm^{-3} and is called the neutron drip point. At such densities, some of the neutrons get detached from the parent nucleus. These neutrons are unbound and stable.

- The fourth region has the density $> 2.8 \times 10^{14}$ gm cm^{-3}, which corresponds to the density regions above the nuclear matter density. Hence, the individual nuclei merge into each other and the resulting effect of such a process is a fluid of neutrons alongwith the other elementary particles protons, electrons and possibly muons, pions, hyperons etc.

The first three regions mentioned above are reasonably well understood. Comprehensive account of the physics of these regions are given by Baym & Pethick (1975, 1979) and Canuto (1974, 1975). These regions form the crust of the star (2.8×10^{14}gm cm^{-3} is the density at the bottom of the crust whereas lower density regions than this represent upper crust and surface) which is a small fraction ($\approx 10\%$) of the total radius of the star. The fourth region which is above the nuclear matter density constitutes the major part of the neutron star interior, hence the main contribution to the mass and the radius of the star comes due to this region. Irvine (1978) and Shapiro & Teukolsky (1983) provide the required background about the structure of neutron stars and the physics of compact objects, respectively. The equations of state corresponding to this density range and above is not yet understood clearly. Though it is well known, that the main constituent at such high density is neutron, the presence of other elementary particles are also not ruled out. Then the main problem in determining equations of state at such high density is regarding the interactions among these particles. Lack of proper many-body techniques to describe these interactions add up further uncertainty about the actual equation of state of these objects. Since systems with such high densities are only available in the astrophysical situations and cannot be studied in the laboratories, reliable experimental information is also not available. Thus, all the calculations involve either extrapolations from known nuclear matter properties or field theoretical approaches.

In our studies, rather than looking into these aspects of the problem, we have selected few of the currently accepted equations of state representing the neutron star matter distribution and have studied the behaviour of ellipticity, centrifugal force and the structure of the magnetic field inside these bodies.

1.5 Plan of thesis

In this thesis we have basically studied the general relativistic effects of rotation and fluid distribution of a compact body on the structure of electromagnetic fields and on its equilibrium configuration. All the studies are carried for a slowly rotating compact body which is represented by the Hartle-Thorne metric. In chapter 2 we have described the formulation of this metric giving the set of equations required to be solved for the equilibrium configuration. Chapter 3 deals with obtaining the electromagnetic fields around the slowly rotating body and the charged particle motion in that field is analyzed. Chapter 4 contains the derivation of 4-force in optical reference geometry and using that the eccentricity is derived for axisymmetric and stationary metric. As a special case, behaviour of centrifugal force and ellipticity is analyzed for a sequence of slowly rotating contracting homogeneous matter distribution. In chapter 5 with the brief discussion of few equations of state, their effects on structure of electromagnetic fields and on centrifugal force and ellipticity are pointed out. We have summarized the results and conclusions of our works in chapter 6.

Chapter 2

Equations of structure for slowly rotating relativistic star: Hartle-metric

2.1 Notation and Signature

In this thesis, we are using +2 signature for the 4-dimensional spacetime. The Latin letters (i, j, k etc.) run from 0 to 3, where 0 represents time-component and $1, 2, 3$ express space-components. The Greek alphabets (α, β etc.) denote space-components only. The components in a local inertial frame are expressed within a parenthesis (). All the quantities are in geometrised units i.e. $G = c = 1$, unless specified otherwise. G is the gravitational constant and c is the speed of light.

2.2 Introduction

An equilibrium fluid distribution in the framework of general relativity is given by Einstein's field equation (Schutz 1985; Misner et al. 1973)

$$R^i{}_j - \frac{1}{2} R\delta^i{}_j = 8\pi T^i_j \tag{2.1}$$

where T^i_j is the energy-momentum tensor describing the distribution of matter and energy whereas $R^i{}_j$ and R are Ricci tensor and its trace, the contracted form of Riemman curvature tensor $R^h_{i\,j\,k}$ and specify the curvature of spacetime. These are functions of the metric component g_{ij} and its first and second derivatives. The line element of such a curved spacetime is

$$ds^2 = g_{ij} dx^i dx^j. \tag{2.2}$$

For a perfect fluid distribution, the energy-momentum tensor is given as

$$T^i_j = (\rho + p) u^i u_j + p\delta^i{}_j \tag{2.3}$$

where ρ is energy density, p is pressure and u^i is the four-velocity of the fluid distribution.

An axisymmetric and stationary metric which represents the spacetime geometry of a rotating body has the most general form :

$$ds^2 = g_{tt}dt^2 + 2g_{t\phi}dtd\phi + g_{\phi\phi}d\phi^2 + g_{rr}dr^2 + g_{\theta\theta}d\theta^2 + g_{r\theta}drd\theta \tag{2.4}$$

where the metric components g_{ij} are functions of r and θ only as ϕ and t are cyclic co-ordinates due to axisymmetry and stationarity of the metric. The components $g_{tr}, g_{t\theta}, g_{\phi r}$ and $g_{\phi\theta}$ vanish due to the geometric symmetries of spacetime which demand the invariance of line element under the inversion of $\phi \to -\phi$ and $t \to -t$. With suitable choice of co-ordinate transformation $r \to f(r)$, $g_{r\theta}$ can be made zero and the metric (2.4) can be rewritten as (Chandrasekhar & Friedman 1972)

$$ds^2 = -e^{2\nu}dt^2 + e^{2\lambda}dr^2 + e^{2\mu}d\theta^2 + e^{2\psi}(d\phi - \omega dt)^2, \tag{2.5}$$

where ν, λ, μ, ψ and ω are functions of r and θ. ω represents the dragging of inertial frame, which appears due to the rotation of the gravitating body. This effect can be noticed by calculating the angular velocity $d\phi/dt$ of a particle falling freely from infinity with its angular momentum $p_\phi = 0$. In this case it is found, that, though the particle's angular momentum remains zero, it acquires angular velocity due to the spacetime geometry surrounding the rotating body as given by

$$\omega = \frac{d\phi}{dt} = \frac{p^\phi}{p^t} = \frac{g^{\phi t}}{g^{tt}} = -\frac{g_{\phi t}}{g_{\phi\phi}} \tag{2.6}$$

When the star is not rotating $g_{t\phi}$ is zero, thus implying no dragging of inertial frames in the absence of rotation. This effect is also known as Lense-Thirring effect (Thirring & Lense 1918). Due to this effect the angular velocity (ϖ) of the fluid observed by a *local* inertial observer situated at a point (r, θ) is $\varpi = \Omega - \omega$, where Ω is the angular velocity of the fluid relative to the distant observer. This fluid velocity ϖ is more important in determining the rotational effects like centrifugal force instead of the angular velocity Ω.

2.3 Hartle-metric

Hartle metric is an approximate metric representing the geometry of spacetime both in the interior and exterior of a slowly rotating star. The rotation is treated to the second order in the angular velocity Ω. The procedure to obtain the metric is as follows:

1. The matter distribution of the rotating star is specified by an equation of state $\rho = \rho(p)$ which gives the relation between the pressure and mass-energy density of the system.

2. The equilibrium configuration for a non-rotating body is obtained. The metric that describes the spherically symmetric geometry of the non-rotating star has the

Schwarzschild form

$$ds^2 = -e^{\nu_0}dt^2 + [1 - 2m/r]^{-1}dr^2 + r^2(d\theta^2 + sin^2\theta d\phi^2), \tag{2.7}$$

and the energy-momentum tensor T^i_j is diag$(-\rho, p, p, p)$. Integrating the Tolman-Oppenheimer-Volkoff equations of hydrostatic equilibrium

$$\frac{dp}{dr} = -(\rho + p)\frac{(m + 4\pi r^3 p)}{r(r - 2m)} \tag{2.8}$$

$$\frac{dm}{dr} = 4\pi r^2 \rho. \tag{2.9}$$

and

$$\frac{d\nu_0}{dr} = -2(\rho + p)^{-1}\frac{dp}{dr} \tag{2.10}$$

from the center $(r = 0)$ to the point where the pressure goes to zero $(r = R)$, one gets the pressure, mass and metric coefficient ν_0 describing the complete structure of the non-rotating body. Initial conditions are $m = 0$ and $p = p_c$, where p_c, the central pressure is obtained for a given central density ρ_c, using the equation of state. ν_0 is matched with Schwarzschild exterior solution at the boundary R having the form

$$(e^{\nu_0})_{r=R} = \left(1 - \frac{2M}{R}\right). \tag{2.11}$$

where, M represents the total mass-energy of the non-rotating body whereas m is the mass inside a shell of radius r in geometrised units when $G = c = 1$.

3. Slow rotation is introduced as the perturbation on the non-rotating body such that the fractional changes in metric coefficients remain small. If the angular velocity $\Omega \ll (M/R^3)^{(1/2)}$, then the slow rotation approximation is valid. This condition also implies that $R\Omega \ll c$, indicating that the particles have non-relativistic velocity.

Metric coefficients for the slowly rotating body are expressed as corrections on the metric components of the non-rotating system and compared with the general form of the axisymmetric stationary metric (equation (2.4)),

$$e^{2\nu} \equiv e^{\nu_0}[1+2h], \tag{2.12}$$

$$e^{2\lambda} \equiv \frac{[1+2m_p/(r-2m)]}{[1-2m/r]}, \tag{2.13}$$

$$e^{2\mu} \equiv r^2[1+2k], \tag{2.14}$$

$$e^{2\psi} \equiv r^2\sin^2\theta[1+2k] \tag{2.15}$$

where, h, m_p, k represent the perturbations expressed in powers of angular velocity Ω. Since the line element should remain invariant under the reversal of direction of rotation, diagonal components of the metric have expansion only in even powers of Ω, whereas $g_{t\phi}$ is expressed in odd powers of angular velocity. In Hartle-metric, corrections are considered upto second order in Ω due to the slow rotation approximation. Hence h, m_p, k are of the order Ω^2 and dragging of inertial frame ω is linear in Ω.

Further, h, m_p, k are expanded in terms of spherical harmonics as

$$a(r,\theta) = \sum_{l=0}^{\infty} a_l(r) P_l(\theta) \tag{2.16}$$

where $P_l(\theta)$ is the Legendre polynomial. As a consequence of slow rotation except $l = 0$ and $l = 2$, all the other terms of the spherical harmonics expansion vanish leaving the form to be

$$h(r,\theta) = h_0(r) + h_2(r)P_2(\theta), \tag{2.17}$$

$$m_p(r,\theta) = m_0(r) + m_2(r)P_2(\theta), \tag{2.18}$$

$$k(r,\theta) = k_0(r) + k_2(r)P_2(\theta). \tag{2.19}$$

$k_0(r) = 0$ is an additional condition obtained by an appropriate co-ordinate transformation of the kind $r \to f(r)$ such that the form of the metric doesn't change. Thus the Hartle metric is expressed as

$$\begin{aligned} ds^2 = {} & [-e^{\nu_0}(1 + 2(h_0 + h_2P_2))]\, dt^2 + \left(1 - \frac{2M}{r}\right)^{-1} \\ & \left[1 + 2\frac{(m_0 + m_2P_2)}{(r - 2M)}\right] dr^2 + r^2 [1 + 2k_2P_2] \\ & \left[d\theta^2 + \sin^2\theta(d\phi - \omega dt)^2\right] + \mathcal{O}\left(\Omega^3\right). \end{aligned} \tag{2.20}$$

The stress-energy tensor for the fluid in the rotating star gets modified as

$$T^i_j = (\rho + \Delta\rho + p + \Delta p)u^i u_j + (p + \Delta p)\delta^i{}_j, \tag{2.21}$$

where

$$\Delta p = (\rho + p)[p_0^* + p_2^* P_2(\theta)] \tag{2.22}$$

$$\Delta \rho = (\rho + p)\frac{d\rho}{dp}[p_0^* + p_2^* P_2(\theta)] \tag{2.23}$$

are the changes in pressure and density in the interior of the star at a given (r, θ) **in a reference frame that is momentarily moving with the fluid.** p_0^* **and** p_2^* **are** dimensionless functions of r proportional to Ω^2, describing the pressure perturbation. The components of four velocity are

$$u^t = (-g_{tt} - 2\Omega g_{t\phi} - g_{\phi\phi}\Omega^2)^{-1/2} \tag{2.24}$$

$$= e^{-\nu_0/2}[1 + \frac{1}{2}r^2 sin^2\theta\varpi^2 e^{-\nu} - h_0 - h_2 P_2], \tag{2.25}$$

$$u^\phi = \Omega u^t, \quad u^r = u^\theta = 0. \tag{2.26}$$

4. Using the above mentioned equations and keeping the terms upto second order in angular velocity in Einstien field equations and hydrodynamical equation of rotating fluid configuration, the functions $\varpi, h_0, m_0, p_0^*, h_2, m_2, k_2$ andp_2^* are calculated. The required set of equations are given in the following subsection.

2.3.1 Evaluation of rotational perturbations

(a) Dragging of inertial frame:

The angular velocity of fluid (ϖ), relative to the local inertial frame is found by integrating the differential equation

$$\frac{1}{r^4}\frac{d}{dr}\left(r^4 j \frac{d\overline{\omega}}{dr}\right) + \frac{4}{r}\frac{dj}{dr}\overline{\omega} = 0, \tag{2.27}$$

from the center ($r = 0$) to the boundary ($r = R$) with the initial conditions $\overline{\omega}_{r=0} = \overline{\omega}_c$ and $(d\overline{\omega}/dr)_{r=0} = 0$, where

$$j = e^{-\nu_0/2}[1 - 2m/r]^{1/2}. \tag{2.28}$$

Outside the star ($r \geq R$), the dragging of the inertial frame is $2J/r^3$, hence

$$\overline{\omega} = \Omega - 2J/r^3. \tag{2.29}$$

where, J is the angular momentum of the star. To integrate equation (2.27) the value of $\overline{\omega}_c$ is chosen arbitrarily and correspondingly the angular momentum J and angular velocity Ω are determined from

$$J = \frac{1}{6}R^4\left(\frac{d\overline{\omega}}{dr}\right)_{r=R} \tag{2.30}$$

and

$$\Omega = \overline{\omega}(R) + \frac{2J}{R^3}. \tag{2.31}$$

If a different value of Ω is desired then the function ϖ can be rescaled as

$$\varpi_{new} = \varpi_{old}(\Omega_{new}/\Omega_{old}) \tag{2.32}$$

and the rescaled angular momentum is calculated from the relation

$$J = I\Omega \tag{2.33}$$

where I is the moment of inertia of the star which depends only on the ratio of angular momentum and angular velocity.

(b) The spherical deformation of the star:

The spherical part of the rotational deformation is obtained by integrating the set of equations corresponding to $l = 0$. The differential equations are in m_0 and p_0^*. h_0 is calculated using an algebraic relation obtained from the hydrodynamic equation, and expressed as

$$h_0 = -p_0^* + \frac{1}{3}r^2 e^{-\nu_0}\varpi^2 + h_{0c}. \tag{2.34}$$

With the initial conditions as $m_0 = p_0^* = 0$, the equations

$$\frac{dm_0}{dr} = 4\pi r^2 \frac{d\rho}{dp}(\rho + p)p_0^* + \frac{1}{12}j^2 r^4 \left(\frac{d\varpi}{dr}\right)^2 - \frac{1}{3}r^3 \frac{dj^2}{dr}\varpi^2, \tag{2.35}$$

$$\frac{dp_0^*}{dr} = -\frac{m_0(1+8\pi r^2 p)}{(r-2m)^2} - \frac{4\pi(\rho+p)r^2}{(r-2m)} p_0^* + \frac{1}{12}\frac{r^4 j^2}{(r-2m)}\left(\frac{d\varpi}{dr}i\right)^2$$

$$+ \frac{1}{3}\frac{d}{dr}\left(\frac{r^3 j^2 \varpi^2}{r-2m}\right), \quad (2.36)$$

are integrated from the center to the surface of the star. These initial conditions enforce the central density of the rotating star to be equal to the density of the non-rotating star at the center. Outside the star, m_0 and h_0, have the form

$$m_0 = \delta M - J^2/r^3, \quad (2.37)$$

$$h_0 = -\frac{\delta M}{r-2m} + \frac{j^2}{r^3(r-2m)}, \quad (2.38)$$

where δM is a constant representing the change in the total mass-energy of the rotating system as $M + \delta M$.

(c) The quadrupole deformations of the rotating star:

The quadrupole deformations due to rotation, are calculated from the equations for $l = 2$, as given by

$$\frac{dv_2}{dr} = -\frac{d\nu_0}{dr}h_2 + \left(\frac{1}{r} + \frac{1}{2}\frac{d\nu_0}{dr}\right)\left[-\frac{1}{3}r^3\frac{dj^2}{dr}\varpi^2 + \frac{1}{6}j^2 r^4\left(\frac{d\varpi}{dr}\right)^2\right], \quad (2.39)$$

$$\frac{dh_2}{dr} = \left[-\frac{d\nu_0}{dr} + \frac{r}{r-2m}\left(\frac{d\nu_0}{dr}\right)^{-1}\left(8\pi(\rho+p) - \frac{4m}{r^3}\right)\right]h_2$$

$$- \frac{4v_2}{r(r-2m)}\left(\frac{d\nu_0}{dr}\right)^{-1} + \frac{1}{6}\left[\frac{1}{2}\frac{d\nu_0}{dr}r - \frac{1}{r-2m}\left(\frac{d\nu_0}{dr}\right)^{-1}\right]r^3 j^2\left(\frac{d\varpi}{dr}\right)^2$$

$$- \frac{1}{3}\left[\frac{1}{2}\frac{d\nu_0}{dr}r + \frac{1}{r-2m}\left(\frac{d\nu_0}{dr}\right)^{-1}\right] r^2 \frac{dj^2}{dr}\overline{\omega}^2, \tag{2.40}$$

where $v_2 = h_2 + k_2$.

Outside the star h_2 and v_2 have the analytic form, obtained as a sum of complementary solution and a particular solution given by,

$$h_2 = J^2\left(\frac{1}{Mr^3} + \frac{1}{r^4}\right) + KQ_2^2\left(\frac{r}{M} - 1\right), \tag{2.41}$$

$$v_2 = -\frac{J^2}{r^4} + K\frac{2M}{[r(r-2M)]^{1/2}}Q_2^1\left(\frac{r}{M} - 1\right). \tag{2.42}$$

where, K is a constant and Q_n^m is the Legendre polynomial of the second kind,

$$Q_2^2(\xi) = \frac{3}{2}(\xi^2 - 1)\log\left(\frac{\xi+1}{\xi-1}\right) - \frac{3\xi^3 - 5\xi}{\xi^2 - 1}, \tag{2.43}$$

$$Q_2^1(\xi) = (\xi^2 - 1)^{1/2}\left[\frac{3\xi^2 - 2}{\xi^2 - 1} - \frac{3}{2}\xi\log\left(\frac{\xi+1}{\xi-1}\right)\right], \tag{2.44}$$

where $\xi = r/M - 1$.

Inside the star the general solution is expressed as

$$h_2 = Ah_2^H + h_2^P, \qquad v_2 = Av_2^H + v_2^P \tag{2.45}$$

where, superscript H denotes the homogeneous solution and P, the particular solution. A is a constant which is calculated alongwith K by matching the interior solution to the exterior solution at the surface of the star. The particular solution is found by integrating equation (2.39) (2.40) from the center with initial conditions as

$$v_2 \rightarrow 2\pi\left[\frac{1}{3}(\rho_c + p_c)(j_c\overline{\omega}_c)^2 - (\frac{1}{3}\rho_c + p_c)\right] r^4, \tag{2.46}$$

$$h_2 \rightarrow r^2 \tag{2.47}$$

The homogeneous solution is obtained by integrating equations

$$\frac{dv_2}{dr} = -\frac{d\nu_0}{dr}h_2, \tag{2.48}$$

$$\frac{dh_2}{dr} = \left[-\frac{d\nu_0}{dr} + \frac{r}{r-2m}\left(\frac{d\nu_0}{dr}\right)^{-1}\left(8\pi(\rho + p) - \frac{4m}{r^3}\right)\right] h_2$$

$$- \frac{4v_2}{r(r-2m)}\left(\frac{d\nu_0}{dr}\right)^{-1} \tag{2.49}$$

when

$$v_2 \rightarrow 2\pi\left(\frac{1}{3}\rho_c + p_c\right) r^4, \tag{2.50}$$

$$h_2 \rightarrow r^2 \tag{2.51}$$

at the center. Using the values of h_2 and v_2, non-radial perturbation factors m_2 and p_2^* are determined from the algebraic relations

$$m_2 = (r - 2m)\left[-h_2 - \frac{1}{3}r^3\left(\frac{dj^2}{dr}\right)\overline{\omega}^2 + \frac{1}{6}r^4 j^2\left(\frac{d\overline{\omega}}{dr}\right)^2\right], \tag{2.52}$$

$$p_2^* = -h_2 - \frac{1}{3}r^2 e^{-\nu}\overline{\omega}^2. \tag{2.53}$$

Thus all the quantities describing the perturbation of the metric are calculated. Deviation from spherical configuration is clearly understood by studying the displacement of constant density surfaces. Due to rotation these spherical surfaces change to spheroidal ones whose radius is given by

$$r + \xi_0(r) + \xi_2(r)P_2(\theta), \tag{2.54}$$

where

$$\xi_0 = -p_0^*(\rho + p)/(dp/dr), \quad \xi_2 = -p_2^*(\rho + p)/(dp/dr) \tag{2.55}$$

are corrections of order Ω^2.

These constant density surfaces are in a particular co-ordinate system. An invariant parametrisation of these surfaces can be obtained by embedding them in a three-dimensional flat spacetime such that the intrinsic geometry of these surfaces is similar to the constant density surface of the rotating system. Thus the obtained spheroid in 3-dimensional flat space has the radius

$$r + \xi_0(r) + (\xi_2(r) + r[v_2(r) - h_2(r)])\, P_2(\theta), \tag{2.56}$$

and the eccentricity

$$\begin{aligned} e &= [1 - r^2_{(pole)}/r^2_{(equator)}]^{1/2} && (2.57) \\ &= [-3(\frac{\xi_2}{r} + v_2 - h_2)]^{1/2}. && (2.58) \end{aligned}$$

Further the change in the binding energy and star's quadrupole moment can be also derived using the above set of equations, but we have only given those equations which are required in our studies. The details and derivation of these equations are given in the original paper by Hartle (1967) and are summarized in Hartle & Thorne (1968). Thorne (1971), Chandrasekhar & Miller (1974) and Demianski (1985) also discuss these sets of equations with slight variations.

2.4 Numerical procedure

The above sets of differential equations are solved numerically using the Runge-Kutta-Verner fifth-order and sixth-order method. The subroutine 'divprk' of IMSL package is used for this purpose, which is based on a code designed by Hull et al. (1976). As main inputs, the number of differential equations (N), independent variable (t) and a subroutine to calculate the derivative of dependent variable 'y' at value 't' are supplied. By providing a value for tolerance, the subroutine controls the norm of the local error such that the global error is proportional to the given value of tolerance. In our programs we set error norms as the absolute error and with the appropriate choice of step size run the program. To evaluate any function at the intermediate values of any given data set, we use the Akima cubic spline interpolation scheme with the help of IMSL subroutine 'dcsakm'. This routine is based on a method by Akima (1970) to combat wiggles in the interpolant.

To test our program, we have reproduced the results obtained by Hartle & Thorne (1968) using the Harrison and Wheeler equation of state (see Harrison et al. 1965, chapter 8). We also checked our result with Chandrasekhar & Miller (1974) for homogeneous slowly rotating contracting body.

Chapter 3

Structure of External Electromagnetic Field around a Slowly Rotating Compact Object and Charged Particle Trajectories Therein

3.1 Introduction

The structure of the electromagnetic field - the flux and the topology of electric and magnetic fields outside a rotating compact object plays a very important role in the understanding of the radiation emission from astrophysical objects like pulsars and quasars. With the discovery of pulsars, the very first model proposed (known in literature as the aligned rotator as given by Goldreich & Julian (1969)) adopted the geometry of a dipole magnetic field and an induced electric field alongwith a co-rotating magnetosphere for accelerating the charges pulled out from within the neutron star surface and producing the emission. Since then there have been several discussions on the structure of the magnetosphere of compact objects (for a review see Michel 1982) including that of black holes (Thorne 1983). Subsequently, though there have been critics of these models (Punsley & Coroniti 1990) no completely understood picture of the magnetosphere of compact objects has emerged yet. More recently there has been a renewed interest, wherein modelists have tried to bring in the general relativistic effects with the hope that it could contribute some more understanding into the structure (Gonthier & Harding 1994; Sengupta 1995). However, these authors continue to use the electromagnetic field structure in curved spacetime as given by that for a static geometry without considering the possible effects that rotation might bring in.

It is indeed important to use the appropriate metric, like the one given by Hartle & Thorne (1968) for the exterior gravitational field of a slowly rotating star and then look at the structure of the magnetic and electric fields in this geometry.In the following, we have presented a part of the possible solution restricting ourselves to look for the solution for the electric field arising out of rotation, while the magnetic field is assumed as given by Ginzburg & Ozernoi (1965).Though a fully appropriate treatment should use all the effects of rotation in the gravitational potentials, we as a first approximation consider only the effects of linear term in rotation which effectively gives a minimal extension of the Schwarzschild field that includes the effect of 'frame dragging' upto linear order in the rotation parameter.Writing Maxwell's equations in this geometry and assuming an ansatz for the electric field and the charge density one can solve for both the fields,with the magnetic field solution being as given earlier. While we appreciate fully the limitations of the so obtained solution,our main aim is to look for the structure of possible trajectories for charged particles in a geometry wherein some linear effects of frame dragging has been incorporated.There is always the doubt that what changes could occur if in addition one considers the radiation reaction terms in the discussion of trajectories. However, as the orbits obtained are for the case of conserved energy and angular momentum of the particles, it is implicitly assumed that the particle if radiating, gets supplied with energy and angular momentum from the background fields and thus could keep their trajectories (Prasanna 1984).The discussion of the trajectories even for this restricted geometry,would give some idea of the magnetosphere of compact objects with magnetic fields.

3.2 Formalism

3.2.1 Maxwell's equations in curved spacetime

In the curved spacetime, which is represented by the line element

$$ds^2 = g_{ij}dx^i dx^j \tag{3.1}$$

in a coordinate frame (x^i), the Maxwell's equations have the form

$$F^{ij}_{\ ;j} = j^i, \quad F_{(ij,k)} = 0, \tag{3.2}$$

First of the equations can be rewritten as

$$\frac{1}{\sqrt{-g}}(\sqrt{-g}F^{ij})_{,j} = j^i. \tag{3.3}$$

where F^{ij} is the electromagnetic field tensor, j^i is the current 4-vector and g is the determinant of g_{ij}.

Electric and magnetic fields are defined as

$$E_\alpha = F_{(0)\ (\alpha)}, \quad B_\alpha = \epsilon_{\alpha\,\beta\,\gamma} F_{(\beta)\ (\gamma)}, \tag{3.4}$$

where $F_{(a)\ (b)}$ is the field tensor in local Lorentz frame and is connected to components in the co-ordinate frame through the tetrad $\lambda^{\ i}_{(a)}$:

$$F_{(a)\ (b)} = \lambda^{\ i}_{(a)} \lambda^{\ j}_{(b)} F_{i\ j} \tag{3.5}$$

For the metric of an axisymmetric and stationary spacetime as expressed in equation (2.5), with the tetrad

$$\lambda^{(a)}_i = \begin{bmatrix} e^\nu & 0 & 0 & 0 \\ 0 & e^\lambda & 0 & 0 \\ 0 & 0 & e^\mu & 0 \\ -\omega e^\psi & 0 & 0 & e^\psi \end{bmatrix} \tag{3.6}$$

the components of field tensor have the form

$$
\begin{aligned}
F_{\phi r} &= e^{\psi+\lambda} F_{(\phi)\,(r)} &&= e^{\psi+\lambda} B_\theta \\
F_{\phi\theta} &= -e^{\psi+\mu} F_{(\phi)\,(\theta)} &&= -e^{\psi+\mu} B_r \\
F_{r\theta} &= e^{\nu+\lambda} F_{(r)\,(\theta)} &&= e^{\nu+\lambda} B_\phi \\
F_{t\phi} &= e^{\nu+\psi} F_{(t)\,(\phi)} &&= e^{\nu+\psi} E_\phi \\
F_{tr} &= e^{\nu+\lambda} F_{(t)\,(r)} - \omega e^{\psi+\lambda} F_{(\phi)\,(r)} &&= e^{\nu+\lambda} E_r - \omega e^{\psi+\lambda} B_\theta \\
F_{t\theta} &= e^{\nu+\mu} F_{(t)\,(\theta)} + \omega e^{\psi+\mu} F_{(\phi)\,(\theta)} &&= e^{\nu+\mu} E_\theta + \omega e^{\psi+\mu} B_r .
\end{aligned}
\tag{3.7}
$$

Contravariant components (F^{ij}) are obtained, using

$$F^{ij} = g^{il} g^{jm} F_{lm} \tag{3.8}$$

If electromagnetic field is assumed to be axisymmetric and stationary then the electric and magnetic fields will be independent of ϕ and t, hence from equations $F_{(rt,\phi)} = 0$ and $F_{(\theta t,\phi)} = 0$, it is clear that the azimuthal component of electric field E_ϕ is zero. Further, assuming the fields to be poloidal in nature, the Maxwell equations (3.2 and 3.3) on an axisymmetric and stationary spacetime (equation 2.5), take the form as

$$
\begin{aligned}
\frac{\partial}{\partial r}\left[e^{(\psi+\mu)} E_r\right] + \frac{\partial}{\partial \theta}\left[e^{(\psi+\lambda)} E_\theta\right] &= e^{\nu+\psi+\lambda+\mu} j^t \\
\frac{\partial}{\partial r}\left[e^{(\nu+\mu)} B_\theta\right] - \frac{\partial}{\partial \theta}\left[e^{(\nu+\lambda)} B_r\right] - \frac{\partial \omega}{\partial r} e^{\psi+\mu} E_r - \frac{\partial \omega}{\partial \theta} e^{\psi+\lambda} E_\theta &= e^{\nu+\psi+\lambda+\mu} j^\phi \\
-\frac{\partial}{\partial r}\left[e^{(\nu+\mu)} E_\theta\right] + \frac{\partial}{\partial \theta}\left[e^{(\nu+\lambda)} E_r\right] - \frac{\partial \omega}{\partial r} e^{\psi+\mu} B_r - \frac{\partial \omega}{\partial \theta} e^{\psi+\lambda} B_\theta &= 0 \\
\frac{\partial}{\partial r}\left[e^{(\psi+\mu)} B_r\right] + \frac{\partial}{\partial \theta}\left[e^{(\psi+\lambda)} B_\theta\right] &= 0
\end{aligned}
\tag{3.9}
$$

3.2.2 Equations of motion in axisymmetric and stationary field

In general relativity, the trajectories of a charged particle of charge e, expressed in the units of its rest mass m_e in an electromagnetic field are given by the covariant Lorentz equations

$$u^i{}_{;j} u^j = e F^i_j u^j, \tag{3.10}$$

where u^i is the 4-velocity.

Since in an axisymmetric and stationary electromagnetic field the quantities are independent of the time co-ordinate t and the azimuthal co-ordinate ϕ, using the Lagrangian formalism two constants of motion associated with the energy E and the specific angular momentum ℓ, are obtained as

$$\frac{\partial \mathcal{L}}{\partial \dot{t}} = -E, \tag{3.11}$$

$$\frac{\partial \mathcal{L}}{\partial \dot{\phi}} = \ell \tag{3.12}$$

where

$$\mathcal{L} = \frac{1}{2} g_{ij} \dot{x}^i \dot{x}^j + e A_i \dot{x}^i, \tag{3.13}$$

is the Lagrangian of motion and A_i is the electromagnetic potential related to field tensor as $F_{ij} = A_{j,i} - A_{i,j}$. In the background geometry specified by the metric (2.4), equations (3.11) and (3.12) are written as

$$g_{tt}u^t + g_{t\phi}u^\phi = -(E + eA_t) \tag{3.14}$$

$$g_{\phi t}u^t + g_{\phi\phi}u^\phi = \ell - eA_\phi, \tag{3.15}$$

which on simplification give two first integrals of motion

$$u^t = -\left[g_{\phi\phi}\left(E + eA_t\right) + g_{t\phi}\left(\ell - eA_\phi\right)\right] / \left(g_{\phi\phi}g_{tt} - g_{t\phi}^2\right) \tag{3.16}$$

$$u^\phi = \left[g_{t\phi}\left(E + eA_t\right) + g_{tt}\left(\ell - eA_\phi\right)\right] / \left(g_{\phi\phi}g_{tt} - g_{t\phi}^2\right) \tag{3.17}$$

3.2.3 Effective potential

Apart from the first integrals of motion obtained above, the metric itself provides one more first integral through the normalization condition

$$g_{ij}u^iu^j = -1 \tag{3.18}$$

which gives the equation for radial velocity u^r for the particle orbiting in the equatorial plane $\theta = \pi/2$ and $u^\theta = 0$ by substituting equations (3.16) and (3.17) in equation (3.18) as

$$\begin{aligned}(u^r)^2 &= \frac{-1}{g_{rr}(g_{\phi\phi}g_{tt} - g_{t\phi}^2)}[(g_{\phi\phi}g_{tt} - g_{t\phi}^2) + g_{tt}(\ell - eA_\phi)^2 + g_{\phi\phi}(E + eA_t)^2 \\ &+ 2g_{t\phi}(E + eA_t)(\ell - eA_\phi)]\end{aligned} \tag{3.19}$$

If the radial component of the velocity is zero at a point, it corresponds to the turning point for the particle in its orbit. At those points where $u^r = 0$, the particle is in equilibrium under the interacting gravitational, electromagnetic and centrifugal forces and hence has the minimum energy. The energy corresponding to the state where $u^r = 0$ is denoted as the effective potential energy (V_{eff})for the particle in its r-motion. Studying the structure of V_{eff} provides the insight to the boundedness and stability of the particle orbits. This approach to analyze the particle trajectories has been adopted in many earlier works (de Felice (1968), Wilkins (1972) used it in connection with the studies of geodesics, whereas Prasanna & Varma (1977), Prasanna & Vishveshwara,Chakraborty & Prasanna (1982) and others have used this approach to study the charged particle trajectories in electromagnetic fields on Schwarzschild, Kerr and Ernst spacetime).

Substituting $u^r = 0$ in equation (3.19), one gets

$$\begin{aligned} V_{eff} \equiv E_{\pm} &= -eA_t - (g_{t\phi}/g_{\phi\phi}(\ell - eA_\phi) \pm (1/g_{\phi\phi}) \\ &\quad ((g_{\phi\phi}g_{tt} - g_{t\phi}^2)[g_{\phi\phi} + (\ell - eA_\phi)^2])^{1/2}. \end{aligned} \tag{3.20}$$

3.3 Field Structure

In the above section the general form of Maxwell's equations and equations of motion are given. As it is apparent from looking at the form of the Maxwell equations (3.9), finding analytical solution for such equations is a tedious task. For simplicity, we have made certain assumptions which make their derivation simpler yet gives insight about the importance of general relativistic effects of rotation.

As an exercise, we consider the case with the spacetime metric

$$ds^2 = -\left(1 - \frac{2M}{r}\right) dt^2 + \left(1 - \frac{2M}{r}\right)^{-1} dr^2 + r^2 d\theta^2 + r^2 \sin^2\theta (d\phi - \omega dt)^2 \quad (3.21)$$

with $\omega = 2J/r^3$,

representing the linearized Kerr metric which is equivalent to an approximated form of the Hartle metric including the corrections due to rotation only upto first order in Ω. As it can be noticed, except for the $g_{t\phi}$ component, other metric coefficients are same as the Schwarzschild exterior solution. Further, by calculating the Ricci tensor it is found that, this represents the vacuum solution upto the first order in Ω.

The components of connection Γ^i_{jk} and curvature R^h_{ijk} are given as

$$
\begin{array}{rclrcl}
\Gamma^\theta_{\phi t} & = & \frac{2J}{r^3}\sin\theta\cos\theta, & \Gamma^r_{\phi t} & = & -\frac{J}{r^2}\left(1-\frac{2M}{r}\right)\sin^2\theta, \\
\Gamma^t_{r\phi} & = & -\frac{3J}{r^2}\left(1-\frac{2M}{r}\right)^{-1}\sin^2\theta, & \Gamma^\theta_{tt} & = & -\frac{4J^2}{r^6}\sin\theta\cos\theta, \\
\Gamma^r_{\theta\theta} & = & \Gamma^r_{\phi\phi}/\sin^2\theta \ = \ (-r+2M), & \Gamma^r_{rr} & = & -\frac{M}{r^2}\left(1-\frac{2M}{r}\right)^{-1}, \\
\Gamma^\phi_{r\phi} & = & \frac{1}{r}-\frac{6J^2}{r^5}\left(1-\frac{2M}{r}\right)^{-1}\sin^2\theta, & \Gamma^\theta_{\phi\phi} & = & -\sin\theta\cos\theta, \\
\Gamma^t_{rt} & = & \left(1-\frac{2M}{r}\right)^{-1}\left(\frac{M}{r^2}+\frac{6J^2}{r^5}\sin^2\theta\right), & \Gamma^\phi_{\theta t} & = & -\frac{2J}{r^3}\cot\theta, \\
\Gamma^\phi_{rt} & = & \frac{J}{r^4}\left(1-\frac{2M}{r}\right)^{-1}\left(1+\frac{12J^2}{r^4}\sin^2\theta\right), & \Gamma^\phi_{\theta\phi} & = & \cot\theta, \\
\Gamma^r_{tt} & = & \frac{M}{r^2}\left(1-\frac{2M}{r}\right)+\frac{8J^2}{r^5}\left(1-\frac{2M}{r}\right)\sin^2\theta, & \Gamma^\theta_{r\theta} & = & \frac{1}{r}.
\end{array}
\qquad (3.22)
$$

and

$$
\begin{array}{rclrcl}
R^r_{\theta r\theta} & = & -\frac{M}{r}, & R^r_{\phi tr} & = & -\frac{J\sin^2\theta}{r^3}\left[3-\frac{4M}{r}+\frac{18J^2}{r^4}\sin^2\theta\right], \\
R^\theta_{\phi\theta\phi} & = & \frac{2M}{r}\sin^2\theta, & R^t_{rtr} & = & \left(1-\frac{2M}{r}\right)^{-1}\left[\frac{2M}{r^3}+\frac{21J^2}{r^6}\sin^2\theta\right], \\
R^t_{\theta\theta\phi} & = & -\frac{3J}{r}\sin^2\theta, & R^t_{rt\theta} & = & -\frac{12J^2}{r^5}\left(1-\frac{2M}{r}\right)^{-1}\sin\theta\cos\theta, \\
R^\theta_{\phi tr} & = & \frac{6J}{r^4}\sin\theta\cos\theta, & R^t_{\theta tr} & = & -\frac{6J^2}{r^5}\left(1-\frac{2M}{r}\right)^{-1}\sin\theta\cos\theta, \\
R^\theta_{\phi t\theta} & = & \frac{3J}{r^3}\left(1-\frac{2M}{3r}\right)\sin^2\theta, & R^t_{\theta r\phi} & = & -\frac{3J}{r^2}\left(1-\frac{2M}{r}\right)^{-1}\sin\theta\cos\theta, \\
R^t_{\theta t\theta} & = & -\left(\frac{M}{r}+\frac{6J^2}{r^4}\sin^2\theta\right), & R^t_{r\theta\phi} & = & -\frac{6J}{r^2}\left(1-\frac{2M}{r}\right)^{-1}\sin\theta\cos\theta, \\
R^t_{rr\phi} & = & \frac{3J}{r^3}\left(1-\frac{2M}{r}\right)^{-1}\sin^2\theta, & R^t_{\phi r\theta} & = & \frac{3J}{r^2}\left(1-\frac{2M}{r}\right)^{-1}\sin\theta\cos\theta, \\
R^t_{\phi t\phi} & = & -\left(\frac{M}{r}+\frac{9J^2}{r^4}\sin^2\theta\right)\sin^2\theta, & R^r_{\theta t\phi} & = & -\frac{3J}{r^2}\left(1-\frac{2M}{r}\right)\sin\theta\cos\theta, \\
R^r_{\phi r\phi} & = & -\left(\frac{M}{r}+\frac{9J^2}{r^4}\sin^2\theta\right)\sin^2\theta, & R^r_{\phi t\theta} & = & \frac{3J}{r^2}\left(1-\frac{2M}{r}\right)\sin\theta\cos\theta.
\end{array}
\qquad (3.23)
$$

The tetrad has the form for metric (3.21), as

$$\lambda_i^{(a)} = \begin{bmatrix} \left(1-\frac{2M}{r}\right)^{1/2} & 0 & 0 & 0 \\ 0 & \left(1-\frac{2M}{r}\right)^{-1/2} & 0 & 0 \\ 0 & 0 & r & 0 \\ -\omega r \sin\theta & 0 & 0 & r\sin\theta \end{bmatrix} \tag{3.24}$$

Assuming the electromagnetic field to be poloidal in character with non-zero charge density j^t, the Maxwell's equations take the form as

$$\frac{\partial}{\partial r}\left[r^2 B_r\right] + \frac{1}{\sin\theta}\frac{\partial}{\partial\theta}\left[r\left(1-\frac{2M}{r}\right)^{-1/2}\sin\theta B_\theta\right] = 0 \tag{3.25}$$

$$\frac{\partial}{\partial r}\left[r\left(1-\frac{2M}{r}\right)^{1/2} E_\theta\right] - \frac{\partial E_r}{\partial\theta} = -\frac{d\omega}{dr} r^2 \sin\theta B_r \tag{3.26}$$

$$\frac{\partial}{\partial r}\left[r^2 E_r\right] + \frac{1}{\sin\theta}\frac{\partial}{\partial\theta}\left[r\left(1-\frac{2M}{r}\right)^{-1/2}\sin\theta E_\theta\right] = -r^2 j^t \tag{3.27}$$

$$\frac{\partial}{\partial r}\left[r\left(1-\frac{2M}{r}\right)^{1/2} B_\theta\right] - \frac{\partial B_r}{\partial\theta} = \frac{d\omega}{dr} r^2 \sin\theta E_r - \omega r^2 \sin\theta j^t \tag{3.28}$$

If there was to be no rotation ($\omega = 0$) then the electric field E would not be present and the equations (3.26) and (3.28) are of the same form as in the case of a static non-rotating body ,solved by Ginzburg & Ozernoi (1965) for a poloidal magnetic field on the Schwarzschild background; the solution for which is given explicitly in the form (Prasanna & Varma 1977)

$$B_r = -\frac{3\mu\cos\theta}{4M^3}\left\{ln\left(1-\frac{2M}{r}\right) + \frac{2M}{r}\left(1+\frac{M}{r}\right)\right\} \tag{3.29}$$

$$B_\theta = \frac{3\mu\sin\theta}{4M^2 r}\left\{\left(1-\frac{2M}{r}\right)^{-1}+\frac{r}{M}ln\left(1-\frac{2M}{r}\right)+1\right\}\left(1-\frac{2M}{r}\right)^{1/2} \tag{3.30}$$

where μ is the asymptotic dipole moment as defined through the field structure of infinity

$$B_r \approx \frac{2\mu}{r^3}\cos\theta \tag{3.31}$$

$$B_\theta \approx \frac{\mu}{r^3}\sin\theta \tag{3.32}$$

Regarding the electric field, instead of assuming it to be simply an induced field (as is familiarly considered), we shall take an ansatz and solve the equations, keeping the magnetic field components in the same format as above. As a consequence of this we find that the charge density is a linear function of radial component of electric field given as

$$j^t = \frac{1}{\omega}\frac{d\,\omega}{dr}E_r \tag{3.33}$$

With this, using

$$E_r = 2\, f_1(r)P_2(\cos\theta), \text{ and } E_\theta = g_1(r)\sin 2\theta \tag{3.34}$$

and B_r, B_θ as given by equation (3.29) and (3.30) in the set of equations (3.25) to (3.28), one finds that f_1 and g_1 have to satisfy the set of ordinary differential equations:

$$\frac{d}{dr}\left(\frac{f_1}{r}\right)+\frac{2g_1}{r^2}\left(1-\frac{2M}{r}\right)^{-1/2}=0 \tag{3.35}$$

$$\frac{d}{dr}\left[r\left(1-\frac{2M}{r}\right)^{1/2} g_1\right]+3f_1=-\frac{9J}{4M^3r^2}\left\{ln\left(1-\frac{2M}{r}\right)+\frac{2M}{r}\left(1+\frac{M}{r}\right)\right\} \tag{3.36}$$

Instead of looking for an exact solution of this set we shall restrict ourselves to finding a solution of the linear order in J and $\frac{M}{r}$ as given by

$$f_1=-\frac{2J\mu}{3r^5}\left(1+\frac{3M}{r}\right),\ g_1=-\frac{2J\mu}{r^5}\left(1+\frac{5M}{2r}\right) \tag{3.37}$$

With these one has an exact dipole magnetic field and an approximate quadrupole electric field to linear order in ω as given by

$$\begin{aligned} B_r &= -\frac{3\mu\cos\theta}{4M^3}\left\{ln\left(1-\frac{2M}{r}\right)+\frac{2M}{r}\left(1+\frac{M}{r}\right)\right\} \\ B_\theta &= \frac{3\mu\sin\theta}{4M^2r}\left\{\left(1-\frac{2M}{r}\right)^{-1}+\frac{r}{M}ln\left(1-\frac{2M}{r}\right)+1\right\}\left(1-\frac{2M}{r}\right)^{1/2} \\ E_r &= -\frac{2\omega\mu}{3r^2}P_2(\cos\theta)\left(1+\frac{3M}{r}\right) \\ E_\theta &= -\frac{\omega\mu}{r^2}\sin 2\theta\left(1+\frac{5M}{2r}\right) \end{aligned} \tag{3.38}$$

and the charge density

$$j^t = \frac{2\omega\mu}{r^3}P_2\left(\cos\theta\right)\left(1+\frac{3M}{r}\right) \tag{3.39}$$

which brings out the effect of 'frame dragging' on the magnetic fields, inducing electric field and an effective charge density.

3.4 Charged Particle Trajectories

Though we have the exact solution of the magnetic field, we have studied the particle trajectories keeping the contributions upto first order in M/r and ω. Hence, the electromagnetic four-potential A_i has the form

$$A_\phi = -\frac{3\mu\sin^2\theta}{8M^3}\left\{r^2\, ln\left(1-\frac{2M}{r}\right)+2Mr\left(1+\frac{M}{r}\right)\right\} \tag{3.40}$$

$$A_t = -\frac{J\mu}{3r^4}\left(1+\frac{12M}{5r}\right) \tag{3.41}$$

which is obtained using the field tensor components

$$F_{r\phi} = -r\left(1-\frac{2M}{r}\right)^{-1/2} B_\theta\sin\theta, \qquad F_{\theta\phi} = r^2\sin\theta B_r \tag{3.42}$$

$$F_{rt} = \frac{4J\mu}{3r^5}\left(1+\frac{3M}{r}\right), \qquad F_{\theta t} = 0 \tag{3.43}$$

The effective potential for 'r-motion' in the equatorial plane $\theta = \pi/2$ is given by (Prasanna 1980)

$$\begin{aligned} V &= \frac{\tilde{J}\lambda}{\rho^4}\left(\frac{1}{3}+\frac{4}{5\rho}\right)+\frac{2\tilde{J}}{\rho^2}\left[\frac{L}{\rho}+\frac{3\lambda\rho}{8}\left\{ln\left(1-\frac{2}{\rho}\right)+\frac{2}{\rho}\left(1+\frac{1}{\rho}\right)\right\}\right] \\ &\pm\left[\left(1-\frac{2}{\rho}\right)\left\{1+\left[\frac{L}{\rho}+\frac{3\lambda\rho}{8}\left\{ln\left(1-\frac{2}{\rho}\right)+\frac{2}{\rho}\left(1+\frac{1}{\rho}\right)\right\}\right]^2\right\}\right]^{1/2} \end{aligned} \tag{3.44}$$

where $\rho = \frac{r}{M}$, $\lambda = \frac{e\mu}{M^2}$, $L = \frac{\ell}{M}$, $\tilde{J} = \frac{J}{M^2}$ are the dimensionless quantities. The constants of motion take the form as

$$\begin{aligned} u^\tau &= \frac{d\tau}{d\sigma} = \left(1-\frac{2}{\rho}\right)^{-1}\left[\left(E - \frac{2\tilde{J}L}{\rho^3}\right) - \frac{\tilde{J}\lambda}{\rho^4}\left\{\frac{1}{3}\right.\right. \\ &+ \left.\left.\frac{4}{5\rho} + \frac{3\rho^3}{4}\left[ln\left(1-\frac{2}{\rho}\right) + \frac{2}{\rho}\left(1+\frac{1}{\rho}\right)\right]\sin^2\theta\right\}\right] \end{aligned} \tag{3.45}$$

and

$$u^\phi = \frac{d\phi}{d\sigma} = \frac{L}{\rho^2 \sin^2\theta} + \frac{3\lambda}{8}\left[ln\left(1-\frac{2}{\rho}\right) + \frac{2}{\rho}\left(1+\frac{1}{\rho}\right)\right] + \frac{2\tilde{J}}{\rho^3}u^\tau \tag{3.46}$$

where $\tau = t/M$ and $\sigma = s/M$ are other dimensionless quantities. Equations of motion in r and θ directions are

$$\begin{aligned} \frac{d^2\rho}{d\sigma^2} &= \left(1-\frac{2}{\rho}\right)\left[-\frac{(u^\tau)^2}{\rho^2} + \rho\sin^2\theta\left(u^\phi\right)^2 + \frac{2\tilde{J}}{\rho^2}\sin^2\theta u^\tau u^\phi + \rho\left(u^\theta\right)^2\right] \\ &+ \left(1-\frac{2}{\rho}\right)^{-1}\frac{(u^\rho)^2}{\rho^2} + \frac{4}{3}\frac{\tilde{J}\lambda}{\rho^5}\left(1+\frac{1}{\rho}\right)u^\tau - \frac{3}{4}\lambda\left(1-\frac{2}{\rho}\right)\sin^2\theta \\ &\left[\rho\, ln\left(1-\frac{2}{\rho}\right) + \left(1-\frac{2}{\rho}\right)^{-1} + 1\right]u^\phi \end{aligned} \tag{3.47}$$

$$\begin{aligned} \frac{d^2\theta}{d\sigma^2} &= \sin\theta\cos\theta\left[\left(u^\phi\right)^2 - \frac{4\tilde{J}}{\rho^3}u^\tau u^\phi - \frac{3}{4}\lambda\left\{ln\left(1-\frac{2}{\rho}\right) + \frac{2}{\rho}\left(1+\frac{1}{\rho}\right)\right\}u^\phi\right] \\ &- \frac{2}{\rho}u^\rho u^\theta \end{aligned} \tag{3.48}$$

It is quite clear from the equations that if initially the particle is on the equatorial plane $\theta = \pi/2$ and has no velocity in the θ-direction $\left(u^\theta\right)_0 = 0$, then it gathers no acceleration in the θ direction and remains confined to the same plane. This is infact significant as one can see that, though in the locally non-rotating frame both components of the electric field are non-zero, (3.38) in the coordinate frame, where the particle motion is being studied, $F_{\theta t}$ turns out to be zero (3.43) and thus in the expression for θ-acceleration (3.48) the particle at rest on the equatorial plane sees no force acting on it in the θ-direction. In general, in order to integrate the set of equations (3.46) to (3.48) one needs five initial conditions viz., the position and velocity. From (3.19) we have

$$\begin{aligned}(u^\rho)^2 &= \left(1-\frac{2}{\rho}\right)\left[-1+\left(1-\frac{2}{\rho}\right)(u^\tau)^2\right. \\ &\left.-\rho^2\left(u^\theta\right)^2-\rho^2\sin^2\theta\left(u^\phi-\frac{2\tilde{J}}{\rho^3}u^\tau\right)^2\right]\end{aligned} \tag{3.49}$$

Starting from the initial position of the particle at $(\rho_0, \pi/2, 0)$, one can find out $(u^\tau)_0$ and $\left(u^\phi\right)_0$ from (3.45) and (3.46) by stipulating the physical parameters E, L, λ and $\tilde{J}$. Using these values of $(u^\tau)_0$ and $\left(u^\phi\right)_0$ and any assumed value of $\left(u^\theta\right)_0$ constrained by the condition:

$$\rho_0\left(u^\theta\right)_0 \leq \left[-1+\left(1-\frac{2}{\rho_0}\right)(u^\tau)_0^2-\rho_0^2\left(\left(u^\phi\right)_0-\frac{2\tilde{J}}{\rho_0^3}(u^\tau)_0\right)^2\right]^{1/2} \tag{3.50}$$

one can calculate $(u^\rho)_0$, the initial velocity in the r-direction from (3.49) and thus get the entire initial data set for the orbits. However, in order to ensure physically plausible trajectories it becomes necessary to ensure that

$$\left(1-\frac{2}{\rho_0}\right)(u^\tau)_0^2-\rho_0^2\left((u^\rho)_0-\frac{2\tilde{J}}{\rho_0^2}(u^\tau)_0\right)^2 \geq 1 \tag{3.51}$$

3.5 Results and Discussions

The study of the 'effective potential' for r-motion for a particle confined to the equatorial plane would give basically the nature of possible orbits, particularly distinguishing the bound and the unbound orbits, as the curves represent V_{eff} as a function of r, for the turning points. The three free parameters of the system L, λ and $\tilde{J}$, would *naturally give a large number of possible configurations within their individual domains and thus one can have sets of effective potential curves for different values of* these three parameters. Figures (3.1)-(3.9) represent some of the possible configurations indicating the trends for bound and unbound orbits. Figures (3.1a) and (3.1b) represent the cases for a fixed value of $\tilde{J}$, how the potential changes with changing L for fixed λ and vice versa, respectively. It is clear from these two that the two arms of the potential well are made up of the two maxima, the inner one representing the magnetic field barrier and the outer one, the centrifugal barrier. For a fixed L, as λ increases the potential minimum shifts outwards in r, whereas for a fixed λ, it moves inwards with increasing L. If both L and λ are high then as shown in figure (3.1c) the potential well appears quite far from the central object indicating the trapping of particles far outside objects like neutron stars ($\rho = 20, 30$). Fig. (3.2) shows an example of the projection of the actual trajectories for a given $\tilde{J}$ but with different E, L and λ values.

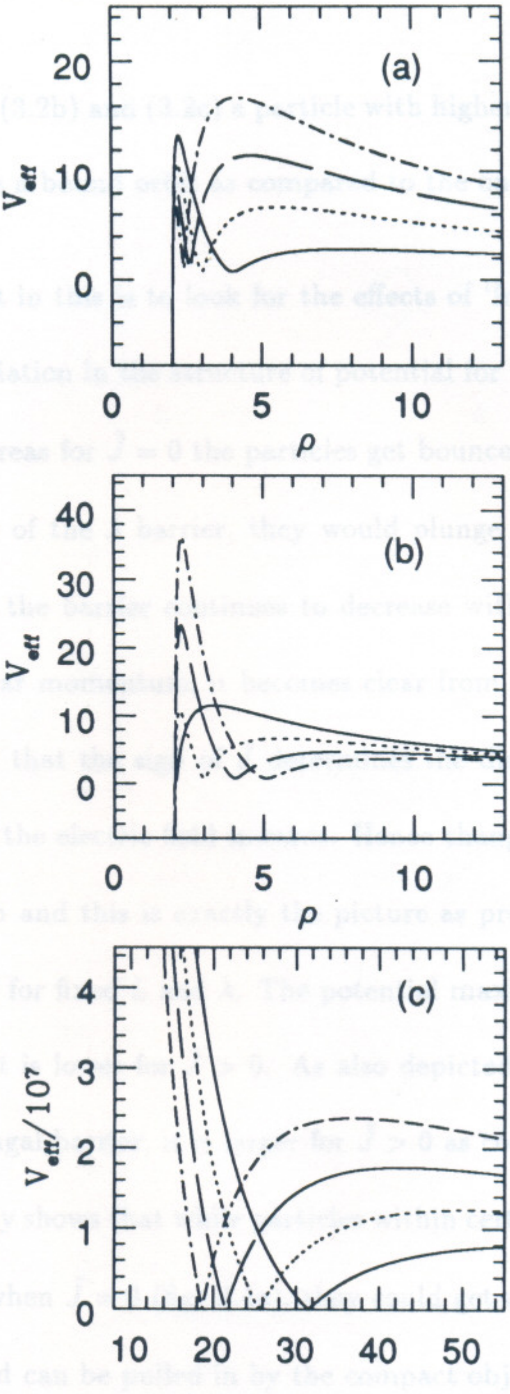

Figure 3.1: Plot for effective potential (V_{eff}) vs. $\rho \left(= \frac{r}{m}\right)$. (a) shows change in L for $\lambda = 100$, $\tilde{J} = 0.310$, $L = 40$ (1), $L = 70$ (2), $L = 100$ (3), $L = 130$ (4), where (1) corresponds to solid line, (2) to dotted line, (3) to dashed line and (4) to dotted dashed line. (b) has fixed $L = 70$, $\tilde{J}$ same as (a) and $\lambda = 25$ (1), $\lambda = 100$ (2), $\lambda = 175$ (3), $\lambda = 250$ (4). (c) is plotted with large values of λ and L. $\tilde{J} = -0.310$, $\lambda = 3.e10$ for $L = 1.e9$ (1), $L = 1.25e9$ (2), $L = 1.5e9$ (3), $L = 1.75e9$ (4).

As seen from figures (3.2b) and (3.2c) a particle with higher energy at the same initial location cannot have a bound orbit as compared to the one with lower energy.

As our main interest in this is to look for the effects of 'frame dragging' $(\tilde{J})$, figure (3.3a) shows the variation in the structure of potential for varying values of $\tilde{J}$ for the same L and λ. Whereas for $\tilde{J} = 0$ the particles get bounced away even upto energies $\sim E = 20$, because of the λ barrier, they would plunge onto the central star if it has non-zero $\tilde{J}$ and the barrier continues to decrease with increasing $\tilde{J}$. Since ω is related to the angular momentum, it becomes clear from the expression (eqn. 3.38) for the electric field that the sign of $\tilde{J}$ determines the direction of the electric field with $\tilde{J} > 0$ yielding the electric field inwards. Hence changing $\tilde{J}$ one could expect to reverse the situation and this is exactly the picture as presented in fig. (3.3b) with $\tilde{J} > 0$, zero and < 0 for fixed L and λ. The potential maximum gets larger for $\tilde{J} < 0$ from $\tilde{J} = 0$, while it is lower for $\tilde{J} > 0$. As also depicted in the same figure, if one looks at the centrifugal barrier, it is larger for $\tilde{J} > 0$ as compared to the cases $\tilde{J} = 0$ and < 0. This clearly shows that while particles within certain energy could be bound in a potential well when $\tilde{J} = 0$ (fig. 3.4a), they could get unbound and move away if $\tilde{J} < 0$ (fig. 3.4b) and can be pulled in by the compact object if $\tilde{J} > 0$ (fig. 3.4c) due to the fact that the electric field acts outwards when $\tilde{J} < 0$ and inwards when $\tilde{J} > 0$.

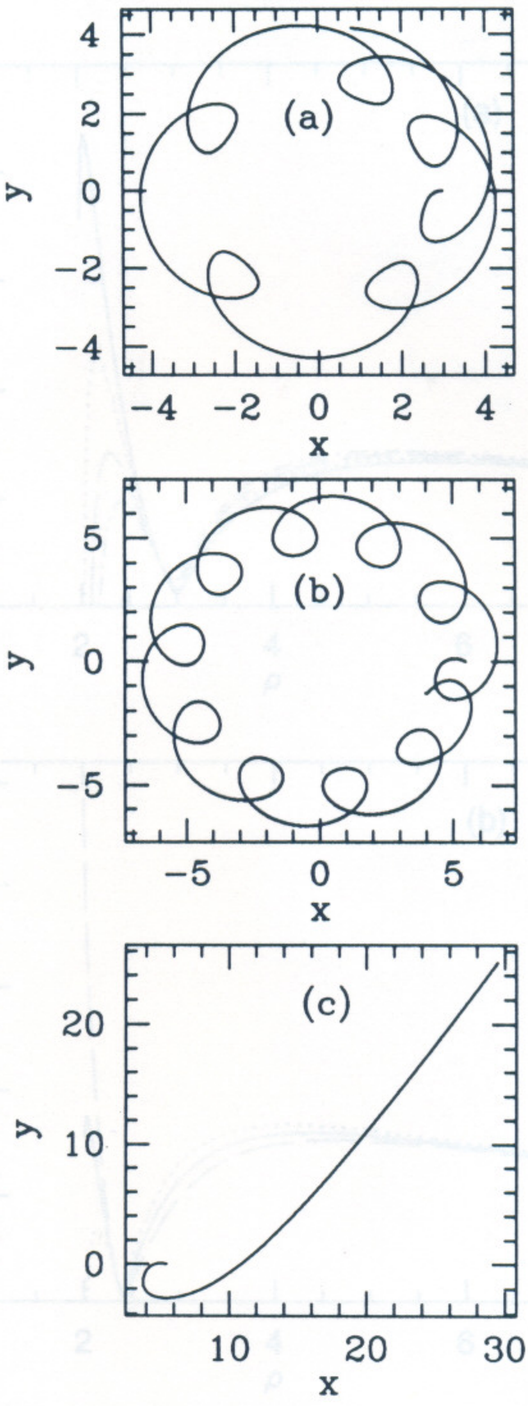

Figure 3.2: Trajectories of particle projected in x-y plane.
(a): $\tilde{J} = 0.311$, $\lambda = 100$, $L = 70.78$, $E = 6$, $\rho_0 = 3$.
(b): $\tilde{J} = 0.311$, $\lambda = 250$, $L = 70.78$, $E = 3$, $\rho_0 = 5.5$.
(c): Same as in (b) but $E = 5$.
The turning points of the gyrating orbits in (a) are $\rho_{min} = 2.56$, $\rho_{max} = 4.29$ and in (b) are $\rho_{min} = 4.39$, $\rho_{max} = 6.72$. In (c) it turns at $\rho_{min} = 3.94$ and shoots out.

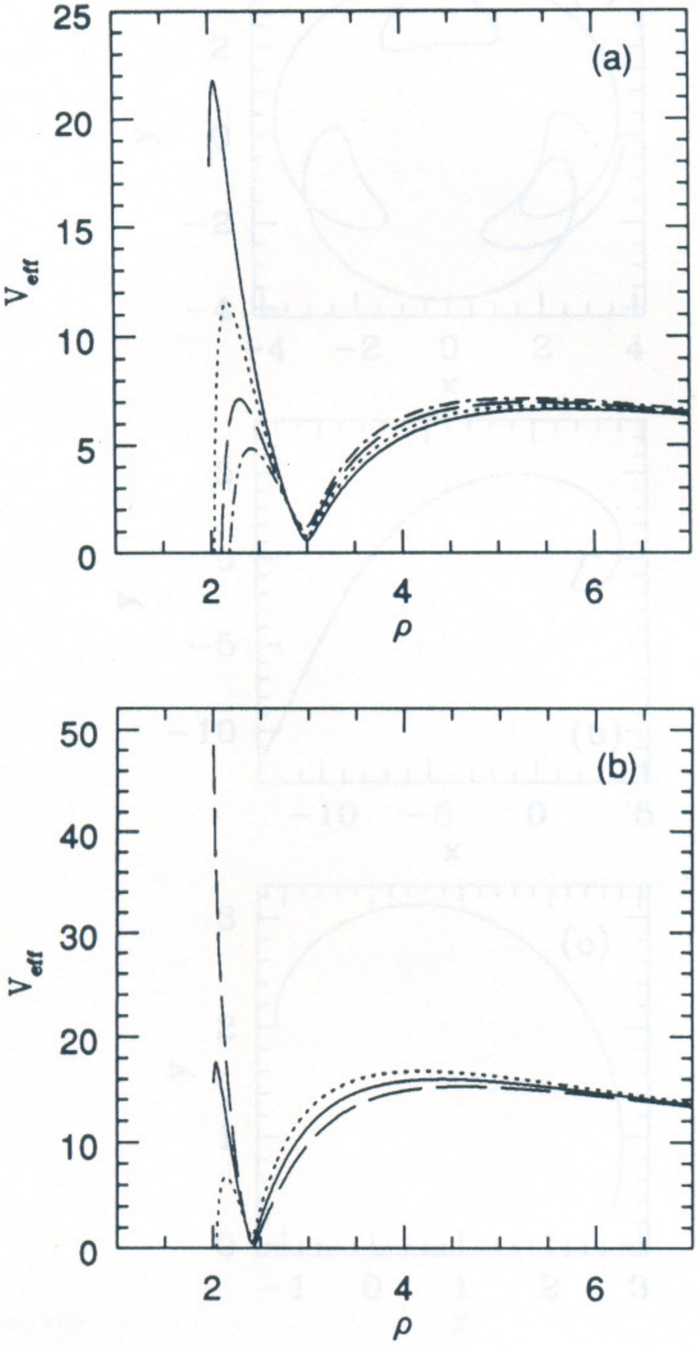

Figure 3.3: (a) shows change in V_{eff} curves for various values of $\tilde{J}$, i.e. $\tilde{J} = 0.0$ (1), $\tilde{J} = 0.271$ (2), $\tilde{J} = 0.541$ (3), $\tilde{J} = 0.813$ (4), where $\lambda = 100$ and $L = 70.78$. In (b) dashed curve represents two sets of J, L and λ i.e. $\tilde{J} = -0.31$, $L = 130$, $\lambda = 100$ and $\tilde{J} = 0.31$, $L = -130$, $\lambda = -100$. Similarly, dotted curve represents other two sets i.e. $\tilde{J} = 0.31$, $L = 130$, $\lambda = 100$ and $\tilde{J} = -0.31$, $L = -130$, $\lambda = -100$. The solid line is for $\tilde{J} = 0$, when both λ and L are positive or negative with the same values as in other two curves.

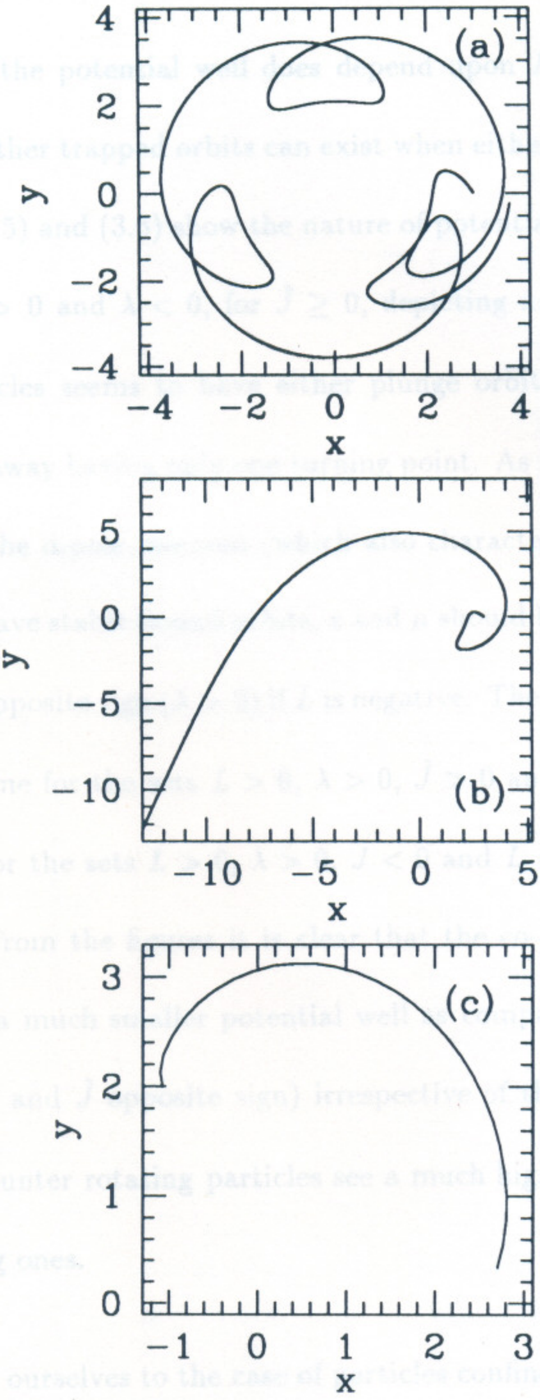

Figure 3.4: *This indicates the distinction of kind of the trajectories for zero and nonzero $\tilde{J}$ and the trapped orbit.* (a) is $\tilde{J} = 0$, $\lambda = 100$, $L = 130$, $E = 15.5$, $\rho_0 = 3$ then $\rho_{min} = 2.085$ and $\rho_{max} = 3.81$. (b) for same input values as of (a), but $\tilde{J} = -0.31$ shows the turning of the particle at $\rho_{min} = 2.147$ and then going away. (c) shows that particle falls inside for same values of L and λ as in (a) and (b), but with $\tilde{J} = 0.31$, $E = 14.0$, $\rho_0 = 2.5$. Its turning point is $\rho_{max} = 3.269$.

As the structure of the potential well does depend upon L and $\lambda(= e\mu/m^2)$, it is necessary to see whether trapped orbits can exist when either one of these parameters is negative. Figs. (3.5) and (3.6) show the nature of potential curves for $\lambda > 0$, $L < 0$ and for the case $L > 0$ and $\lambda < 0$, for $\tilde{J} \geq 0$, depicting no possible potential well. In either case particles seems to have either plunge orbits if they are sufficiently energetic or escape away having only one turning point. As λ involves e the charge of the particle and μ the dipole moment (which also characterizes the direction of the dipole) in order to have stable bound orbits, e and μ should have the same sign, if L is positive, and be of opposite sign ($\lambda > 0$) if L is negative. The structure of the potential well remains the same for the sets $L > 0$, $\lambda > 0$, $\tilde{J} > 0$ and $L < 0, \lambda < 0, \tilde{J} < 0$ on the one hand and for the sets $L > 0$, $\lambda > 0$, $\tilde{J} < 0$ and $L < 0$, $\lambda < 0$, $\tilde{J} > 0$ on the other (fig. 3.3b). From the figures it is clear that the co-rotating particles (L and $\tilde{J}$ same sign) have a much smaller potential well as compared to the ones that are counter rotating (L and $\tilde{J}$ opposite sign) irrespective of the sign of the charge and consequently the counter rotating particles see a much higher magnetic field barrier than the co-rotating ones.

So far we addressed ourselves to the case of particles confined to the equatorial plane having initial conditions $\theta_0 = \pi/2$, $\left(u^\theta\right)_0 = 0$. On the other hand if $\left(u^\theta\right)_0 \neq 0$ then as the equations show the particle would have acceleration in the θ direction and thus it leaves the equatorial plane.

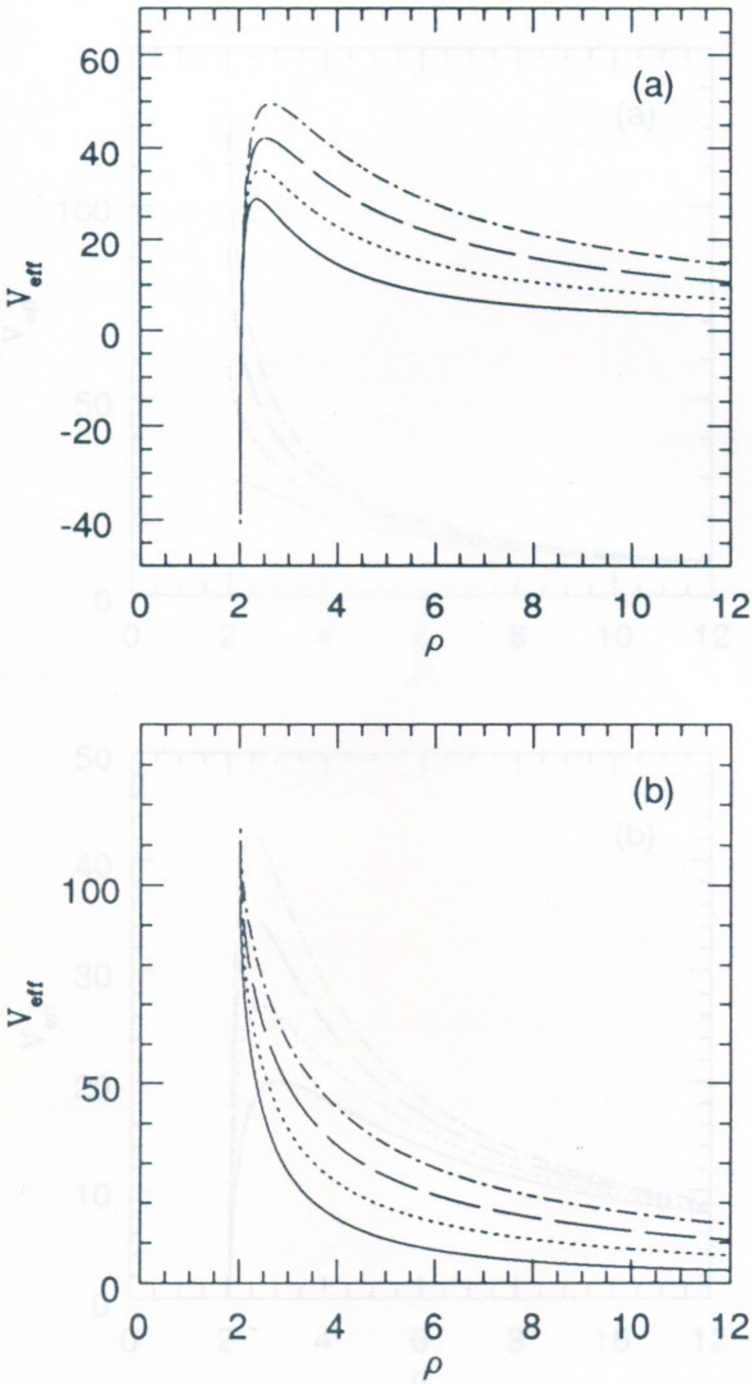

Figure 3.5: This is V_{eff} vs. ρ curve, showing distinction due to the change in sign of J for varying values of L. In (a), $\lambda = 150$, $\tilde{J} = 0.31$ and $L = -25$ (1), $L = -75$ (2), $L = -125$ (3), $L = -175$ (4), while (b) is same as (a), but $\tilde{J} = -0.31$.

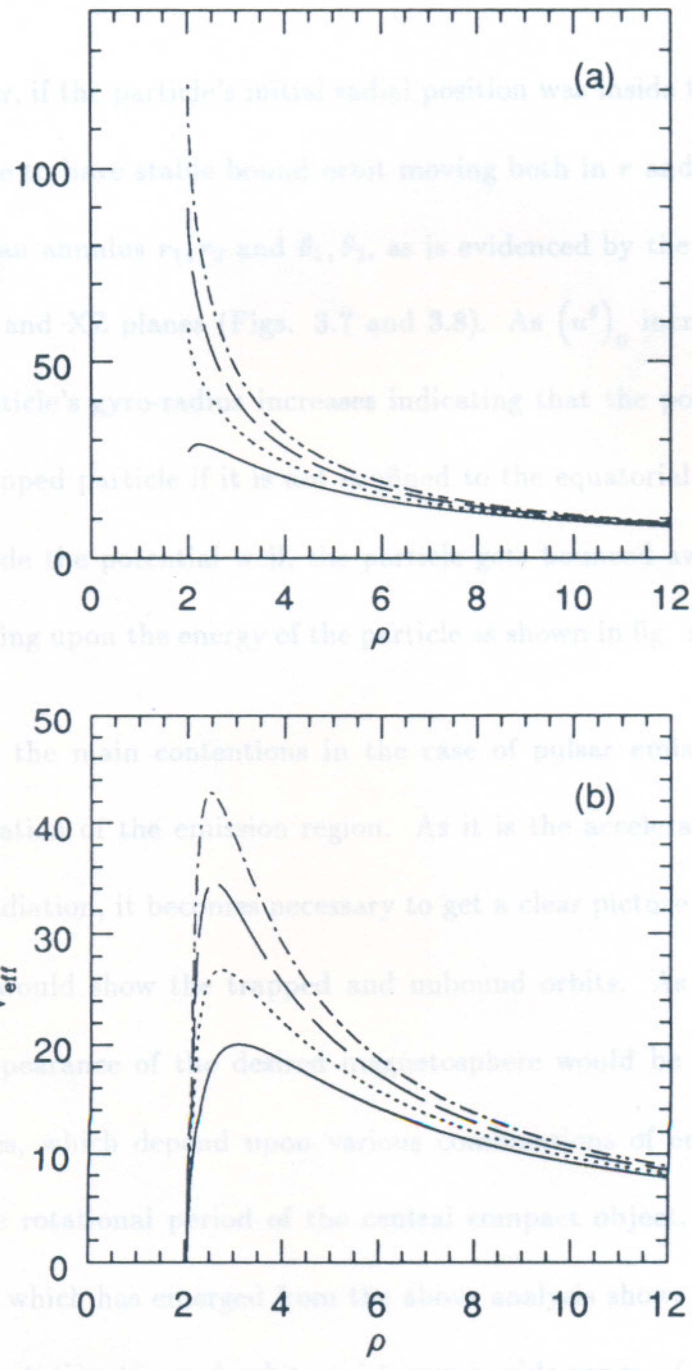

Figure 3.6: These curves correspond to varying values of λ. (a) has $L = 100$, $\tilde{J} = 0.31$ and $\lambda = -25$ (1), $\lambda = -75$ (2), $\lambda = -125$ (3), $\lambda = -175$ (4) whereas (b) is same as (a), but $\tilde{J} = -0.31$.

However, if the particle's initial radial position was inside the potential well, it could continue to have stable bound orbit moving both in r and θ directions but confined within an annulus r_1, r_2 and θ_1, θ_2, as is evidenced by the projection of these orbits on XY and XZ planes (Figs. 3.7 and 3.8). As $\left(u^{\theta}\right)_0$ increases to its limiting value the particle's gyro-radius increases indicating that the potential well is broader for any trapped particle if it is not confined to the equatorial plane. When the particle is outside the potential well, the particle gets bounced away by one of the barriers depending upon the energy of the particle as shown in fig. (3.9) even when $\left(u^{\theta}\right)_0 \neq 0$.

One of the main contentions in the case of pulsar emission mechanism has been the location of the emission region. As it is the accelerated charged particles that emit radiation, it becomes necessary to get a clear picture of the particle trajectories which would show the trapped and unbound orbits. As seen above, the existence and appearance of the desired magnetosphere would be a consequence of trapped particles, which depend upon various combinations of energy, angular momentum and the rotational period of the central compact object. However, the qualitative picture which has emerged from the above analysis shows that both co-rotating and contra-rotating trapped orbits exist over a wide range of physical parameters. The example shown in (Fig. 3.1c) matches with the poloidal field strength of the order of 10^{11} to 10^{12} gauss and in such a case the specific angular momentum needs to be sufficiently large to acquire trapped orbits for low energy particles.

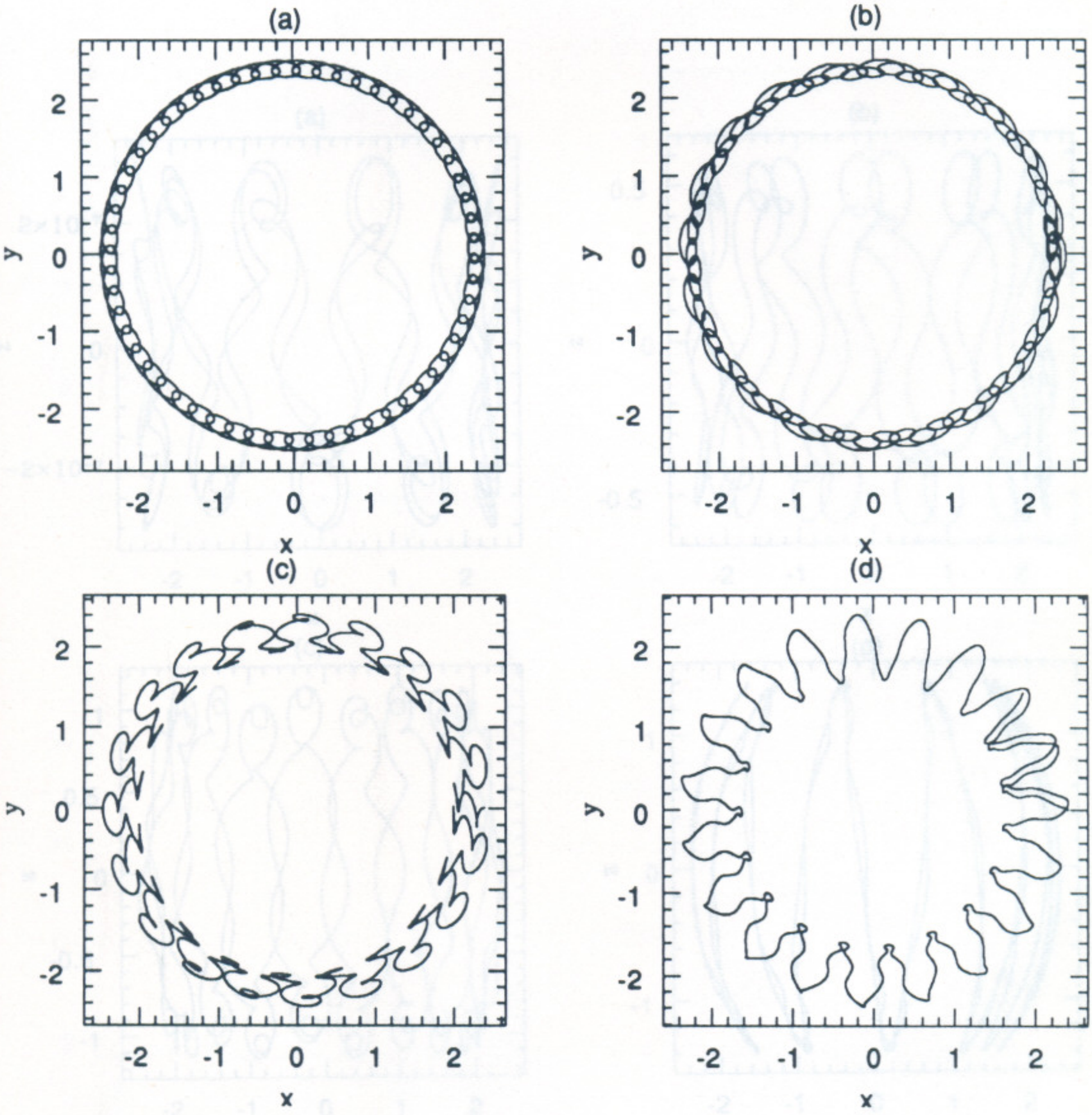

Figure 3.7: It has $\tilde{J} = 0.31$, $\lambda = 100$, $L = 130$, $E = 4.0$, $\rho_0 = 2.4$.
(a): $\left(u^\theta\right)_0 = 0$ which gives $\rho_{min} = 2.299$, $\rho_{max} = 2.515$.
(b): $\left(u^\theta\right)_0 = 1.154$, $\rho_{min} = 2.283$, $\rho_{max} = 2.509$.
(c): $\left(u^\theta\right)_0 = 2.308$, $\rho_{min} = 2.205$, $\rho_{max} = 2.480$.
(d): $\left(u^\theta\right)_0 = 3.462$, $\rho_{min} = 2.128$, $\rho_{max} = 2.407$.

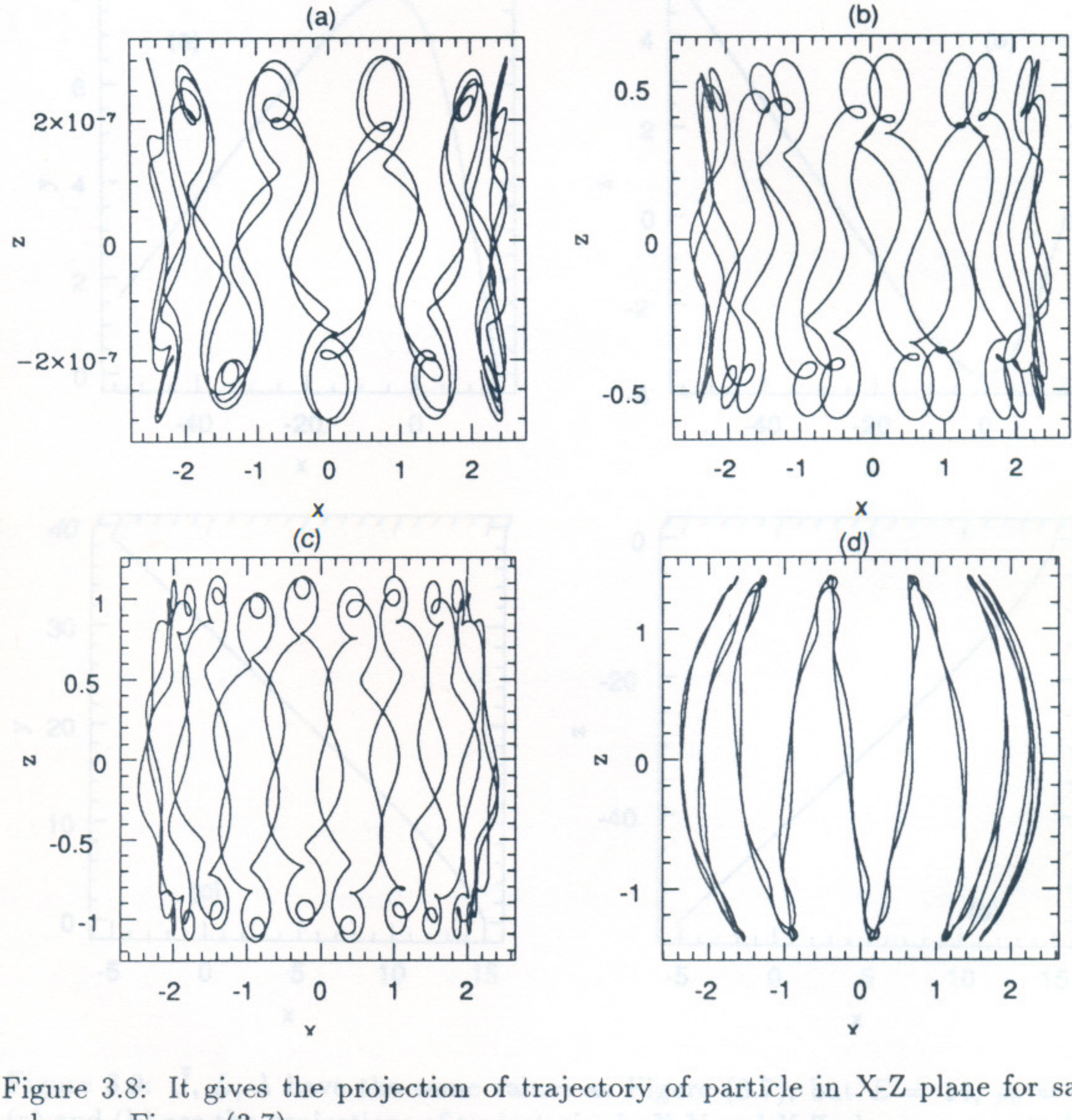

Figure 3.8: It gives the projection of trajectory of particle in X-Z plane for same values as Figure (3.7).

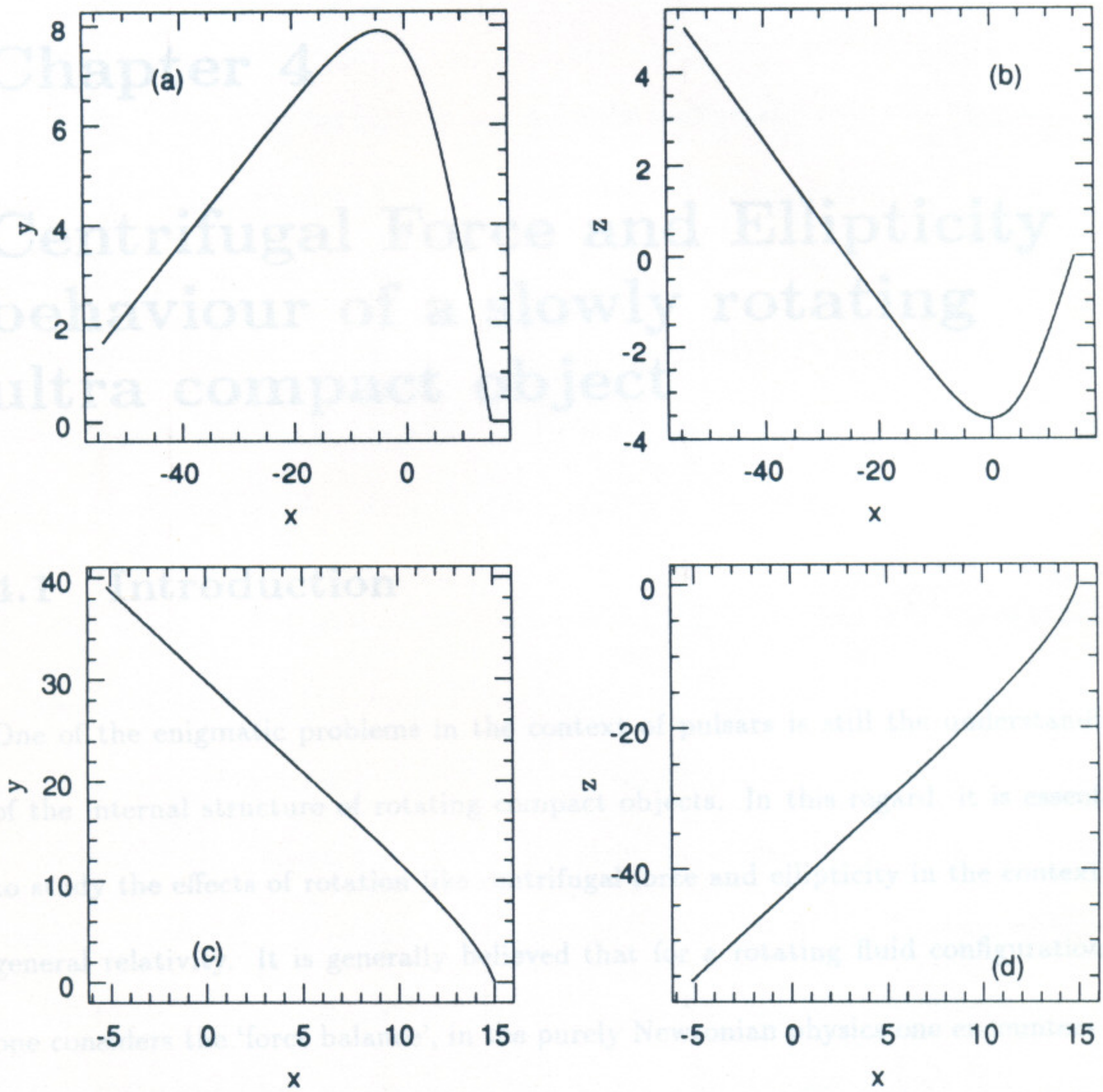

Figure 3.9: $\tilde{J}$, L, λ have the same values as Figure (3.7), but $E = 14$, $\rho_0 = 15.0$. (a) and (b) are the projections of trajectories in X-Y and X-Z planes respectively for $\left(u^\theta\right)_0 == 2.762$ and turning point is $\rho_{min} = 8.217$. (c) and (d) are for $\left(u^\theta\right)_0 = 8.286$ with $\rho_{min} = 14.884$.

ıapter 4

entrifugal Force and Ellipticity ehaviour of a slowly rotating tra compact object

l Introduction

e of the enigmatic problems in the context of pulsars is still the understanding he internal structure of rotating compact objects. In this regard, it is essential study the effects of rotation like centrifugal force and ellipticity in the context of ıeral relativity. It is generally believed that for a rotating fluid configuration if e considers the 'force balance', in the purely Newtonian physics one encounters no ange behaviour irrespective of the size of the compact object as the two traditional als the gravitation vis-a-vis the centrifugal force acting on a fluid element would vays be opposing each other. However, as mentioned in section (1.3), in the context general relativity Abramowicz & Prasanna (1990) showed that for a sufficiently small size object, the centrifugal force acting on a test particle of mass m_0 in circular orbit outside the object with mass M is given by

$$F_{cfg} = \frac{m_0 \tilde{v}^2}{r}(1 - \frac{3M}{r}), \tag{4.1}$$

where $\tilde{v}$ is the speed of the particle as seen in the conformally projected 3-space of the optical reference geometry (ACL) . As seen from the above expression the centrifugal force would not oppose gravity if the particle is situated at a distance $r \leq 3M$. As there could exist ultra compact bodies (Iyer et al. 1985) of size $2M \leq R \leq 3M$, it would become relevant to consider the effect of such a centrifugal force reversal on a fluid element of a possible ultra compact rotating configuration.

Another important manifestation of the same result viz, introducing Newtonian forces in general relativity is the explanation of ellipticity maximum for a rotating configuration given by Abramowicz & Miller (1990), an effect discovered by Chandrasekhar & Miller (1974). Though the explanation given by Abramowicz and Miller is qualitatively viable, quantitatively there appears a difference in the location of the ellipticity maximum, which perhaps is due to the fact that they considered only the Schwarzschild background geometry, which does not take into account the influence of rotation of the central body inherently.

We have re-examined the scenario by studying the possible centrifugal reversal and the ensuing ellipticity maximum for a slowly rotating fluid configuration by adopting the Hartle - Thorne solution.

We start with a general axisymmetric, stationary fluid configuration and introduce a formalism to treat the 'four-force' on a fluid element in the 3+1 conformal splitting and then adopting Hartle's solution as a specific example consider the centrifugal force. Using the Newtonian principle of force balance equation for a rotating spheroid we then derive a general expression for the ellipticity and again study its behaviour for the Hartle solution. We find that the result matches closer to that of the Chandrasekhar and Miller result thus validating the more general expression derived.

4.2 Formalism

4.2.1 Equation of motion

The equation of motion for a perfect fluid distribution on a general curved space time

$$ds^2 = g_{ij}dx^i dx^j, \tag{4.2}$$

is given by

$$(\rho + p)(u^i_{;j}u^j) = -h^{ij}p_{,j} \tag{4.3}$$

where ρ is the matter density, p the pressure, u^i the four velocity and h^{ij} the projection tensor $(g^{ij}+u^i u^j)$ with i and j taking values from 0 to 3. This may indeed be expressed as the 'four-force' acting on a fluid element

$$f_i := (\rho + p)(u_{i;j}u^j) + h_i^j p_{,j} \tag{4.4}$$

$$= (\rho + p)[u^j \partial_j u_i - \frac{1}{2} u^m u^j \partial_i g_{jm}] + h_i^j p_{,j} , \tag{4.5}$$

which when $p = 0$ and $\rho = m_0$, reduces to the well known four-force expression acting on a particle (ACL)

$$m_0 f_i \equiv P^j \partial_j P_i - \frac{1}{2} P^j P^m \partial_i g_{jm}, \tag{4.6}$$

where P_i is the 4-momentum of the particle.

4.2.2 3 + 1 splitting of spacetime

A general four-dimensional curved spacetime (equation(4.2)) can be written as

$$ds^2 = g_{00}(dx^0)^2 + 2g_{0\alpha}dx^0 dx^\alpha + g_{\alpha\beta}dx^\alpha dx^\beta \tag{4.7}$$

which can be further split in terms of a positive definite metric specifying an absolute 3-space, with metric components $\gamma_{\alpha\beta}$ and terms associated with the time co-ordinate as

$$ds^2 = dl^2 - \Phi(dt + 2\omega_\alpha dx^\alpha)^2 \tag{4.8}$$

where

$$dl^2 = \gamma_{\alpha\beta}dx^\alpha dx^\beta, \tag{4.9}$$

$$g_{00} = -\Phi, \qquad g_{0\alpha} = -2\Phi\omega_\alpha, \qquad g_{\alpha\beta} = \gamma_{\alpha\beta} - 4\Phi\omega_\alpha\omega_\beta. \tag{4.10}$$

Then the covariant components of 4-velocity can be expressed as

$$u_0 = -\Phi(u^0 + 2\omega_\alpha u^\alpha), \tag{4.11}$$

$$u_\alpha = \gamma_{\alpha\beta}u^\beta + 2\omega_\alpha u_0, \tag{4.12}$$

and using equation (4.5), four-force is rewritten in the form

$$f_0 = \Phi^{-1}(\rho + p)u^\mu \partial_\mu u_0 + h_0^\mu p_\mu \tag{4.13}$$

$$f_\alpha = (\rho + p)[u^\beta \partial_\beta u_\alpha - \frac{1}{2}\{u^\mu u^\beta \partial_\alpha(\gamma_{\mu\beta} - 4\Phi\omega_\mu\omega_\beta)$$

$$+ 2u^0 u^\beta \partial_\alpha(-2\Phi\omega_\beta) + (u^0)^2 \partial_\alpha(-\Phi)^2\}] + h_\alpha^\beta p_{,\beta} \tag{4.14}$$

4.2.3 Optical reference geometry

In a conformally transformed absolute 3-space

$$d\tilde{l}^2 = \tilde{g}_{\alpha\beta}dx^\alpha dx^\beta \tag{4.15}$$

where $\tilde{g}_{\alpha\beta} = \gamma_{\alpha\beta}/\Phi$ and $dl^2 = \Phi\, d\tilde{l}^2$, the 3-velocity is defined as

$$\tilde{u}^\alpha = \Phi u^\alpha, \tag{4.16}$$

such that the contravariant components of 3-velocity in this conformally transformed reference frame are obtained using the metric $\tilde{g}_{\alpha\beta}$ as

$$\tilde{u}_{\alpha} = \tilde{g}_{\alpha\beta}\tilde{u}^{\beta}. \tag{4.17}$$

Then, equation (4.13) and (4.14) take the form :

$$f_0 = \Phi^{-1}(\rho + p)\tilde{u}^{\mu}\partial_{\mu}u_0 + h_0^{\mu}p_{,\mu} \tag{4.18}$$

$$\begin{aligned} f_{\alpha} &= \Phi^{-1}(\rho + p)\left[\tilde{u}^{\mu}\tilde{\nabla}_{\mu}\tilde{u}_{\alpha} + 2u^0\tilde{u}^{\mu}\omega_{\mu\alpha} + \frac{M_0^2}{2\Phi}\partial_{\alpha}\Phi\right] \\ &\quad + 2\omega_{\alpha}f_0 + (h_{\alpha}^{\mu} - 2\omega_{\alpha}h_0^{\mu})p_{,\mu} \end{aligned} \tag{4.19}$$

where

$$M_0^2 = u_0^2 - \tilde{g}_{\mu\nu}\tilde{u}^{\mu}\tilde{u}^{\nu} \tag{4.20}$$

$$\omega_{\mu\alpha} = \partial_{\mu}\omega_{\alpha} - \partial_{\alpha}\omega_{\mu} \tag{4.21}$$

$$\tilde{\nabla}_{\mu}\tilde{u}^{\alpha} = \partial_{\mu}\tilde{u}_{\alpha} - \frac{1}{2}\tilde{g}^{\nu\sigma}\tilde{u}_{\nu}(\tilde{g}_{\mu\sigma,\,\alpha} + \tilde{g}_{\alpha\sigma,\,\mu} - \tilde{g}_{\mu\alpha,\,\sigma}). \tag{4.22}$$

For an axisymmetric and stationary spacetime (equation(2.5)),

$$ds^2 = -e^{2\nu}dt^2 + e^{2\lambda}dr^2 + e^{2\mu}d\theta^2 + e^{2\psi}(d\phi - \omega dt)^2, \tag{4.23}$$

adopting the 3 + 1 conformal slicing on the locally non-rotating frame (LNRF) (Bardeen et al. 1972), the 3-components of the forces ((4.19)) simplify to

$$f_\alpha = \Phi^{-1}(\rho + p)\left[\tilde{u}^\mu \tilde{\nabla}_\mu \tilde{u}_\alpha + \frac{M_0^2}{2\Phi}\partial_\alpha \Phi\right] + h^\mu_\alpha p_{,\mu} \tag{4.24}$$

which in fact, when zero, gives the equation of hydrodynamic equilibrium for a rotating fluid configuration. The terms $\tilde{u}^\mu \tilde{\nabla}_\mu \tilde{u}_\alpha$ and $(M_0^2/2\Phi)\partial_\alpha \Phi$ correspond to the 'centrifugal acceleration' and the 'gravitational acceleration' respectively. The radial components of these forces for metric (4.23) are

$$\begin{aligned} F_{cf} &= e^{2\psi+2\nu}(\Omega-\omega)^2(\psi'-\nu')\left[e^{2\nu}-e^{2\psi}(\Omega-\omega)^2\right]^{-1} \\ F_g &= e^{2\nu}\nu', \end{aligned} \tag{4.25}$$

where prime denotes differentiation with respect to r.

4.2.4 Ellipticity

It is well known that a rotating fluid configuration deviates from spherical symmetry and depending upon the degree of rotation the equatorial diameter expands whereas the polar diameter contracts thereby producing a change in shape. The various equilibrium configurations of rotating fluids have been well discussed in the literature, and the sequence goes through Maclaurin spheroids to Jacobi ellipsoids (Chandrasekhar 1969). For slowly rotating configuration one can consider the Maclaurin spheroid the ellipticity defined through the usual definition of

$$\epsilon = \frac{1-(1-e^2)^{1/2}}{(1-e^2)^{1/6}}, \tag{4.26}$$

ng the eccentricity defined as $e = (1 - b^2/a^2)^{1/2}$, where b and a are polar and torial radii respectively.

aurin had shown (Chandrasekhar 1969) that the acceleration due to gravity at quator and pole has the values

$$\begin{aligned} g_{equator} &= 2\pi G\rho a \frac{(1-e^2)^{\frac{1}{2}}}{e^3}[sin^{-1}e - e(1-e^2)^{\frac{1}{2}}] \\ g_{pole} &= 4\pi G\rho a \frac{(1-e^2)^{\frac{1}{2}}}{e^3}[e - (1-e^2)^{\frac{1}{2}} sin^{-1}e], \end{aligned} \tag{4.27}$$

ein he had considered the possible effects that could arise due to the internal es in the body. However, as we are looking for a solution in general relativity, ein the gravitational field inside the body is described through a metric which olution of Einstein's equations for a perfect fluid distribution, the gravitational tials g_{ij} would be incorporating the effects of all characteristics of the fluid bution . With this proviso, in the new language of optical reference geometry it ficient to consider the modified expression for the gravitational and centrifugal rations as given by (4.25) and use the Newtonian force balance equation to relate ccentricity with the acceleration. Thus generalizing the Newtonian equation

$$g_{equator} - a\Omega^2 = g_{pole}(1-e^2)^{\frac{1}{2}}. \tag{4.28}$$

with the ellipticity defined through the usual definition of

$$\epsilon = \frac{1-(1-e^2)^{1/2}}{(1-e^2)^{1/6}}, \tag{4.26}$$

e being the eccentricity defined as $e = (1 - b^2/a^2)^{1/2}$, where b and a are polar and equatorial radii respectively.

Maclaurin had shown (Chandrasekhar 1969) that the acceleration due to gravity at the equator and pole has the values

$$\begin{aligned} g_{equator} &= 2\pi G\rho a\frac{(1-e^2)^{\frac{1}{2}}}{e^3}[sin^{-1}e - e(1-e^2)^{\frac{1}{2}}] \\ g_{pole} &= 4\pi G\rho a\frac{(1-e^2)^{\frac{1}{2}}}{e^3}[e - (1-e^2)^{\frac{1}{2}}sin^{-1}e], \end{aligned} \tag{4.27}$$

wherein he had considered the possible effects that could arise due to the internal stresses in the body. However, as we are looking for a solution in general relativity, wherein the gravitational field inside the body is described through a metric which is a solution of Einstein's equations for a perfect fluid distribution, the gravitational potentials g_{ij} would be incorporating the effects of all characteristics of the fluid distribution . With this proviso, in the new language of optical reference geometry it is sufficient to consider the modified expression for the gravitational and centrifugal accelerations as given by (4.25) and use the Newtonian force balance equation to relate the eccentricity with the acceleration. Thus generalizing the Newtonian equation

$$g_{equator} - a\Omega^2 = g_{pole}(1-e^2)^{\frac{1}{2}}. \tag{4.28}$$

to

$$F_{ge} - F_{cf} = F_{gp}(1-e^2)^{1/2} \tag{4.29}$$

and using the force expression as given by

$$(\theta = \pi/2) : F_{ge} \;=\; e^{2\nu_0(r,\pi/2)}\nu_0'(r,\pi/2), \tag{4.30}$$

$$(\theta = 0) : F_{gp} \;=\; e^{2\nu_0(r,0)}\nu_0'(r,0), \tag{4.31}$$

and F_{cf} as in (4.25), the eccentricity of the configuration would be given by

$$e^2 = \left(1 - \left[\frac{F_{cf} - F_{ge}}{F_{gp}}\right]^2\right) \tag{4.32}$$

and the ellipticity in the limit of slow rotation $e << 1$, is

$$\epsilon = \frac{1}{2}e^2. \tag{4.33}$$

4.3 Hartle potentials and optical reference geometry

In the previous section we have described the forces on an axisymmetric and stationary spacetime considering the optical reference geometry and then generalized the Newtonian force balance equation to derive the ellipticity for a slowly rotating spheroid. As the Hartle metric represents a slowly rotating body, expressing the forces as obtained above in terms of the Hartle-Thorne potentials upto second order in Ω, one gets

$$F_{cf} = r^2\bar{\omega}^2(1/r - \nu_0'/2), \tag{4.34}$$

$$F_{ge} = \frac{1}{2}e^{\nu_0}[\nu_0'(1 + 2h_0 - h_2) + 2h_0' - h_2'], \tag{4.35}$$

$$F_{gp} = \frac{1}{2}e^{\nu_0}[\nu_0'(1 + 2h_0 + 2h_2) + 2h_0' + 2h_2'], \tag{4.36}$$

yielding for the ellipticity

$$\epsilon = 3(h_2 + h_2'/\nu_0') + \frac{r^2\bar{\omega}^2}{e^{\nu_0}}(2/r\nu_0' - 1) \tag{4.37}$$

in optical reference geometry.

4.4 Quasi-stationary and semi-adiabatic contraction

As described in chapter 2, for a given central density and angular velocity, we can obtain all quantities describing the structure of a slowly rotating body. A sequence of such configurations with decreasing radii R can approximately indicate the quasi-stationary and semi-adiabatic collapse of the body if mass M and angular momentum J are conserved throughout the sequence (Chandrasekhar & Miller 1974, Miller 1977). This is so because, for an axisymmetric gravitational contraction, the gravitational radiation does not carry away angular momentum and the change in mass due to energy liberated through radiation is of the fourth order in Ω. Since we are keeping corrections upto Ω^2, J and M are constant in this approximation. While studying the homogeneous distribution numerically, we can fix mass and angular momentum separately for the whole sequence, as pressure is not related to energy density. In that case, for a fixed value of M and varying radius R, we can calculate the corresponding values of energy density thus describing the structure of the non-rotating body. Further, using equations (2.31) and (2.32), for a fixed value of angular momentum J, we calculate the angular velocity and dragging of inertial frame, which are used to obtain all other rotational perturbations.

4.5 Results and Discussion

As a first attempt we have studied the behaviour of centrifugal force and ellipticity in optical reference geometry for a slowly rotating, contracting homogeneous fluid distribution and have compared the results with the ellipticity

$$\epsilon_{H-T}(r) = -\frac{3}{2}\left[\frac{\xi_2(r)}{r} + v_2(r) - h_2(r)\right], \tag{4.38}$$

which is derived using equations (2.57) and (4.33), and has been studied by Chandrasekhar & Miller (1974).

For the homogeneous distribution, the non-rotating structure is described by the Schwarzschild interior solution. Hence, using the analytical forms of pressure, mass and metric function ν_0, the rotational corrections are computed by integrating the set of differential equations (equations 2.27 to 2.49) with the specified initial conditions, using Runge-Kutta method. Then the centrifugal force and ellipticity are obtained by substituting these quantities in equations (4.34) and (4.37).

Writing the expressions in dimensionless units

$$\bar{F}_{cf} = \frac{F_{cf}}{(J^2/R_s^5)}, \quad \bar{\epsilon} = \frac{\epsilon}{(J^2/R_s^4)}, \tag{4.39}$$

where $R_s(= 2M)$ is the Schwarzschild radius, we have evaluated these quantities for a sequence of homogeneous slowly rotating configurations with decreasing radii keeping M and J conserved.

A comparison of Fig (4.1) and Fig (4.2) demonstrates the correspondence in the general behaviour of the ellipticity and the centrifugal force, which supports the conjecture of Abramowicz & Miller (1990) that the main cause of the reversal in the behaviour of ellipticity is not associated with dragging of inertial frames, but instead, can be connected to the general change in behaviour of centrifugal effects in general relativistic situations i.e., in strong fields.

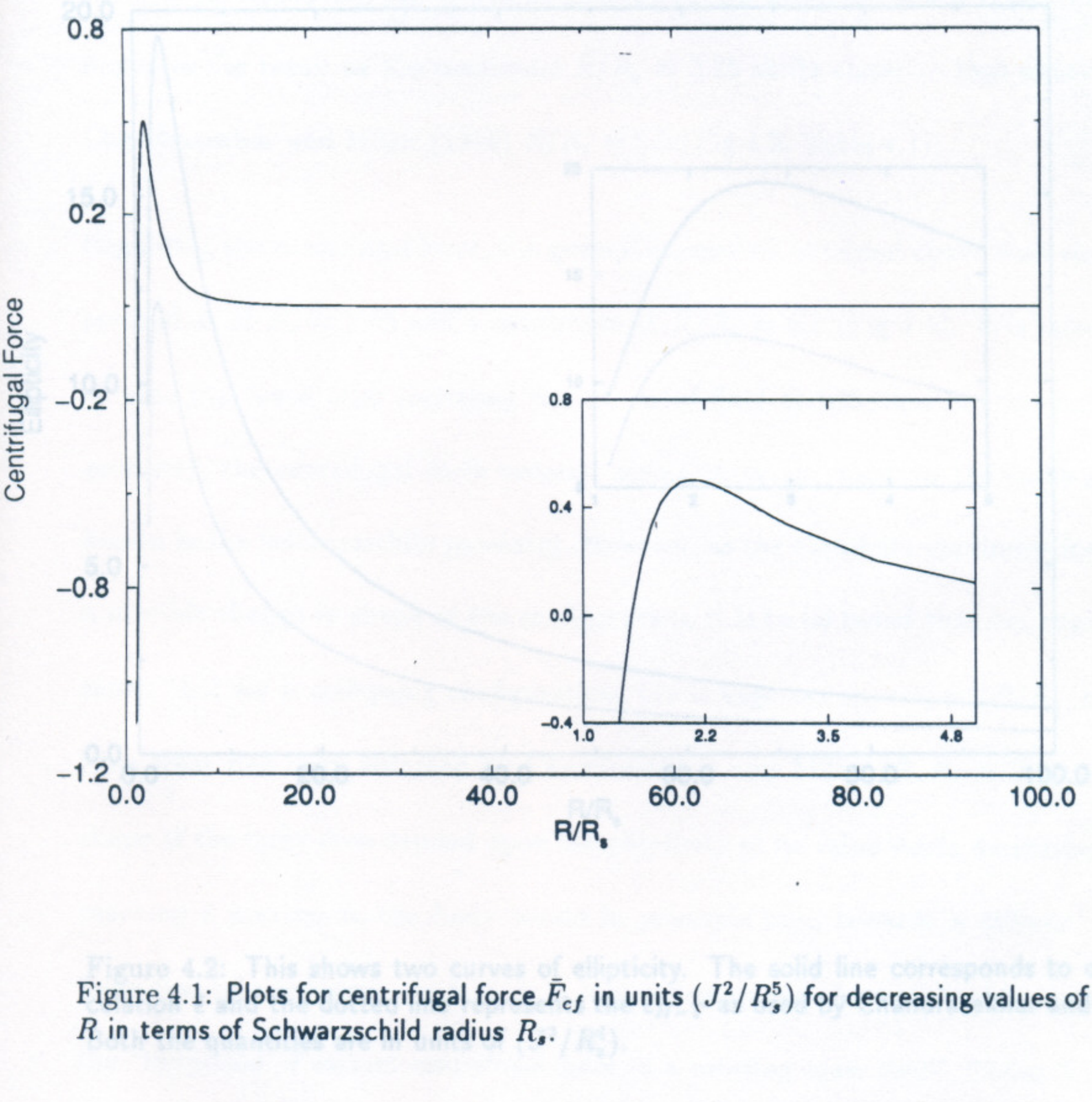

Figure 4.1: Plots for centrifugal force $\bar{F}_{cf}$ in units (J^2/R_s^5) for decreasing values of radius R in terms of Schwarzschild radius R_s.

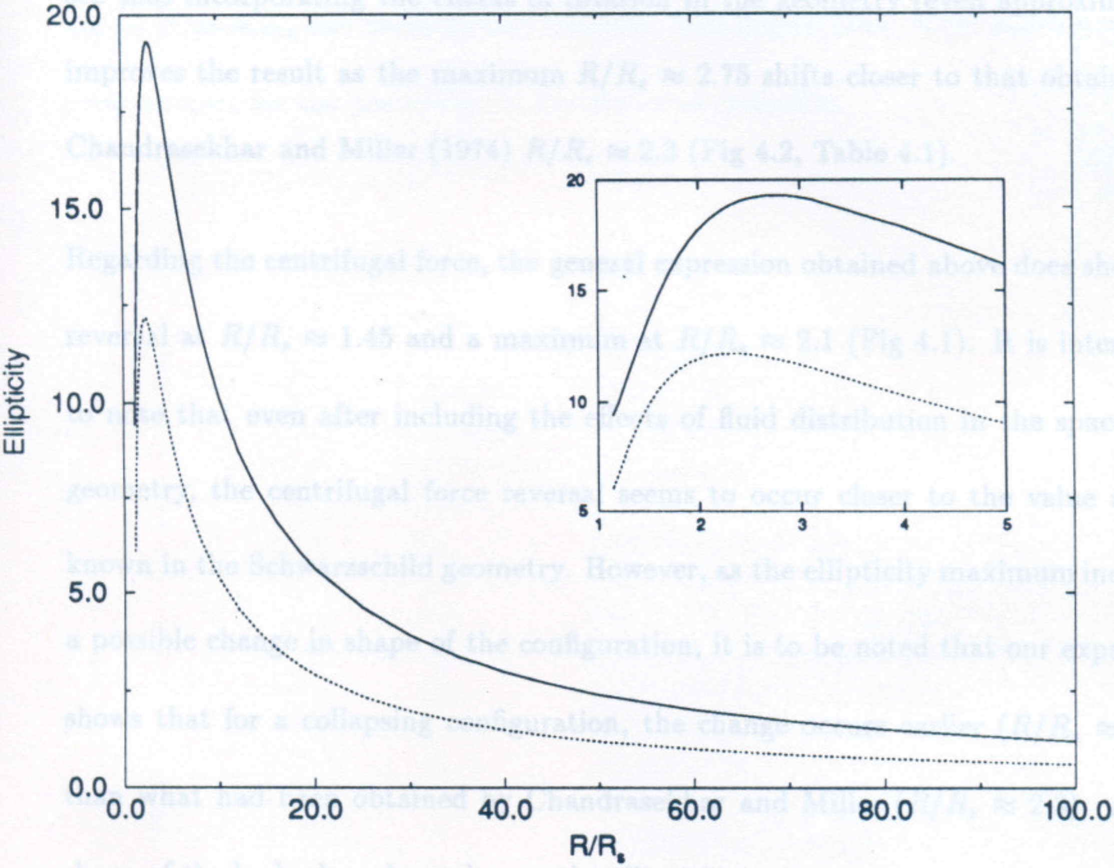

Figure 4.2: This shows two curves of ellipticity. The solid line corresponds to our calculation $\bar{\epsilon}$ and the dotted line represents the $\bar{\epsilon}_{H-T}$ as used by Chandrasekhar and Miller. Both the quantities are in units of (J^2/R_s^4).

However, comparing our present result with that of Abramowicz and Miller, who had obtained the maximum at $R/R_s = 3$, using pure Schwarzschild geometry, we see that incorporating the effects of rotation in the geometry (even approximately) improves the result as the maximum $R/R_s \approx 2.75$ shifts closer to that obtained by Chandrasekhar and Miller (1974) $R/R_s \approx 2.3$ (Fig 4.2, Table 4.1).

Regarding the centrifugal force, the general expression obtained above does show the reversal at $R/R_s \approx 1.45$ and a maximum at $R/R_s \approx 2.1$ (Fig 4.1). It is interesting to note that even after including the effects of fluid distribution in the space time geometry, the centrifugal force reversal seems to occur closer to the value as was known in the Schwarzschild geometry. However, as the ellipticity maximum indicates a possible change in shape of the configuration, it is to be noted that our expression shows that for a collapsing configuration, the change occurs earlier ($R/R_s \approx 2.75$) than what had been obtained by Chandrasekhar and Miller ($R/R_s \approx 2.3$). As the shape of the body does depend upon the ellipticity as its value starts decreasing after reaching a maximum, the body would in principle tend towards a different shape from that of a spheroid. In fact, it is interesting to note here that while discussing the "induction of correct centrifugal force in a rotating mass shell" Pfister & Braun (1985) have also observed that the ellipticity function shows a behaviour of reaching a maximum, while the function itself is negative indicating the shape of the shell to be prolate. However, as the inside of the shell is considered to be flat, one cannot compare our result exactly with this. But the fact that introduction of the correct centrifugal force in the kinematics does lead to a change in the shape of the body is indeed interesting and needs further analysis. This deformation might have interesting consequences for the generation of gravitational radiation.

R/R_s	$\bar{\epsilon}_{H-T}$	$\bar{\epsilon}$	$\bar{F}_{cf}$
1.125	5.604732E+0	9.135673E+0	-1.105476E+0
1.150	6.090158E+0	9.419599E+0	-1.111393E+0
1.200	6.728176E+0	9.973936E+0	-1.006851E+0
1.300	7.970848E+0	1.121079E+1	-6.367954E-1
1.400	9.033281E+0	1.249040E+1	-2.781407E-1
1.500	9.893101E+0	1.370501E+1	1.036231E-4
1.600	1.056893E+1	1.479904E+1	1.982318E-1
1.700	1.108810E+1	1.575131E+1	3.318464E-1
1.800	1.147746E+1	1.656041E+1	4.172701E-1
1.900	1.176069E+1	1.723471E+1	4.679588E-1
2.000	1.195771E+1	1.778676E+1	4.941394E-1
2.100	1.208496E+1	1.823045E+1	5.033122E-1
2.200	1.215588E+1	1.857943E+1	5.008806E-1
2.300	1.218139E+1	1.884639E+1	4.906997E-1
2.400	1.217034E+1	1.904277E+1	4.755023E-1
2.500	1.212995E+1	1.917867E+1	4.572160E-1
2.600	1.206606E+1	1.926295E+1	4.371926E-1
2.700	1.198343E+1	1.930324E+1	4.163726E-1
2.750	1.193634E+1	1.930894E+1	4.058754E-1
2.800	1.188595E+1	1.930607E+1	3.954040E-1
2.900	1.177679E+1	1.927725E+1	3.747254E-1
3.000	1.165855E+1	1.922168E+1	3.546271E-1
4.000	1.029998E+1	1.788030E+1	2.021015E-1
5.000	9.029724E+0	1.615380E+1	1.209157E-1
10.000	5.351696E+0	1.014123E+1	1.982923E-2
20.000	2.896627E+0	5.641617E+0	2.794844E-3
35.000	1.710614E+0	3.370030E+0	5.475721E-4
50.000	1.213098E+0	2.400532E+0	1.914418E-4
80.000	7.668072E-1	1.523602E+0	4.751822E-5
100.000	6.157617E-1	1.224927E+0	2.446291E-5

Table 4.1: It shows the ellipticity $\bar{\epsilon}$ (equation 4.37), $\bar{\epsilon}_{H-T}$ (equation 4.38) and the centrifugal force $\bar{F}_{cf}$ (equation 4.34) (units of these quantities are described in equation 4.39) for a sequence of decreasing radius with conserved mass and angular momentum for a homogeneous distribution.

Chapter 5

Effects of equations of state on electromagnetic fields and equilibrium structure

5.1 Introduction

As mentioned in the chapter 1, the structure and dynamics of neutron star depend sensitively on the equations of state (EOS) at high densities $\rho > 2.8 \times 10^{14}\mathrm{gm\ cm^{-3}}$. Due to lack of exact theory for the interactions among the particles at such high densities, a number of equations of state exist which are considered to be good candidates to model neutron star's interior. Each of these equations of state are in agreement with some of the observational facts. Though a number of studies (Sabbadini & Hartle 1973; Chitre & Hartle 1976; Iyer et al. 1985 etc.) are devoted to estimate the maximum and minimum stable masses, radius etc. of these objects based on some general assumptions, these quantities are sensitive to the choice of equation of state. Cook et al. (1994) and Salgado et al. (1994a, b) studied general properties of a rapidly rotating neutron star for a large number of ($\approx 10 - 15$) equations of state. Weber & Glendenning (1992) studied and tabulated the properties of rotating neutron star for 17 EOS considering the Hartle metric. Further Datta et al. (1995a) and Bhattacharya & Datta (1996) discussed neutron star crustal density profiles and the magnetic field evolution inside the star for several EOS models. They found that the stiffer the equation of state, larger the crust thickness for a given neutron star mass, leading to the larger time scales for field decay.

Since centrifugal force and ellipticity become important to understand the shape and the deformation of a rotating body, we have studied their behaviour for slowly rotating contracting system for four equations of state, and further extended the analysis of electromagnetic field structure inside the star for these equations of state. Though the choice of these equations of state is not very exhaustive, it serves to illustrate the role of equations of state (especially dependence on the softness and stiffness) in deciding the shape and magnetic fields of these objects. A brief description of these equations of state models is given in the following section. In section 3 their effects on centrifugal force and ellipticity are discussed, whereas description of the form of magnetic field inside the star and its dependence on equations of state and rotation is given in section 4 and 5.

5.2 Equations of state

Model A : Pandharipande (1971a, b) studied the behaviour of dense neutron matter and hyperon matter respectively using a many-body theory based upon the variational approach suggested by Jastrow (1955). To describe the nuclear interactions, the Reid nucleon-nucleon potential was used (Reid 1968) which was suitably altered to represent the different isospin states of the hyperonic matter ($\Lambda, \Sigma^{\pm}$). The suggestion that hyperons may be additional baryonic constituent of neutron star interiors was first made by Ambartsumyan & Saakyan (1960). There have been several theoretical attempts aimed at deriving the equations of state of baryonic liquid made up of neutrons, protons and hyperons. However, this still remains an open problem as knowledge of hyperon-nucleon and hyperon-hyperon interactions and their coupling constants have large uncertainties. In our studies we are considering the Pandharipande (1971 b) equation of state representing the hyperonic matter.

Model B : Wiringa et al. (1988) proposed a model for dense nuclear and neutron matter which is firmly based on available nuclear data. This is a non-relativistic model based on the variational method and includes three-nucleon interactions. The nuclear matter is in beta equilibrium with electrons, protons and muons. The three-body potential considered by the authors, includes long-range repulsive parts that are adjusted to give light nuclei binding energies and nuclear matter saturation properties, alongwith the intermediate and short-range parts coming from exchange of pions, heavier mesons or overlaps of composite quark systems. The model is an improvement over the calculations of Friedman & Pandharipande (1981) regarding the long-range attraction term in the Hamilton. These authors gave three models denoted as: AV14+UVII, UV14+UVII and UV14+TNI, the first term in each of it expresses the two-body potential whereas second term in each of this model denotes the phenomenological three-nucleon interaction. We are considering the model, UV14+UVII, and will be referred in our studies as Model B.

Model C : Walecka (1974) gave an EOS for pure neutron matter at high densities based on a relativistic approach, using scalar and vector meson exchange interactions. The exchange of these mesons among nucleons is known to provide the short-range repulsion and intermediate-range attraction in the nucleon-nucleon potential. The effective interaction is characterized by the meson parameters such as their masses and coupling constants, which are adjusted to reproduce the saturation property of equilibrium nuclear matter.

Model D : Sahu et al. (1993) gave a field theoretical EOS for high density matter, assuming the composition to be neutron rich matter in beta equilibrium based on the chiral sigma model. The model includes an isoscalar vector field generated dynamically and reproduces the empirical values of the saturation density and binding energy of equilibrium nuclear matter. It also gives the right isospin symmetry coefficient for asymmetric nuclear matter by incorporating the interactions due to the isospin triplet ρ meson. The energy per nucleon of nuclear matter is in good agreement upto about four times the equilibrium nuclear matter density with estimates inferred from heavy-ion collision experimental data.

An equation of state is said to be stiff, if for a given density it has larger net pressure which comes due to more repulsion among the constituent particles. In the case of soft EOS it will mean higher attraction. Model A and B are relatively soft EOS whereas Model C and D represent very stiff EOS. Fig (5.1), show logarithmic plot (ρ vs p) for these four EOS. These EOS are joined with EOS Negele & Vautherin (1973), Baym et al. (1971) and Feynman et al. (1949) for density 10^{14} to 5×10^{10} gm cm^{-3}, till $\approx 10^3$ gm cm^{-3} and below 10^3 gm cm^{-3} respectively, to give the entire span of neutron star densities.

5.3 Centrifugal force and ellipticity

In the case of non-homogeneous distribution, while computing the set of equations, it is not possible to keep M and J conserved independently, but since all the quantities expressing deformation can be determined as functions of r/R in the units of R/R_s and J/M^2, the sequence of equilibrium configurations with fixed J/M^2 can be used to describe approximately, the contraction of slowly rotating body.

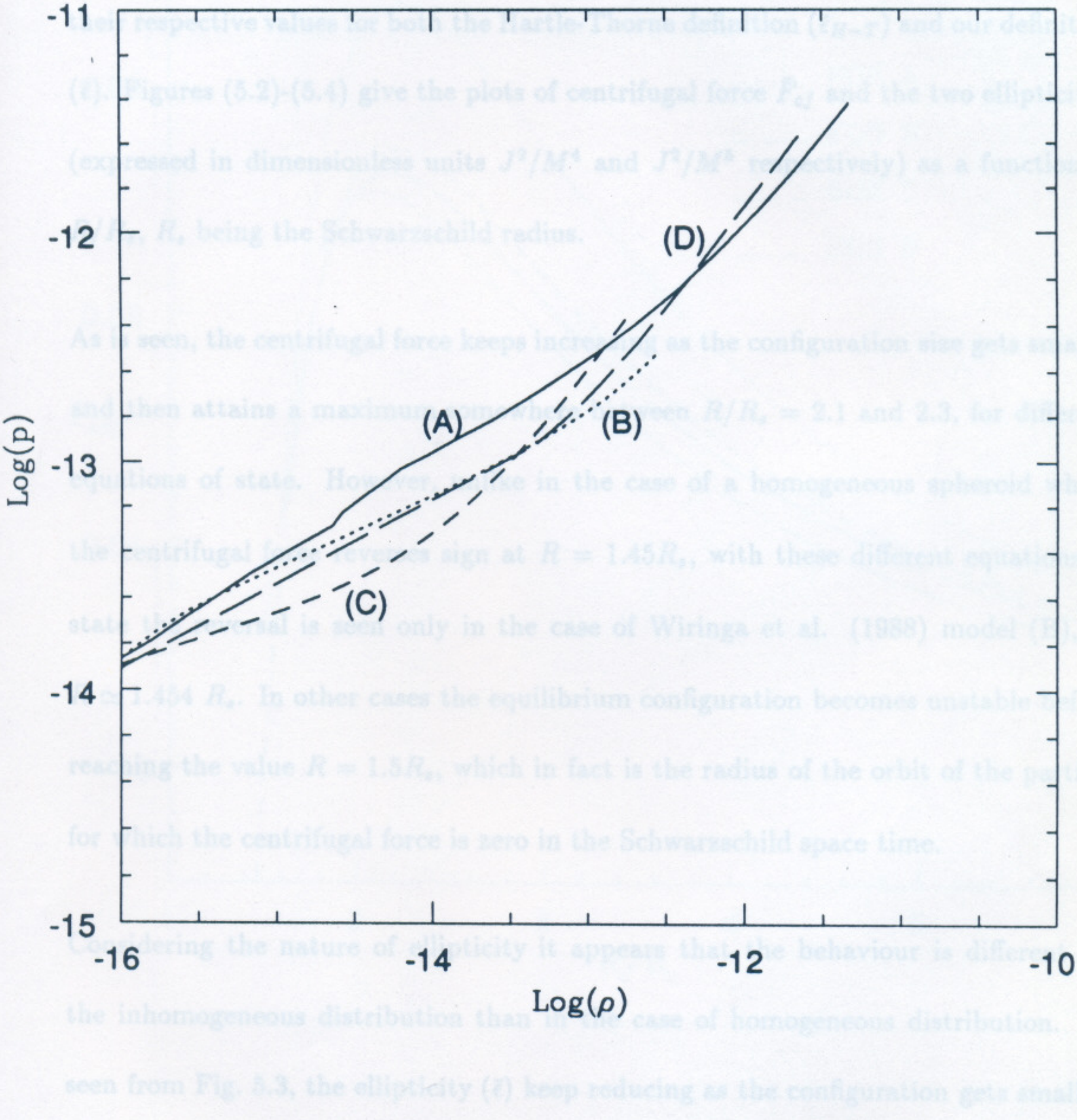

Figure 5.1: Logarithmic plot of density (ρ) vs. pressure (p) in geometrized units ($G = c = 1$).

The equations and procedure used are similar as discussed in chapter 4. Table 5.1 shows the location of extrema for the centrifugal force as well as for the ellipticity and their respective values for both the Hartle-Thorne definition ($\bar{\epsilon}_{H-T}$) and our definition ($\bar{\epsilon}$). Figures (5.2)-(5.4) give the plots of centrifugal force $\bar{F}_{cf}$ and the two ellipticities (expressed in dimensionless units J^2/M^4 and J^2/M^5 respectively) as a function of R/R_s, R_s being the Schwarzschild radius.

As is seen, the centrifugal force keeps increasing as the configuration size gets smaller and then attains a maximum somewhere between $R/R_s = 2.1$ and 2.3, for different equations of state. However, unlike in the case of a homogeneous spheroid where the centrifugal force reverses sign at $R = 1.45R_s$, with these different equations of state the reversal is seen only in the case of Wiringa et al. (1988) model (B), at $R \simeq 1.454\ R_s$. In other cases the equilibrium configuration becomes unstable before reaching the value $R = 1.5R_s$, which in fact is the radius of the orbit of the particle for which the centrifugal force is zero in the Schwarzschild space time.

Considering the nature of ellipticity it appears that the behaviour is different for the inhomogeneous distribution than in the case of homogeneous distribution. As seen from Fig. 5.3, the ellipticity ($\bar{\epsilon}$) keep reducing as the configuration gets smaller, becomes zero (meaning that the shape becomes spherical) and further on gets to a negative value. However, the negative value attains a minimum and then again the ellipticity starts increasing.

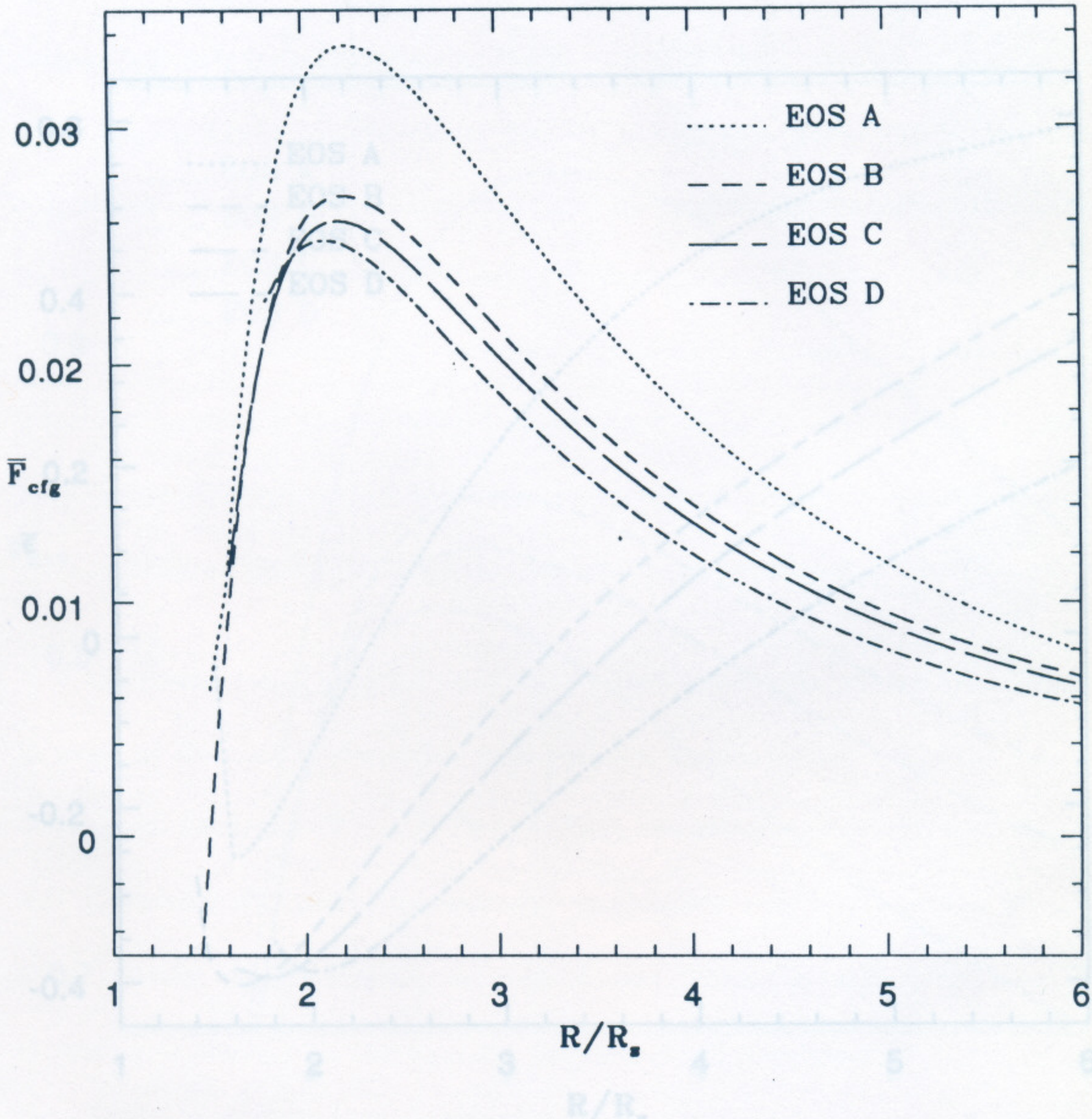

Figure 5.2: Centrifugal force $\bar{F}_{cfg}$ in units (J^2/M^5) for decreasing values of radius R in terms of Schwarzschild radius R_s for various equations of state. EOS A is the softest and EOS D represents the stiffest equation of state among the four considered equations of state.

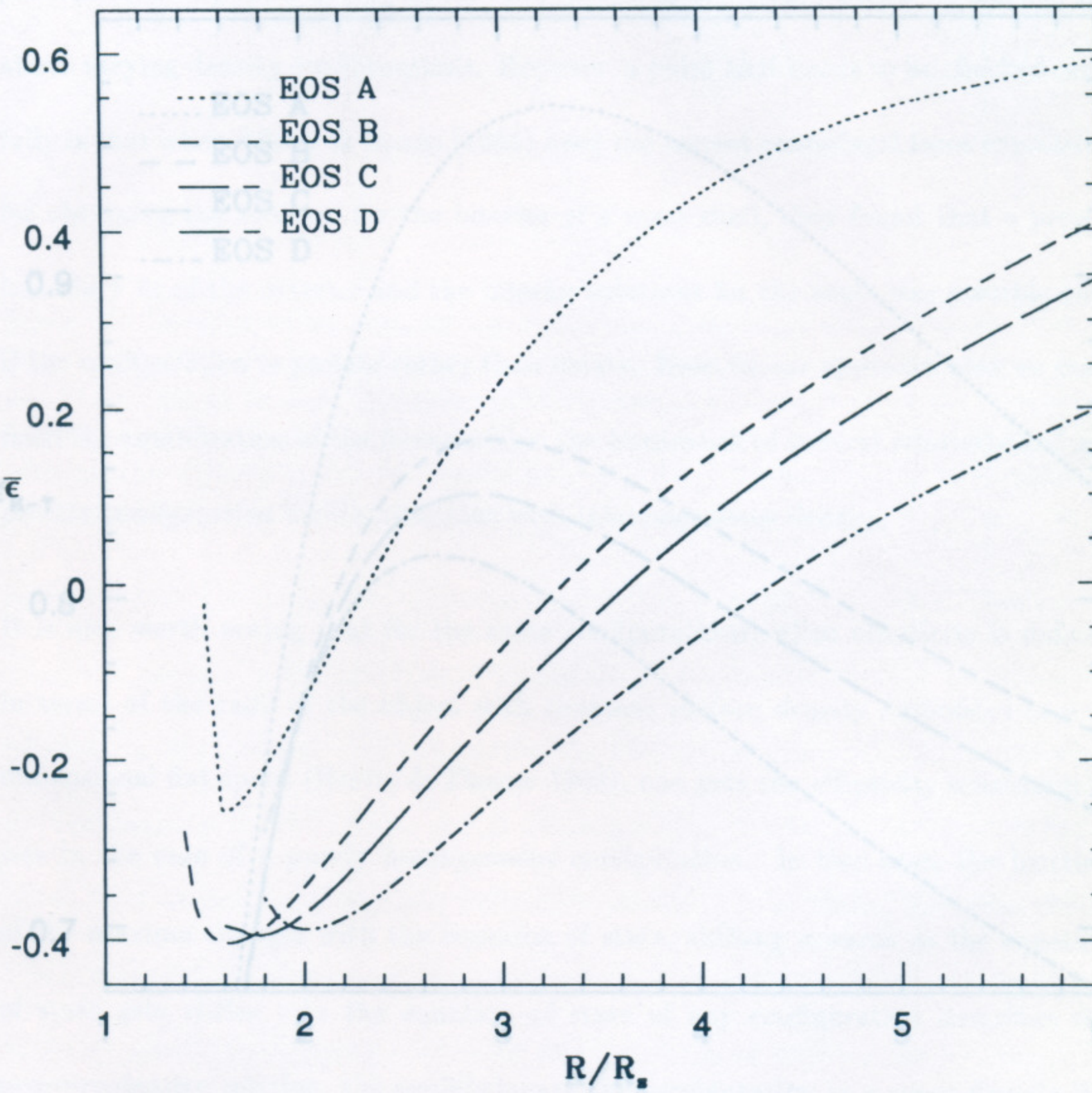

Figure 5.3: Ellipticity $\bar{\epsilon}$ in units of J^2/M^4, derived in optical reference geometry.

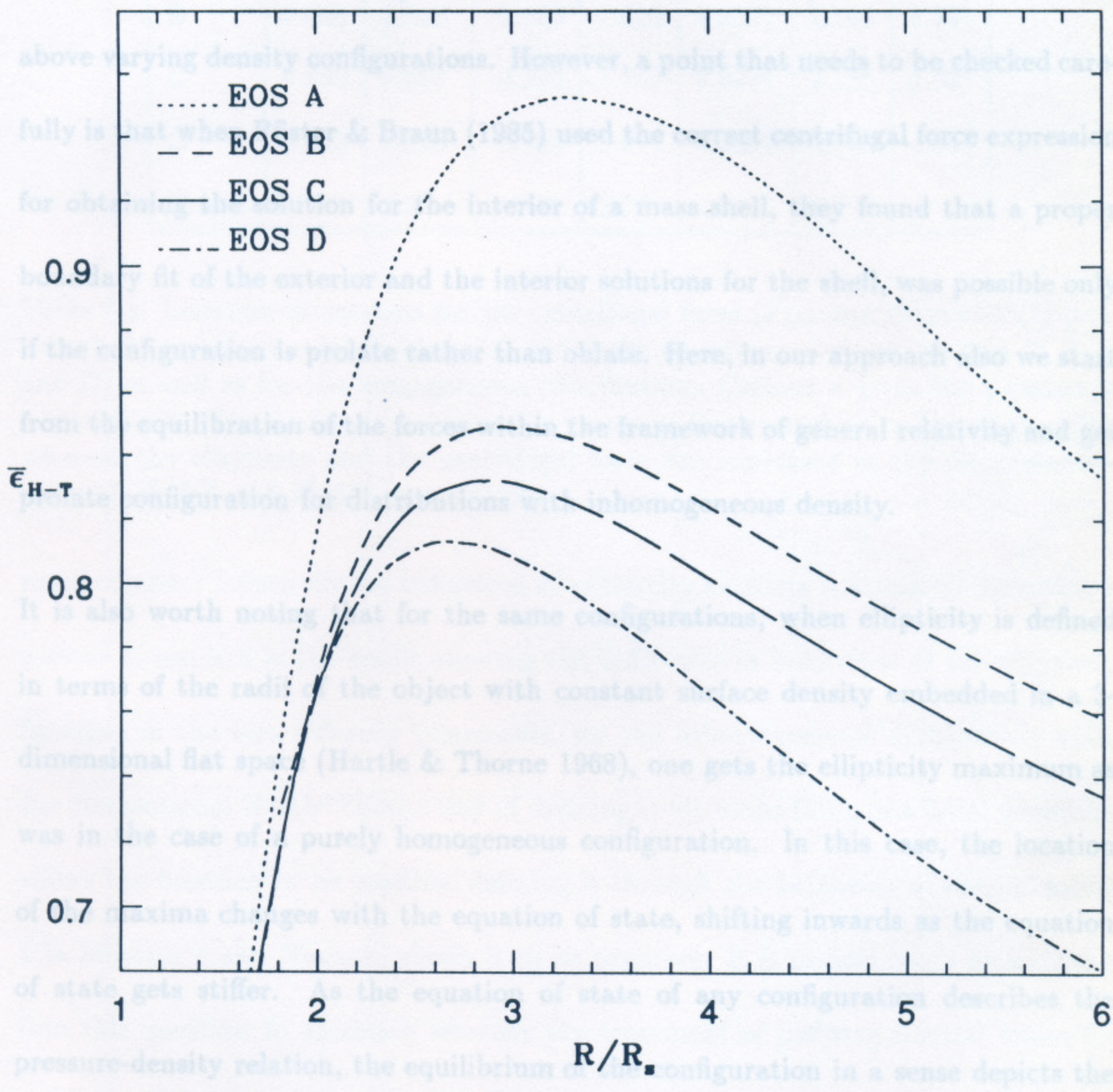

Figure 5.4: Ellipticity $\bar{\epsilon}_{H-T}$ as defined by Hartle and Thorne in the units of J^2/M^4.

The fact that the ellipticity starts decreasing and further becomes negative, could be due to the reason that the force balance equation used in defining the ellipticity is perhaps true only for a homogeneous distribution of the fluid, whereas we have in the above varying density configurations. However, a point that needs to be checked carefully is that when Pfister & Braun (1985) used the correct centrifugal force expression for obtaining the solution for the interior of a mass shell, they found that a proper boundary fit of the exterior and the interior solutions for the shell, was possible only if the configuration is prolate rather than oblate. Here, in our approach also we start from the equilibration of the forces within the framework of general relativity and get prolate configuration for distributions with inhomogeneous density.

It is also worth noting that for the same configurations, when ellipticity is defined in terms of the radii of the object with constant surface density embedded in a 3-dimensional flat space (Hartle & Thorne 1968), one gets the ellipticity maximum as was in the case of a purely homogeneous configuration. In this case, the location of the maxima changes with the equation of state, shifting inwards as the equation of state gets stiffer. As the equation of state of any configuration describes the pressure-density relation, the equilibrium of the configuration in a sense depicts the balancing of the various forces like gravity, material binding and the centrifugal force. As the equations of state gets stiffer the intra-nucleonic forces, which are effectively repulsive at very short range become larger, thus requiring the configuration to get

EOS	$\bar{\epsilon}_{H-T}$	$R_{\bar{\epsilon}_{H-T}}$	$\bar{\epsilon}$	$R_{\bar{\epsilon}}$	$\bar{F}_{cf}$	$R_{\bar{F}_{cf}}$	$R_{\bar{\epsilon}_{rev.}}$
A	0.953	3.278	-0.257	1.603	0.0335	2.234	2.297
B	0.849	2.948	-0.403	1.610	0.0271	2.204	3.301
C	0.832	2.857	-0.395	1.769	0.0261	2.180	3.631
D	0.813	2.625	-0.388	2.014	0.0252	2.112	4.343
Homo.	0.761	2.3	1.207	2.75	0.0157	2.1	

Table 5.1: Location of extrema for the centrifugal force ($\bar{F}_{cf}$) and ellipticity ($\bar{\epsilon}$) (column 7, 5) and their values (column 6, 4) for the equations of state: Models A, B, C and D, as well as for the homogeneous distribution. Column 8 gives the location of reversal in $\bar{\epsilon}$. The radius is expressed in terms of Schwarzschild radius $R_s (= 2M)$, whereas the ellipticity and the centrifugal force are expressed in the dimensionless units of J^2/M^5 and J^2/M^4, respectively.

more compact before similar behaviour of ellipticity extrema is attained. However, a matter of concern is the result showing the difference in behaviour of the ellipticity function in the two different treatments, for the inhomogeneous distribution while the conventional Hartle-Thorne way of defining it via embedding in a 3-flat geometry shows the function to be positive, defining it through the balancing of inertial forces a la Maclaurin and Newton, shows it to be negative. It is important to look deeper into this question to ascertain whether the treatment of defining inertial forces for a fluid configuration has to be different from the approach used for a single particle dynamics, particularly for inhomogeneous distributions.

5.4 Electromagnetic fields

The studies of electromagnetic fields inside the neutron stars become important in connection with understanding the mechanisms of pulsar glitches, superfluidity, thermal evolution etc. Apart from that, the evolution and origin of these fields also affect the field strength on the surface. In recent years number of works (Thompson & Duncan 1993; Urpin & Ray 1994; Wiebicke & Geppert 1995; Urpin & Shalybkov 1995; Bhattacharya & Datta 1996) have discussed the generation and evolution of internal magnetic fields in the non-relativistic approach. As for relativistic effects in studying the structure of magnetic field inside a rotating neutron star, one of the studies made is, by Bocquet et al. (1995). They solved numerically the coupled Einstein-Maxwell equations in full general relativistic framework considering magnetic field to be axisymmetric and poloidal in nature. Further they studied its effects on the structure of neutron star employing different equations of state. Rather than solving the complete set of coupled equations numerically, we have extended our studies of the electromagnetic fields (as discussed in chapter 3) inside the slowly rotating body, in the same approach as was done for the external field.

5.4.1 Maxwell's equations for inside the star

Interior of neutron star is considered to be a perfect conductor. Hence the electric field inside the star is zero, but due to the rotation the magnetic field gets modified as

$$B_r = B_r^0 + \delta B_r, \qquad B_\theta = B_\theta^0 + \delta B_\theta \tag{5.1}$$

where B_r^0 and B_θ^0 are the fields for the body when it is not rotating and δB_r and δB_θ are the corrections due to the rotation of the order Ω^2. The Maxwell's equations inside the star, using the corrections of angular velocity for $l = 0$ are written as

$$\begin{aligned} &\frac{\partial}{\partial r}\left[re^{\nu_0/2}(1+h_0)B_\theta\right] \\ -\frac{\partial}{\partial \theta}\left[e^{\nu_0/2}\left(1-\frac{2m}{r}\right)^{-1/2}\left(1+h_0+\frac{m_0}{r-2m}\right)B_r\right] &= 0 \end{aligned} \tag{5.2}$$

$$\frac{\partial}{\partial r}\left[r^2\sin\theta B_r\right] + \frac{\partial}{\partial \theta}\left[r\sin\theta\,(1-2mr)^{-1/2}(1-\frac{m_0}{r-2m})B_\theta\right] = 0 \tag{5.3}$$

Assuming the magnetic field to be dipolar in nature, the field components can be written as

$$B_r = f(r)\cos\theta, \qquad B_\theta = g(r)\sin\theta \tag{5.4}$$

then the equations (5.2) and (5.3), reduce to ordinary differential equations

$$\begin{aligned} r(1+h_0)\frac{dg}{dr} + g\left[(1+h_0)\left(1+\frac{1}{2}r\frac{d\nu_0}{dr}\right)+r\frac{dh_0}{dr}\right] & \\ +\left(1-\frac{2m}{r}\right)^{-1/2}\left(1+h_0+\frac{m_0}{r-2m}\right)f &= 0 \end{aligned} \tag{5.5}$$

$$r\frac{df}{dr} + 2f + 2\left(1-\frac{2m}{r}\right)^{-1/2}\left(1-\frac{m_0}{r-2m}\right)g = 0. \tag{5.6}$$

5.4.2 Initial conditions

Further taking the fields to be continuous at the surface of the star, the inside fields are integrated from boundary to the center. The form of the fields at boundary is obtained to be

$$B_r^{\,0}(R) = -\frac{3\mu}{4M^3}\left[\ln\left(1-\frac{2M}{R}\right)+\frac{2M}{R}+\frac{2M^2}{R^2}\right]\cos\theta \tag{5.7}$$

$$\begin{aligned} B_\theta^{\,0}(R) = {} & \frac{3\mu}{4M^2R}\left[\left(1-\frac{2M}{R}\right)^{-1}+\frac{R}{M}\ln\left(1-\frac{2M}{R}\right)+1\right] \\ & \left(1-\frac{2M}{R}\right)^{1/2}\sin\theta \end{aligned} \tag{5.8}$$

$$\delta B_r(R) = \frac{12\mu}{R^4}\left[\delta M\left(\frac{1}{4}+\frac{4}{5}\frac{M}{R}\right)-\frac{J^2}{R^3}\left(\frac{1}{14}+\frac{3}{10}\frac{M}{R}\right)\right]\cos\theta \tag{5.9}$$

$$\delta B_\theta(R) = \frac{\mu}{R^4}\left[\delta M\left(\frac{1}{2}+\frac{37}{5}\frac{M}{R}\right)-\frac{J^2}{R^3}\left(\frac{8}{7}+\frac{163}{35}\frac{M}{R}\right)\right]\sin\theta \tag{5.10}$$

which we have derived by taking an ansatz and keeping the terms linear in M/R and Ω^2.

5.5 Results and Discussions

Taking initial conditions as equations (5.7 to 5.10) and using the Hartle metric for the above mentioned equations of state, we have integrated equations (5.5 and 5.6) thus obtaining the B_r and B_θ components inside the star from equation (5.4).

We have plotted field lines for different configurations and studied the field line topology which represents the constant magnetic flux and can be found by rotating a given filed line about the polar co-ordinate θ. The flux from $\theta = 0$ to any θ is given by

$$b(\theta) = \int_0^\theta B \,.\, da = \int_0^\theta B_r\, r^2 \sin\theta \, d\theta \, d\phi. \tag{5.11}$$

For the dipole field as given by equation (5.4), the field lines are

$$b(\theta) = \pi r^2 f(r) \sin^2\theta = constant. \tag{5.12}$$

Transforming these field lines to cartesian co-ordinate system with the magnetic dipole aligned about the z-axis, we have plotted them in the x-z plane (Fig 5.5) for the configurations with varying potential m/r, As the potential increases the field lines get denser.

For a given central density the field strength is higher for softer equation of state (Model A) (Fig 5.6), as well as for a given equation of state change in the field strength with respect to increase in central density is larger for softer equations of state. This shows that for the stiffer equations of state the field strength does not change substantially but it is comparatively more sensitive to the central density in the case of softer equations of state.

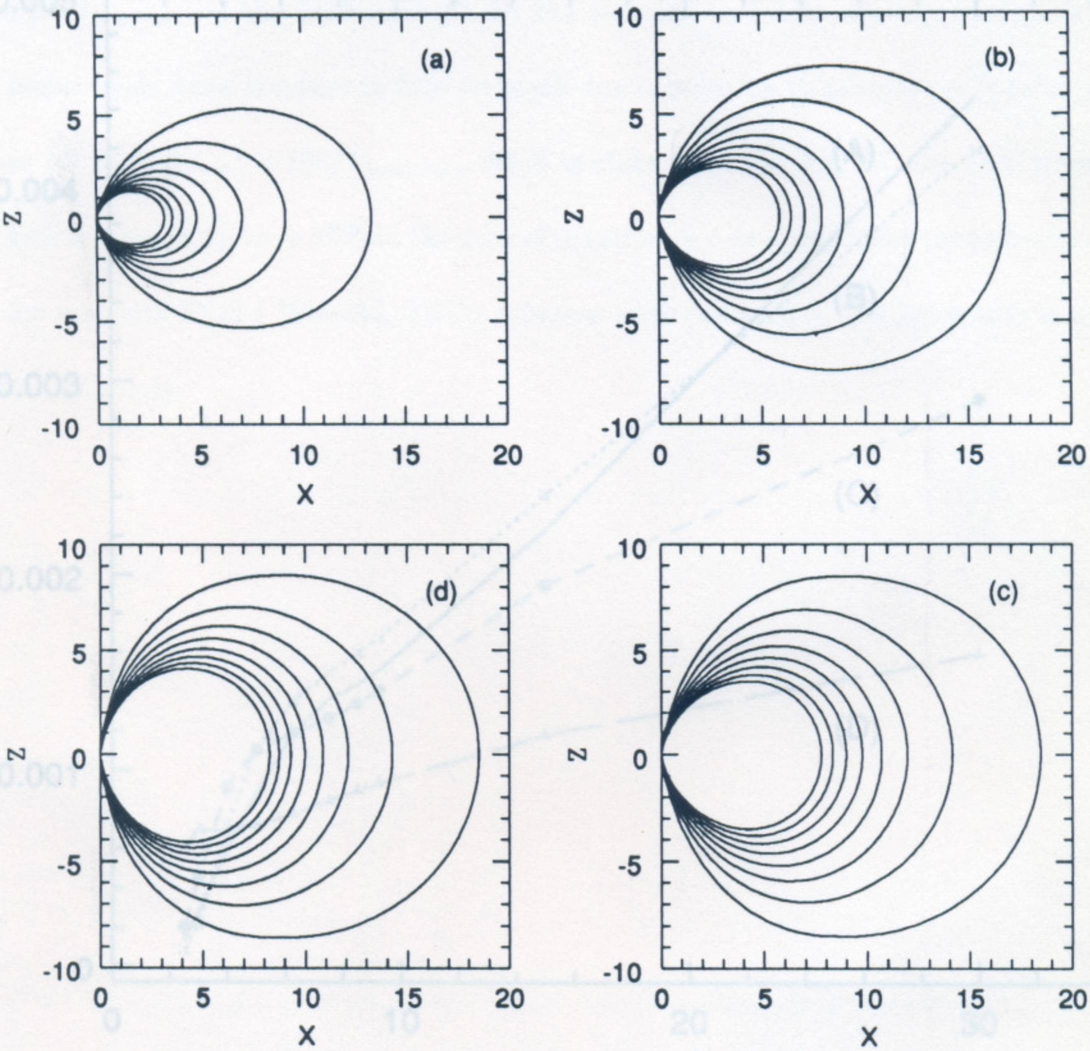

Figure 5.5: Field lines are plotted in x-z plane. Field strength is weaker for small gravitational potential (fig (a): $M/R = 0.039$) as compared to higher gravitational potential (fig (d): $M/R = 0.282$). Fig (b) has $M/R = 0.177$ and fig (c) has $M/R = 0.266$.

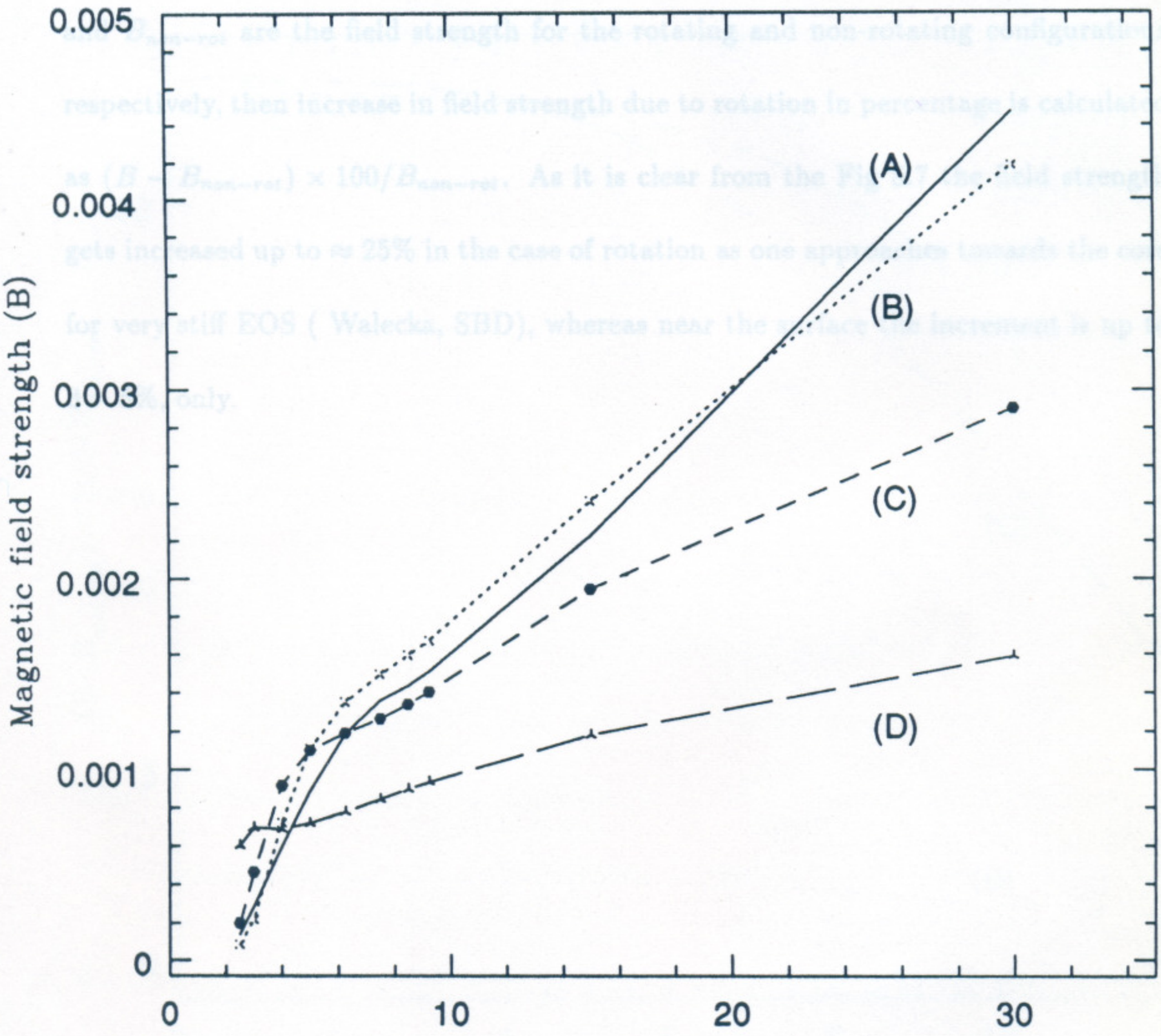

Figure 5.6: Shows change in the field strength with respect to increase in central density for a given EOS. Density is in gm cm^{-3} and B is in geometrized units.

Rotation also modifies the field strength, Fig 5.7 shows the increase in the field strength from the surface to the center for the considered equations of state. If B and $B_{non-rot}$ are the field strength for the rotating and non-rotating configurations respectively, then increase in field strength due to rotation in percentage is calculated as $(B - B_{non-rot}) \times 100/B_{non-rot}$. As it is clear from the Fig 5.7 the field strength gets increased up to $\approx 25\%$ in the case of rotation as one approaches towards the core for very stiff EOS (Walecka, SBD), whereas near the surface the increment is up to $3 - 5\%$, only.

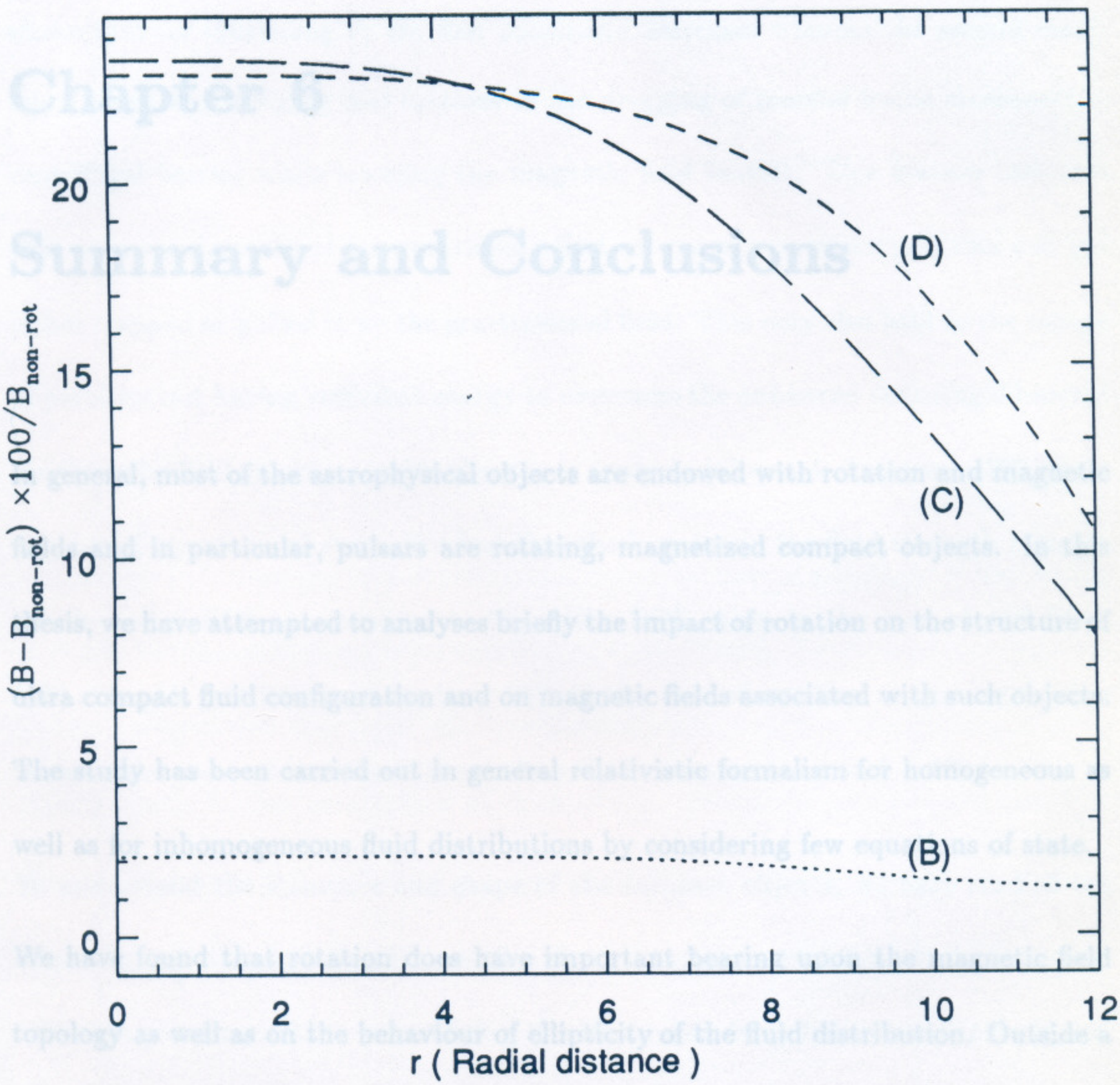

Figure 5.7: Percentage increase in the field strength (B) due to rotation from center to the surface. Radial distance (r) is in km. For Model A, increase is much smaller.

Chapter 6

Summary and Conclusions

In general, most of the astrophysical objects are endowed with rotation and magnetic fields and in particular, pulsars are rotating, magnetized compact objects. In this thesis, we have attempted to analyses briefly the impact of rotation on the structure of ultra compact fluid configuration and on magnetic fields associated with such objects. The study has been carried out in general relativistic formalism for homogeneous as well as for inhomogeneous fluid distributions by considering few equations of state.

We have found that rotation does have important bearing upon the magnetic field topology as well as on the behaviour of ellipticity of the fluid distribution. Outside a slowly rotating body, the structure of electromagnetic field is obtained (Prasanna & Gupta 1997) taking an ansatz and then the charged particle trajectories are studied. We find that for high values of L and λ the potential well appears far away from the body indicating the possible trapping of particles far outside the objects like neutron stars ($r = 20m, 30m$). Trapping of particles far away from the star indicates the possible formation of magnetospheres. The study of potential curves for varying $\tilde{J}$ shows that for increasing $\tilde{J}$, the first maximum decreases whereas the second maximum increases, implying that increase in the dragging of inertial frame increases the centrifugal barrier while lowering the magnetic field barrier. This feature indicates that as a consequence of the rotational effect on spacetime, more particles can get either trapped or pulled in by the gravitational field. This may also lead to the escape of particles not having sufficient energy to overcome the enhanced centrifugal barrier. Further, the field structure inside the star is analyses (Gupta & Prasanna 1997) for a number of equations of state. We find that the increase in the field strength is larger for the softer EOS as compared to the stiffer EOS. Also, in the case of stiff EOS, field strength gets increased up to $\approx 25\%$ in the case of rotation as one approaches towards the core, whereas near the surface the increment is up to $3 - 5\%$.

To understand the structure and shape of the compact objects, we have studied the ellipticity and the centrifugal force of a slowly rotating contracting body in optical reference geometry. After generalizing the Newtonian force balance equation by using the inertial forces as obtained in optical reference geometry, we have derived the expression for ellipticity and then compared it with ellipticity derived by Hartle & Thorne (1968). In the case of homogeneous matter distribution(Gupta et al. 1996a), comparison of general behavior of the ellipticity and centrifugal force support the conjecture of Abramowicz & Miller (1990) that the main cause of the reversal in behavior of ellipticity is not associated with dragging of inertial frames, but instead, can be connected to the general change in behavior of centrifugal effects in general relativistic situations i.e., in strong gravitational fields. Further, comparing our present result with that of Abramowicz and Miller, who had obtained the maximum at $R/R_s = 3$, using pure Schwarzschild geometry, we see that incorporating the effects of rotation in the geometry (even approximately) improves the result as the maximum $R/R_s \approx 2.75$ shifts closer to that obtained by Chandrasekhar & Miller (1974) $R/R_s \approx 2.3$, which indeed is more exact.

In the case of inhomogeneous distributions, the behaviour of ellipticity is not similar as it is in the case of homogeneous case(Gupta et al. 1996b). Ellipticity keeps reducing as the configuration contracts and becomes negative, implying that it acquires the prolate shape in the later stages of contraction. The negative ellipticity could be due to the reason that the force balance equation used in defining the ellipticity is perhaps true only for a homogeneous distribution of the fluid, and further analysis is needed to understand this aspect fully. The behaviour of centrifugal force and ellipticity as defined by Hartle & Thorne (1968) show similar behaviour as in the case of homogeneous distribution. In both the cases, maxima occur which shifts inward as the equation of state gets stiffer.

As this is only a beginning of the investigation we have found results of sufficient interest, which clearly show that further, more detailed analysis would perhaps give better insights into the structure and stability of rotating magnetized ultra compact objects, particularly within the framework of general relativity.

Bibliography

[1] Abramowicz M. A. and Miller J. C., 1990, *Ellipticity behaviour of relativistic Maclaurin spheroids*, Mon. Not. R. Astron. Soc., **245**, 729.

[2] Abramowicz M. A. and Prasanna A. R., 1990, *Centrifugal-force reversal near a Schwarzschild black hole*, Mon. Not. R. Astron. Soc., **245**, 720.

[3] Abramowicz M. A., Carter B. and Lasota J. P., 1988, *Optical reference geometry for stationary and static dynamics*, Gen. Rel. Grav., **20**, 1173.

[4] Abramowicz M. A., Nurowski P. and Wex N., 1993, *Covariant definition of inertial forces*, Class. Quant. Grav., **10**, L183.

[5] Abramowicz M. A., Nurowski P. and Wex N., 1995, *Optical reference geometry for stationary and axially symmetric spacetimes* , Class. Quant. Grav., **12**, 1467.

[6] Aguirregabiria J. M., Chamorro A., Nayak K. R., Suinaga J. and Vishveshwara C. V., 1996b, *Equilibrium of a charged test particle in the Kerr-Newman spacetime : Force analysis*, Class. Quant. Grav., **13**, 2179.

[7] Aguirregabiria J. M., Chamorro A., Suinaga J. and Vishveshwara C. V., 1995, *Equilibrium of a charged test particle in the Kerr-Newman spacetime*, Class. Quant. Grav., **12**, 699.

[8] Aguirregabiria J. M., Chamorro A., Suinaga J. and Vishveshwara C. V., 1996a, *Equilibrium of a charged test particle with spin in the Kerr-Newman spacetime*, Class. Quant. Grav., **13**, 417.

[9] Akima H., 1970, *A new method of interpolation and smooth curve fitting based on local procedures*, Journ. of the ACM., **17**, 589.

[10] Ambartsumyan V. A. and Saakyan G. S., 1960, *The degenerate superdense gas of elementary particles*, Sov. Astr., **4**, 187 (Translation of Astronomicheskii Zhurnal Vol. **37**, No: 2 (1960) p.193-209).

[11] Anderson J. L. and Cohen J. M., 1970, *Gravitational collapse of magnetic neutron stars*, Astrophys. Space Sci., **9**, 146.

[12] Anderson M. R. and Lemos J. P. S., 1988, *Viscous shear in the Kerr metric*, Mon. Not. R. Astron. Soc., **233**, 489.

[13] Baade W. and Zwicky F., 1934, *Supernovae and cosmic rays*, Phys. Rev., **45**, 138.

[14] Balek V., Bicak J. and Stuchlik Z., 1989, *The motion of the charged particles in the field of rotating charged black holes and naked singularities*, Bull. Astron. Inst. Czechosl., **40**, 133.

[15] Bardeen J. M., Press W. H. and Teukolsky S. A., 1972, *Rotating black holes: Locally non-rotating frames, energy extraction and scalar synchroton radiation*, Astrophys. J., **178**, 347.

[16] Barrabes C., Boisseau B. and Israel W., 1995, *Orbits, forces and accretion dynamics near spinning black holes*, Mon. Not. R. Astron. Soc., **276**, 432.

[17] Baym G. and Pethick C., 1975, *Neutron stars*, Ann. Rev. Nucl. Sci., **25**, 27.

[18] Baym G. and Pethick C., 1979, *Physics of neutron stars*, Ann. Rev. Astron. Astrophys., **17**, 415.

[19] Baym G., Pethick C. and Sutherland P. G., 1972, *The ground state of matter at high densities: Equation of state and stellar models*, Astrophys. J., **170**, 299.

[20] Bhattacharya D. and Datta B., 1996, *Ohmic decay of magnetic flux expelled from neutron star interiors*, Mon. Not. R. Astron. Soc., **282**, 1059.

[21] Bocquet M., Bonazzola S., Gourgoulhon E and Novak J., 1995, *Rotating neutron star models with a magnetic field*, Astron & Astrophys., **301**, 757.

[22] Bonazzola S., Gourgoulhon E., Salgado and Marck J. A., 1993, *Axisymmetric rotating relativistic bodies: a new numerical aprroach for "exact" solutions*, J. Astron. Astrophys., **278**, 421.

[23] Butterworth E. M. and Isper J. R., 1976, *On the structure and stability of rapidly rotating fluid bodies in general relativity. I. The numerical method for computing structure and its application to uniformly rotating homogeneous bodies*, Astrophys. J., **204**, 200.

[24] Cameron A. G. W., 1959, *Neutron star models*, Astrophys. J., **130**, 884.

[25] Canuto V., 1974, *Equation of state of ultrahigh densities, Part I.*, Ann. Rev. Astron. Astrophys., **12**, 167.

[26] Canuto V., 1975, *Equation of state of ultrahigh densities, Part II.*, Ann. Rev. Astron. Astrophys., **13**, 335.

[27] Chakrabarti S. K. and Prasanna A.,R., 1990, *The Newtonian forces in the Kerr geometry*, J. Astron. & Astrophys., **11**, 29.

[28] Chakraborty D. K. and Prasanna A. R., 1982, *Motion of the charged particles off the equatorial plane of a Kerr black hole in an electromagnetic field*, Pramana, **19**, 141.

[29] Chandrasekhar S., 1967, *An Introduction to the Study of Stellar Structure*, Dover Publications, New York., 62.

[30] Chandrasekhar S., 1969, *Ellipsoidal figures of equilibrium*, (New Haven and London: Yale University press).

[31] Chandrasekhar S. and Friedman J. L., 1972, *On the stability of axisymmetric systems to axisymmetric perturbations in general relativity. I. The equations governing nonstationary, and perturbed systems*, Astrophys. J., **175**, 379.

[32] Chandrasekhar S. and Miller J. C., 1974, *On slowly rotating homogeneous masses in general relativity*, Mon. Not. R. Astron. Soc., **167**, 63.

[33] Chitre D. M. and Hartle J. B., 1976, *Stationary configurations and the upper bound on the mass of nonrotating, causal neutron stars*, Astrophys. J., **207**, 592.

[34] Chitre D. M. and Vishveshwara C. V., 1975, *Electromagnetic field around a current loop in a Kerr black hole*, Phys. Rev. D, **12**, 1538.

[35] Cohen J. M. and Wald R. M., 1971, *Point charge in the vicinity of a Schwarzschild black hole*, Journ. Math. Phys. **12**, 1845.

[36] Cohen J. M., Kegeles L. S., Vishweshwara C. V. and Wald R. M., 1974, *Point charge in the vicinity of a Kerr black hole*, Ann. Phys. (NY), **82**, 597.

[37] Cook G. B., Shapiro S. L. and Teukolsky S. A., 1994, *Rapidly rotating netron stars in general relativity: relativistic equations of state*, Astrophys. J., **424**, 823.

[38] Datta B. and Ray A., 1983, *Lower bounds on neutron star mass and moment of inertia implied by the millisecond pulsar*, Mon. Not. R. Astron. Soc., **204**, 75.

[39] Datta B., Hasan S. S. and Sahu P. K., 1992, *Eigenfrequencies of radial pulsations of rotating neutron stars*, Phys. Lett. B, **283**, 313.

[40] Datta B., Thampan A. V. and Bhattacharya D, 1995a, *A numerical survey of neutron star crustal density profiles*, J. Astron & Astrophys., **16**, 375.

[41] Datta B., Thampan A.V. and Wiita P. J., 1995b, *Accretion onto weak field neutron stars: Disk luminosity and angular momentum for accreting, weak field neutron stars in the 'slow' rotation approximation*, J. Astron. & Astrophys., **16**, 357.

[42] de Felice F., 1968, *Equatorial geodesic motion in the gravitational field of a rotating source*, Il Nuovo Cimento , **57**, 351.

[43] de Felice F., 1991b, *Rotating frames and measurements of forces in general relativity*, Mon. Not. R. Astron. Soc., **252**, 197.

[44] de Felice F., 1994, *Kerr metric : The permitted angular velocity pattern and the pre-horizon regime.*, Class. Quant. Grav. **11**, 1283.

[45] de Felice F. and Usseglio- Tomaset S., 1991a, *On the pre-horizon regime in the Kerr metric*, Class. Quant. Grav. **8**, 1871.

[46] Demianski M., 1985, *Relativistic Astrophysics* PWN-Polish scientific publishers; Pergamon press, 120.

[47] Dolginov A. Z., 1988, *Magnetic field generation in celestial bodies*, Phys. Rep., **162**, 337.

[48] Eriguchi Y., Hachisu I. and Nomoto K., 1994, *Structure of rapidly rotating neutron stars*, Mon. Not. R. Astron. Soc., **266**, 179.

[49] Feynman R. P., Metropolis N. and Teller E., 1949, *Equation of state of elements based on the generalised Fermi-Thomas theory*, Phys. Rev., **75**, 1561.

[50] Fowler W. A., 1964, *Massive stars, relativistic polytropes, and gravitational radiation*, Rev. Mod. Phys., **36**, 545.

[51] Fowler W. A., 1966, *The stability of supermassive stars*, Astrophys. J., **144**, 180.

[52] Friedman B. and Pandharipande V. R., 1981, *Hot and cold, nuclear and neutron matter*, Nucl. Phys., **A 361**, 502.

[53] Friedman J.L., Ipser J. R. and Parker L.,1986, *Rapidly rotating neutron star models*, Astrophys. J., **304**, 115.

[54] Giacconi R., Gursky H., Paolini F. R. and Rossi B. B., 1962, *Evidence for x-rays from source outside the solar system*, Phys. Rev. Lett., **9**, 439.

[55] Ginzburg V.L. and Ozernoi, 1965, *On the gravitational collapse of magnetic stars*, Sov. Phys. JETP, **20**, 689.

[56] Glendenning N. K., 1985, ***Neutron stars are giant hypernuclei ?***, Astrophys. J., **293**, 170.

[57] Gold T., 1968, ***Rotating neutron stars as the origin of the pulsating radio sources***, Nature, **218**, 731.

[58] Goldreich P. and Julian W. H.,1969, ***Pulsar electrodynamics***, Astrophys. J., **157**, 869.

[59] Gonthier P. L. and Harding A. K., 1994, ***General relativistic corrections in the gamma-ray emissiom from the pulsars***, Astrophys. J., **425**, 767.

[60] Gupta Anshu and Prasanna A. R., 1997, ***Effects of rotation and equations of state on the structure of the electromagnetic field inside a slowly rotating body***, in preparation.

[61] Gupta Anshu, Iyer Sai and Prasanna A. R., 1996a, *Centrifugal force and ellipticity behaviour of a slowly rotating ultra compact object*, Class. and Quant. Grav., **13**, 2675.

[62] Gupta Anshu, Iyer Sai and Prasanna A. R., 1996b, *Behaviour of the centrifugal force and of ellipticity for a slowly rotating fluid configuration with different equations of state* communicated to Class. and Quant. Grav.

[63] Hanni R. S. and Ruffini R., 1973, *Black Holes, edited by C. Dewitt and B. S. Dewitt, New York, Gordon and Breach.*

[64] Harrison B. K., Wakano M. and Wheeler J. A., 1958, *Matter-energy at high density; end point of thermonuclear evolution* in La Structure et l'evolution de l'univers, Onzieme Conseil de Physique Solvay, Stoops, Brussels, Belgium.

[65] Harrison B. K., Thorne K. S., Wakano M. and Wheeler J. A., (HTWW), 1965, *Gravitation Theory and Gravitational Collapse*, University of Chicago Press, Chicago, Illinois.

[66] Hartle J. B., 1967, *Slowly rotating relativistic stars I. Equations of structure*, Astrophys. J., **150**, 1005.

[67] Hartle J. B. and Thorne K. S.,1968, *Slowly rotating relativistic stars II. Models for neutron stars and supermassive stars*, Astrophys. J., **153**, 807.

[68] Hewish A., Bell S. J., Pilkington J. D. H., Scott P. F. and Collins R. A., 1968, *Observation of a rapidly pulsating radio source*, Nature, **217**, 709.

[69] Hoyle F., Narlikar J. V. and Wheeler J. A., 1964, *Electromagnetic waves from very Dense Stars*, Nature, **203**, 914.

[70] Hull T. E., Enright W. H. and Jackson K. R., 1976, *Users guide for DVERK-A subroutine for solving non-stiff ODES*, Deptt. of Computer Science Technical Report 100, Univ. Of Toronto.

[71] Irvine J. M., 1978, *Neutron Stars*, (Oxford university press).

[72] Iyer B. R., Vishveshwara C. V., and Dhurandhar S. V., 1985, *Ultracompact ($R < 3M$) objects in general relativity*, Class. and Quant. Grav., **2**, 219.

[73] Iyer Sai and Prasanna A.,R., 1993, *Centrifugal force in Kerr geometry*, Class. and Quant. Grav., **10**, L13.

[74] Jastrow R., 1955, *Many-body problem with strong forces*, Phys. Rev., **98**, 1479.

[75] Kapoor R. C., 1991, *The contribution of light bending and redshift to the pulse characteristics of a pulsar in the case of smaller neutron stars*, Astrophys. J., **378**, 227.

[76] Kapoor R. C. and Datta B, 1985, *Fast Pulsars: Effects of spacetime curvature and rotation on the pulse characteristics*, Astrophys. J., **297**, 413.

[77] Meltzer D. W. and Thorne K. S, 1966, *Normal modes of radial pulsation of stars at the end point of thermonuclear evolution*, Astrophys. J., **145**, 514.

[78] Meszaros P. and Riffert H., 1987, *On the radius of neutron stars*, Astrophys. J., **323**, L 127.

[79] Meszaros P. and Riffert H., 1988, *Gravitational light bending near neutron stars.II. Accreting pulsar spectra as a function of phase*, Astrophys. J., **327**, 712.

[80] Meszaros P., Bagoly Z. and Riffert H., 1989, *Magnetized neutron stars as gamma-ray bursters: Detection rates at high energies* , Astrophys. J., **337**, L 23.

[81] Michel F. C., 1982, *Theory of pulsar magnetospheres*, Rev. Mod. Phys., **54**, 1.

[82] Miller J. C., 1977, *Quasi-stationary gravitational collapse of slowly rotating bodies in general relativity*, Mon. Not. R. Astron. Soc., **179**, 483.

[83] Misner C. W., Thorne K. S. and Wheeler J. A.,1973, *Gravitation*, W. H. Freeman and Company, San Francisco.

[84] Nayak K. R. and Vishveshwara C. V., 1996a, *Gyroscopic precession and centrifugal force in the Ernst spacetime*, (to be published).

[85] Nayak K. R. and Vishveshwara C. V., 1996b, *Gyroscopic precession and centrifugal force in the Kerr-Newman spacetime*, Class. Quant. Grav., **13**, 1783.

[86] Negele J. W. and Vautherin D., 1973, ***Neutron star matter at sub-nuclear densities***, Nucl. Phys., **A 207**, 298.

[87] Newman E. and Penrose R., 1962, *An approach to gravitational radiation by a method of spin coefficients*, Journ. Math. Phys., **3**, 566.

[88] Oppenheimer J. R. and Volkoff G. M., 1939, *On massive neutron cores*, Phys. Rev., **55**, 374.

[89] Ostriker J. P. and Gunn J. E., 1969, *On the nature of pulsars. I. Theory*, Astrophys. J., **157**, 1395.

[90] Pacini F., 1967, *Energy emission from a neutron star*, Nature, **216**, 567.

[91] Pandharipande V. R., 1971a, *Dense neutron matter with realistic interactions*, Nucl. Phys., **A 174**, 641.

[92] Pandharipande V. R., 1971b, *Hyperonic matter*, Nucl. Phys., **A 178**, 123.

[93] Petterson J. A., 1974, *Magnetic field of a current loop around a Schwarzschild black hole*, Phys. Rev. D, **10**, 3166.

[94] Petterson J. A., 1975, *Stationary axisymmetric electromagnetic fields around a rotating black hole*, Phys. Rev. D, **12**, 2218.

[95] Pfister H. and Braun K. H., 1985, *Induction of correct centrifugal force in a rotating mass shell*, Class. and Quant. Grav., **2**, 909.

[96] Prasanna A. R., 1980, *General relativistic analysis of charged particle motion in electromagnetic fields surrounding black holes*, Revista del Nuovo Cimento, **3**, 1.

[97] Prasanna A. R., 1984, A Random walk in relativity and cosmology, 192.

[98] Prasanna A. R., 1991, *Centrifugal force in Ernst spacetime*, Phys. Rev. D, **43**, 1418.

[99] Prasanna A.R. and Chakrabarti S. K., 1990, *Angular momentum coupling and optical reference geometry in Kerr space-time*, Gen. Rel. Grav., **22**, 987.

[100] Prasanna A. R. and Gupta Anshu, 1997, *Structure of external electromagnetic field around a slowly rotating compact object and charged particle trajectories therein* to appear in Il Nuovo Cimento.

[101] Prasanna A. R. and Iyer Sai, 1991, *The radial force on a charged particle in superimposed magnetic fields on Schwarzschild spacetime*, Pramana, **37**, 405.

[102] Prasanna A. R. and Sengupta S., 1994, *Charged particle trajectories in the presence of a toroidal magnetic field on a Schwarzschild background*, Phys. Lett. A, **193**, 25.

[103] Prasanna A. R. and Varma R. K., 1977, *Charged particle trajectories in a magnetic field on a curved space-time*, Pramana, **8**, 229.

[104] Prasanna A. R. and Vishveshwara C. V., 1978, *Charged particle motion in an electromagnetic field on Kerr background geometry*, Pramana, **11**, 359.

[105] Punsley B. and Coroniti F. V., 1990, *Relativistic winds from pulsar and black hole magnetospheres*, Astrophys. J., **350**, 518.

[106] Ray A. and Datta B., 1984, *Rotating neutron star structure: Implications of the millisecond pulsar PSR 1937 + 214*, Astrophys. J., **282**, 542.

[107] Reid R. V. Jr., 1968, *Local phenomological nucleon-nucleon potentials*, Ann. Phys., **50**, 411.

[108] Riffert H. and Meszaros P., 1988, *Emissions from columns and hot spots*, Astrophys. J., **325**, 207..

[109] Riffert H., Meszaros P. and Bagoly Z., 1989, *High-energy gamma-ray absorptions in relativistic magnetospheres* , Astrophys. J., **340**, 443.

[110] Ruderman M. A. and Sutherland P. G., 1975, *Theory of pulsars: polar gaps, sparks and coherent microwave radiation*, Astrophys. J., **196**, 51.

[111] Sabbadini A. G. and Hartle J. B., 1973, *Upper bound on the mass of non-rotating neutron stars*, Astrophys. Space Sci., **25**, 117.

[112] Sahu P. K., Basu R. and Datta B., 1993, *High-density matter in the chiral sigma model*, Astrophys. J., **416**, 267.

[113] Salgado M., Bonazzola S., Gourgoulhon E. and Haensel P., 1994a, *High precession rotating neutron star models I. Analysis of neutron star properties*, Astron. & Astrophys., **291**, 155.

[114] Salgado M., Bonazzola S., Gourgoulhon E. and Haensel P., 1994b, *High precession rotating neutron star models II. Large sample of neutron star properties*, Astron. & Astrophys. Supl., **108**, 455.

[115] Sandage A., 1961, *The ability of the 200 inch telescope to discriminate between selected world models*, Astrophys. J., **133**, 355.

[116] Schmidt M., 1963, *3C 273: A star-like object with large red-shift*, Nature, **197**, 1040.

[117] Schutz B. F., 1985, ***A First Course in General Relativity***, Cambridge University Press.

[118] Seguin F. H., 1975, ***The stability of nonuniform rotation in relativistic stars***, Astrophys. J., **197**, 745.

[119] Sengupta S., 1995, ***General relativistic effects on the induced electric field exterior to pulsars***, Astrophys. J., **449**, 224).

[120] Shapiro S. L. and Teukolsky S. A., 1983, ***Black holes, White dwarfs and Neutron stars: The physics of compact objects***, (John Wiley & sons: Wiley publications).

[121] Shapiro S. L. and Teukolsky S. A., 1985, ***Relativistic stellar dynamics on the computer I. Motivation and numerical method***, Astrophys. J., **298**, 34.

[122] Sonego S. and Massar M.,1996, ***On the notions of gravitational and centrifugal force in static spherically symmetric space-times*** , Mon. Not. R. Astron. Soc., **281**, 659.

[123] Stuchlik Z., 1983, ***The motion of test particles in the black-hole backgrounds with non-zero cosmological constant***, Bull. Astron. Inst. Czechosl., **34**, 129.

[124] Stuchlik Z., 1990, ***Note on the properties of the Schwarzschild-de-Sitter space-time***, Bull. Astron. Inst. Czechosl., **41**, 341.

[125] Teukolosky S. A., 1973, ***Perturbations of a rotating black hole. I. Fundamental equations for gravitational, electromagnetic and interior field perturbations***, Astrophys. J., **185**, 635.

[126] Thirring H. and Lense J., 1918, ***Uber den Einfluss der Eigenrotation der Zentralkorper auf die Bewegung der Planeten Und Monde Nach der Einsteinschen Gravitationstheorie***, Phys. Zeits., **19**, 33.

[127] Thompson C. and Duncan R. C., 1993, ***Neutron star dynamos and the origin of pulsar magnetism***,Astrophys. J, **408**, 194.

[128] Thorne K. S., 1971, ***General relativity and cosmology***, Course XLVII, Proceedings of the International School of Physics 'Enrico Fermi',ed. R. K. Sachs, Academic press, New York, 272.

[129] Thorne K. S., 1967, ***Relativistic Stellar Structure and Dynamics***, Proc. 1966 Ecale d Ete de Physique Theorique (New York: Gordon and Breach).

[130] Thorne K. S., 1983, ***Black Hole a Membrane Paradigm***, (New Haven and London: Yale University press).

[131] Tolman R. C., 1939, *Static solutions of Einstein's field equations for spheres of fluid*, Phys. Rev., **55**, 364.

[132] Tooper R. F., 1966, *The standard model for massive stars in general relativity*, Astrophys. J., **143**, 465.

[133] Tsuruta S. and Cameron A. G. W., 1966, *Rotation of neutron stars*, Nature, **211**, 356.

[134] Tsuruta S. and Cameron A. G. W., 1967, *The rotation of neutron stars*, Proc. 1966 Ecale d Ete de Physique Theorique (New York: Gordon and Breach)

[135] Urpin V. A. and Ray A., 1994, *Circulation of matter and the evolution of the internal magnetic field in neutron stars*, Mon. Not. R. Astron. Soc., **267**, 1000.

[136] Urpin V. A. and Shalybkov D. A., 1995, *Magnetothermal evolution of neutron stars*, Astron. & Astrophys., **294**, 117.

[137] Vokrouhlicky D. and Karas V., 1991, *Motion of charged particles around a black hole in a magnetic field*, Astron. & Astrophys., **243**, 165.

[138] Walecka J. D., 1974, *A theory of highly dense matter*, Ann. Phys., **83**, 491.

[139] Weber F. and Glendenning N. K., 1992, *Application of the improved Hartle method for the construction of general relativistic rotating neutron star models*, Astrophys. J., **390**, 541.

[140] Wheeler J. A., 1966, *Superdense stars* Ann. Rev. in Astron. & Astrophys., **4**, 393.

[141] Wiebicke H. J. and Geppert U., 1995, *Amplification of neutron star magnetic fields by thermoelectric effects*, Astron. & Astrophys., **294**, 303.

[142] Wilkins D., 1972, *Bound geodesics in the Kerr metric*, Phys. Rev. D, **5**, 814.

[143] Wiringa R. B., Fiks V. and Fabrocini A., 1988, *Equation of state for dense nucleon matter*, Phys. Rev. C, **38**, 1010.

[144] Woltjer L., 1964, *X-Rays from Type I supernova remnants*, Astrophys. J., **140**, 1309.